A KINETIC STUDY OF THE CATALYTIC OXIDATION OF BENZENE

A THESIS SUBMITTED TO
THE UNIVERSITY OF BOMBAY
FOR THE DEGREE OF Ph.D. (Tech.)
BY

K. VAIDYANATHAN, B.Sc., B.Sc. (Tech.)

NATIONAL CHEMICAL LABORATORY, POONA.

1967

Statement required to be submitted under Rule 0.413 of the University of Bombay

No part of this thesis has been submitted for a degree or diploma or other academic award. The literature concerning the problem investigated has been surveyed, and all the necessary references are given in the thesis. The present work has been clearly indicated separately. The experimental work has been carried out entirely by me. In accordance with the usual practice, due acknowledgement has been made wherever the work presented is based on the results of other workers.

K. Vaidyanathan
CANDIDATE

POONA
May 1967

L. K. Doraiswamy
RESEARCH GUIDE

TABLE OF CONTENTS

SUMMARY AND CONCLUSIONS

SUMMARY AND CONCLUSIONS

The published literature on the oxidation of benzene to maleic anhydride in the vapour phase is quite vast, but only a small part of it relates to the kinetics of the oxidation process. As a first step in the present study, the available literature on the kinetics of the reaction was collected and tabulated. It was observed that though benzene oxidation proceeds through a number of intermediate steps (including the formation of phenol, hydroquinone and benzoquinone), for the kinetic analysis the following scheme has generally been accepted.

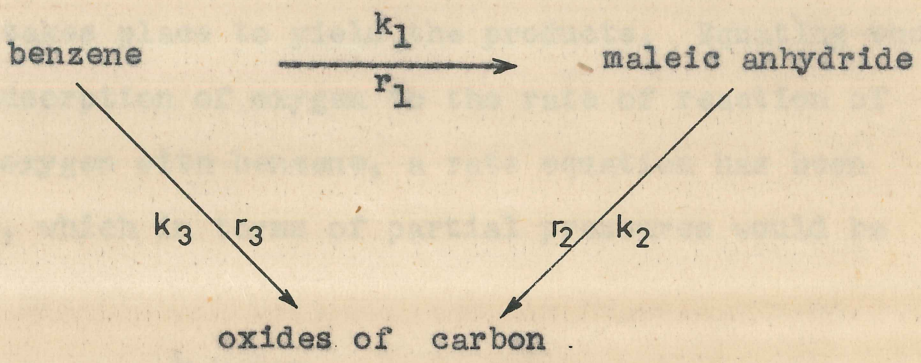

Moreover each of the three principal steps involved apparently follows first-order kinetics. According to Hammar (Svensk Kem. Tid., 64, 165 (1952); Chem. Abst., 46, 8945d (1952)) all these three steps have equal apparent activation energies, where as Ioffe and Lyubarskii (Kinetika i Kataliz, 3, 261 (1962);

Chem. Abst., 58, 55g (1963)) found the activation energies to be unequal.

Apparently no attempt has been made to postulate a plausible model for benzene oxidation, except the solitary attempt of Hayashi et al (Can. J. Chem. Eng., 41, 220 (1963)) who applied the Hinshelwood model to benzene oxidation, the scheme being,

$$\text{benzene} + nO_2 \longrightarrow \text{products}$$

In this model it is assumed that first oxygen is adsorbed over the catalyst surface, then benzene from the gas phase strikes the adsorbed oxygen whence the chemical reaction takes place to yield the products. Equating the rate of adsorption of oxygen to the rate of reaction of adsorbed oxygen with benzene, a rate equation has been developed, which in terms of partial pressures would be

$$r = \frac{k_a k_r p_B p_O}{k_a p_O + n k_r p_B} \qquad .. \qquad (1)$$

This rate equation is restricted to the overall reaction of hydrocarbon with oxygen and not to the individual steps involved. Also the equations are not of general applicability since the value of the specific

adsorption constant of oxygen has been found to vary for different hydrocarbons for a given temperature and catalyst, though the fact that only oxygen is assumed to be adsorbed would require that this constant should have the same value for all the hydrocarbons.

Hence a systematic study of the oxidation of benzene was carried out with the following objectives:

To establish the first-order rate constants and then to suggest a suitable composition of V_2O_5 and MoO_3 (on silica gel) on the basis of a comparative assessment of the kinetic parameters for different catalyst compositions; to examine the Hinshelwood model proposed earlier; to propose plausible models of the Hougen-Watson type for all the principal steps involved; and to elucidate the effect (if any) of mass transfer and pore diffusion.

Experiments were carried out in an integral reactor with outside fluidized bed heating to obtain isothermal conditions. Rate data were collected at four different ratios of benzene to air (1:50, 1:80, 1:110 and 1:140) covering a temperature range of 310-400°C. and a contact time (W/F) range of 60-400 gm.hr./gm-mole. Results of all the runs are expressed in terms of the partial pressures of the products of oxidation, viz., unreacted

benzene and oxygen, maleic anhydride, carbon dioxide and water (as benzoquinone and carbon monoxide were formed in traces, they were not included in the partial pressure calculations).

The rate data conform to pseudo first-order kinetics for all the catalysts employed. The first-order equations for the reaction scheme presented earlier are:

$$-\frac{dp_B}{d(W/F)} = (k_1+k_3)\, p_B \qquad .. \qquad (2)$$

$$\frac{dp_M}{d(W/F)} = k_1 p_B - k_2 p_M \qquad .. \qquad (3)$$

$$\frac{dp_C}{d(W/F)} = (2k_1+6k_3)\, p_B + 4k_2 p_M \qquad .. \qquad (4)$$

The accuracy of the rate constants has been checked by back calculating the disappearance of benzene and formation of maleic anhydride and comparing them with the observed values. The deviation is about 8%. The temperature dependence of these constants has been expressed in the form of the usual Arrhenius relationship, which clearly showed that all the three steps involved have equal activation energies; but the value of the activation energies depends on the temperature region, being about

20 kcal./gm-mole in the region 310-350°C. and about 2 kcal./gm-mole in the region 350-400°C. The magnitude of the activation energy (2 kcal./gm-mole) in the higher temperature range (350-400°C.) suggests that in this region mass transfer might be the controlling step.

A comparative assessment of the kinetic parameters, $k_1/(k_1+k_3)$ and k_2/k_1, for different catalyst compositions indicates that probably a total oxides content ~~constant~~ of 14% and V_2O_5 to MoO_3 ratio 1:1 is the most suitable composition for benzene oxidation.

As pointed out earlier, the Hinshelwood model is not of general applicability. Moreover, the present data also do not uphold this mechanism. Hence, starting from Bretton's postulate (Ind. Eng. Chem., 44, 594 (1952)) that hydrocarbon is adsorbed in preference to oxygen, a modified Hinshelwood model has been developed, according to which benzene is first adsorbed on the catalyst surface and oxygen from the gas phase then strikes the adsorbed benzene leading to chemical reaction. Equating the rate of adsorption of benzene to the rate of reaction of benzene at steady state, the rate equation developed is of the form,

$$r = \frac{k_B k_r p_B p_O}{k_B p_B + k_r p_O} \qquad .. \qquad (5)$$

This equation holds good for the initial conditions only. An empirical correlation has been developed to extend the equation to other conditions by setting,

$$k_r = k_{ro} (1 - ax) \quad .. \quad (6)$$

where

a = empirical constant

The validity of the rate equation has been tested by calculating the rates and comparing them with the experimental values. The Arrhenius relationship developed for the specific rate constant k_{ro} (for the initial condition) yields an activation energy comparable with that obtained from first-order kinetics.

An attempt was then made to delineate the controlling steps for the reactions under study using the Hougen-Watson models. The models proposed after the usual elimination procedure are as follows:

For reaction step 1, adsorption of benzene is the controlling step, reaction occurring between adsorbed benzene and oxygen in the gas phase with carbon dioxide and water not adsorbed.

$$r_1 = \frac{k_{1s}}{(1 + K_M p_M)} \quad .. \quad (7)$$

For reaction step 2, adsorption of maleic anhydride is the controlling step, reaction occurring between adsorbed maleic anhydride and oxygen in the gas phase, with carbon dioxide and water not adsorbed.

$$r_2 = k_{2s} p_M \quad .. \quad (8)$$

For reaction step 3, adsorption of benzene is the controlling step, the reaction occurring between adsorbed benzene and oxygen in the gas phase, with carbon dioxide and water not adsorbed.

$$r_3 = k_{3s} p_B \quad .. \quad (9)$$

The equation developed for steps 2 and 3 are identical with the equation based on first-order kinetics, whose validity was established earlier. For reaction step 1, the accuracy of the constants, k_{1s} and K_M, was checked by calculating the rates from the equation developed for this step and comparing with the observed rates. The deviation is about 13-15%.

The low activation energy (2 kcal./gm-mole) for the higher temperature range (350-400°C.) indicates that mass transfer might be the controlling step in this regime.

Since according to Petersen ("Chemical Reaction Analysis," Prentice-Hall, Inc., New Jersey (1965)) mass transfer alone cannot be the controlling step, being always accompanied by pore diffusional resistance, an attempt was made to determine the influence of pore diffusion. For this purpose rate constants were calculated for different particle sizes, viz.,

-5 +12, -12 +22, -22 +36, -36 +60 (B.S.S. mesh)

Then, from a plot of the observed values of k (rate constant for total benzene disappearance) as a function of particle size, the intrinsic value of k was determined. In view of the similarity in the behaviour of all the rate constants this analysis has been restricted to the total disappearance of benzene. Using this value of k, the effectiveness factor ϵ was calculated from,

$$\epsilon = \frac{\text{observed value of k}}{\text{intrinsic value of k}} \quad .. \quad (10)$$

The Thiele modulus (ϕ) was estimated for different particle sizes from

$$\phi = L \sqrt{\frac{k\ (\text{intrinsic})}{D_e}} \quad .. \quad (11)$$

In the present case, the effectiveness factor was found to be practically unity, and in the plot of ϵ vs. ϕ the experimental points also coincide with the theoretical $\epsilon - \phi$ curve.

Three regions can be identified in the curve:

(i) $\phi < 0.2$ where $\epsilon = 1$;

(ii) $0.2 < \phi < 2$, the transition region; and

(iii) $\phi > 2$ where $\epsilon = 1/\phi$.

Petersen has postulated a mass transfer factor (σ) and has established a relationship between this factor and the Thiele modulus (ϕ) for region (iii), which can be put in the form,

$$\sigma = \frac{1}{1 + 3\phi(D_e/D)} \qquad .. \qquad (12)$$

where the ratio (D_e/D) is a measure of the tortuous diffusion inside the catalyst. This equation can be modified to provide

$$\sigma = \frac{1}{1 + 3\phi^2(D_e/D)} \qquad .. \qquad (13)$$

for region (i) where pore diffusion is absent. A scrutiny of Equation (13) shows that, in the case of benzene oxidation, the value of (D_e/D) being 5.102×10^{-3}, the mass transfer factor (δ) is unity. This fact, combined with the earlier observation that the effectiveness factor is also unity, suggests that neither external mass transfer nor pore diffusion offers any significant resistance in this reaction.

The above analysis was carried out for the high temperature range only since, in the low temperature range, chemical reaction is evidently the controlling step. It is a reasonable conclusion that in the high temperature range also chemical reaction is the controlling step, the unusually low value of the activation energy being attributable to a favourable change in the chemical structure of the catalyst.

Note: The nomenclature is given in pages 156-9.

CHAPTER-1

LITERATURE REVIEW AND PROBLEM OUTLINE

Chapter 1

LITERATURE REVIEW AND PROBLEM OUTLINE

1.1 INTRODUCTION

Maleic anhydride has uses in many branches of the chemical industry. This compound, an internal anhydride of an unsaturated dicarboxylic acid, with its enhanced reactive olefinic linkage, contributes (with its many derivatives) to the manufacture of a variety of chemicals ranging from oil additives to pharmaceuticals.

Maleic anhydride/acid may be obtained by the oxidation of benzene, biphenyl (28), α-pinene (13,14), succinic acid (22), furfural (29,48,51,56), crotonaldehyde (2,7,11,15), butene (9,45,57,60), n-butane (6,35), furan (42), butadiene (6), furfuraldehyde (53), isobutylene (6), phenanthrene (50), cyclopentadiene (49), etc. The pyrolysis of diglycolic anhydride (38) and electrolytic oxidation of benzene (81) and cyclohexanone (27) also yield maleic acid. It is also obtained as a by-product in the production of phthalic anhydride from o-xylene (33) and naphthalene (24,25,73), of benzaldehyde/benzoic acid from toluene oxidation (62), and in the oxidation of ethyl benzene (61).

Attempts have been made to oxidize benzene in the liquid phase, but without success. Potassium permanganate has no marked effect on benzene in the liquid phase (74), hydrogen peroxide in the presence of iron salts yields a

mixture of phenol and diphenyl (16), and the action of air under pressure yields about 0.5 per cent phenol (37).

Of all the raw materials used benzene (25,58,59, 75,76), crotonaldehyde (5,12) and butene (55) are of commercial importance. However more than 90% of the total production of maleic anhydride is based on benzene oxidation.

In the following paragraphs a brief review is presented highlighting the general aspects of benzene oxidation, the various catalysts used, the mechanism of oxidation and the kinetic models proposed. Based on this survey the scope of the present work is outlined in Section 1.6.

1.2 MALEIC ANHYDRIDE FROM BENZENE OXIDATION - A GENERAL SURVEY

An account of the earlier papers dealing with the oxidation of benzene has been presented by Egloff (23) and by Marek and Hahn (46).

As early as 1870, Carius obtained a then unknown derivative of maleic acid as a result of treating benzene with perchloric acid. Kekule repeated this experiment, and identified this product to be β-trichloroacetocecrylic acid ($CCl_3COCH = CH - COOH$). The mechanism of the reaction was explained by supposing that simultaneous oxidation and chlorination of benzene led to a large number of

intermediate compounds, viz. chlorinated benzene, phenol, chlorinated phenols, quinones and finally chlorinated quinones.

In 1891 Zincke and his collaborators undertook a study of the action of chlorine (potassium chlorate + hydrochloric acid) on various derivatives of hydroxy benzenes. In their investigation they came across hexachloro-o-diketone, pentachloro-m-diketone derivatives and dichloro maleic acid. Further, the cleavage of the benzene ring by chlorine in alkaline solution was studied by Hantzsch.

Döbner oxidized phenol with potassium permanganate and obtained meso tartaric acid. It was presumed that hydroquinone, quinone and maleic acid were intermediate steps of oxidation.

In 1906, during a study connected with the structure of benzene, Kempf noted the formation of maleic acid as a result of the liquid phase oxidation of quinone with silver peroxide. He noted that this also resulted by the electrolytic oxidation of quinone.

However, the first step towards the oxidation of aromatics in the vapour phase was undertaken by Orloff in 1908. He obtained benzaldehyde by oxidizing toluene in the vapour phase over copper sieve contact mass. But in the case of benzene a number of unidentified compounds

were reported.

Further studies relating to the oxidation of hydrocarbons were conducted by Gilles and his associates, working at the Bureau of Chemistry in Washington and by Weiss and Downs and their associates, working in the laboratories of the Barret Company at Edgewater, New Jersey. The investigations carried out by them were said to have paralleled each other to a great extent. Very few details concerning the work were published. However, a number of patents were taken on the production of phthalic anhydride from naphthalene, anthraquinone from anthracene, phenanthrequinone from phenanthrene and benzaldehyde from toluene.

The first paper on the vapour phase oxidation of benzene was published in 1920 by Weiss and Downs (77). According to them the oxidation of benzene at high temperatures yielded diphenyl, tarry products and other products of complete oxidation. However, with certain catalysts, conversion to phenol to the extent of 0.3 per cent was possible, with quinone being formed in slightly larger amounts. In the case of a few catalysts, in particular with vanadium pentoxide, maleic acid was formed. Under their experimental conditions, the proportion of quinone to that of maleic acid formed remained almost unaltered. A small quantity of formaldehyde was also reported; but neither the amount nor the mode of its analysis

was indicated. The reaction velocity of the partial oxidation of benzene was said to be less than that of the oxidation rate of sulphur dioxide to sulphur trioxide or of ammonia to nitric acid. The apparatus used by these authors mainly consisted of a vaporizer through which air was bubbled and a 'U' tube reactor held in a bath of molten lead maintained at constant temperature. The reaction products were scrubbed with distilled water and analysed.

In an article published in 1926, Downs (19) had indicated that both alumina and iron, among other materials, were without catalytic activity. Several aspects of the laboratory scale investigations, including the mode of temperature control (through a molten lead bath) as well as the details of a commercial size reactor, consisting of a number of small diameter tubes inserted in a liquid mercury bath (heat exchanger type reactor) for controlling the temperature gradient, have been given. It has been indicated that a yield of 60 pounds of maleic acid per 100 pounds of benzene was feasible on a commercial scale.

Following the introduction of maleic anhydride in the market, Downs (26) published a paper on the possible ~~plausible~~ applications of maleic anhydride.

In 1929 Yabuta and Simose (82) reviewed the oxidation of benzene over vanadium oxide catalyst,

emphasizing the influence of diluent gases, mode of catalyst preparation and effect of other metallic oxides in the catalyst.

Zalkind (83) reported that, at the optimum temperature of 410-430°C., yields of 14 to 17 per cent maleic acid on the basis of benzene used could be obtained. The reaction probably took place via phenol to quinone, to maleic acid and subsequently to the complete oxidation products.

Pigulevskii (54) conducted experiments over ammonium meta vandate catalyst in atmospheres rich in oxygen. Working in the temperatures 370-450°C. with mixtures of benzene from 3 to 8 per cent and 19.7 to 89 per cent oxygen by volume, and at contact times (0.4 to 20.6 sec.) it was reported that a maximum yield of 38 per cent could be obtained.

Kiprianov and Shostak (44) obtained 24 per cent of maleic acid by weight of benzene fed over vanadium pentoxide deposited on pumice, and concluded that the yield could be doubled with 70 per cent vanadium oxide and 30 per cent molybdenum oxide catalyst. Moreover they ascertained, from experimental evidences, the effect of adding small amounts of some metallic oxides as promoters for their catalysts, and found that whilst cobalt enhanced the efficiency of oxidation, bismuth, tin and

lead were innocuous, and addition of iron, nickel, chromium or manganese was deleterious.

Takikawa (63) made use of multicomponent catalysts - vanadium and molybdenum oxides, vanadium, molybdenum and titanium oxides - for the oxidation of the parent compound.

In 1952, Hammar (34) published his studies on the reaction kinetics of the oxidation of benzene over vanadium - molybdenum catalysts deposited over alumina. The reactor consisted of a stainless steel tube heated both externally and internally with dowtherm. The only solid product identified was maleic anhydride and the gaseous products of oxidation were analysed by the conventional Orsat apparatus.

Fakuda (26) studied the relationship between the yield and the ratio of air to benzene, composition of the catalyst, etc., to evolve the optimum conditions for industrial production.

Norrish (52) and his collaborators conducted the oxidation of benzene at a higher temperature of 685°C. and at residence times up to two hours without a catalyst. The idea was to ascertain the mode of oxidation of benzene to the final products. According to the results published, the oxidation has been shown to proceed via successive hydroxylations of the ring to the dihydroxy

stage, whence the ring cleavage takes place, the fission products being rapidly degraded to C_2 hydrocarbons, formaldehyde, carbon oxides, hydrogen and water.

Bhattacharya and Venkataraman (2) have made a systematic study pertaining to the addition of various modifiers like oxides of cobalt, tungsten, uranium, cerium, thorium, zirconium and titanium to the vanadium - molybdenum mixed oxide catalyst over different catalyst supports like kieselguhr, pumice, kaolin, silica gel, metallic aluminium and calcium sulphate. Best yields of maleic acid (50 per cent conversion of benzene) were obtained with a vanadium pentoxide - molybdenum trioxide (ratio 1-2.3 : 1) catalyst supported on kieselguhr with 5 per cent of cobalt oxide as promoter. According to them the mode of preparation of metal oxide and the pre-treatment of the supports also affected the yields.

Sherwood (59) has discussed the various processes used in maleic anhydride production, the significance of the oxidation step, the variables involved in the reaction, the composition of the catalyst used, the product recovery step and the different techniques used (viz. the fixed and fluidized bed techniques).

Due to the short supply of benzene, and the fact that out of 6 carbon atoms in benzene only 4 atoms are utilized in procuring maleic acid whereas the other 2 atoms are lost as oxides of carbon during the reaction, the

recent trends are to utilize hydrocarbons having 4 carbon atoms as the starting material, like butene (CH_3-CH = CH-CH_3) or crotonaldehyde (CH_3-CH = CH.CHO).

Crotonaldehyde (4,5,12) is used by Germans in the production of maleic anhydride. The crotonaldehyde needed for this process is obtained from acetaldehyde by aldol condensation carried out in a continuous converter.

Irrespective of the starting materials used, the reaction is highly exothermic. In order to prevent the consequent temperature gradients in the catalyst bed, which hamper the progress of the reaction to the intermediate products of oxidation, many new ideas have been put into practice.

At present, besides the conventional fixed bed technique for the maleic anhydride production, fluidized (58) and moving (64) bed techniques have also been employed.

A recent French patent (30) proposes a novel method which consists in packing the fixed bed reactor with three layers of catalyst of different compositions. The compositions of these catalysts are so adjusted that the reaction proceeds smoothly and a high yield of maleic anhydride is obtained.

Another method has been reported (10) in which

two catalytic reactors are operated in series. These two fixed bed reactors are packed with different quantities of the catalyst maintained at different temperatures and at specified conditions. The first reactor yields about 37.5 per cent and the second about 37.6 per cent, thus fetching a total of about 75 per cent of maleic anhydride per pass. This method appears to be in consonance with modern techniques of temperature optimization.

1.3 CATALYSTS USED IN BENZENE OXIDATION

A great variety of catalysts has been patented for use in the vapour phase oxidation of benzene to maleic anhydride. The use of the metals of the fifth and sixth groups of the periodic system or mixturesof these oxides has been particularly stressed. Vanadium pentoxide has been studied more in this connection than any other oxide because of its selective role in the oxidation of benzene.

Weiss, Burns and Downs (78) investigated the mechanism by which vanadium oxide catalyses the oxidation of benzene. It was found that the colour of the catalyst changed from reddish yellow in the initial condition to bluish green to grey after the reaction. Hence it was assumed that the pentavalent vanadium dissociates as

$$V_2O_5 \underset{\text{air}}{\overset{\text{benzene}}{\rightleftharpoons}} V_2O_4 + O$$

To verify this phenomenon, different catalysts of known composition were prepared and analysed at the end of the reaction. It was found that the equilibrium composition depended only on the ratio of air to benzene at a given temperature. But the proportion of vanadium pentoxide in the catalyst at equilibrium decreased with increase of temperature. At the same time, at higher temperatures, as the products of total oxidation from the reaction increased, it was suggested that the degree of complete oxidation was not solely dependent on the ratio of V_2O_5 to V_2O_4. They attributed the relative proportions of the various products of oxidation from the parent compound to some other property of the catalyst, perhaps the structure of the crystalline lattice.

The effect of various promoters like molybdenum oxide (63), boric acid (63), chromic acid (39), tungstic oxide (65), in conjunction with the vanadium pentoxide, has been studied. Of these promoters, only molybdenum oxide is widely used.

Ioffe and his co-workers (39) have made a systematic study of the oxidation of benzene over a varied proportion of vanadium and molybdenum oxides. According to them, the increased activity of the catalyst is associated with the solid solution formation of MoO_3 with V_2O_5 lattice. Thus a 25 to 30 mole per cent of MoO_3 with V_2O_5 has been shown to form a good solid solution.

But according to others the ideal mixture proportion is 1:1 (2,66,67).

Addition of small quantities of "additives" or "modifiers" to V_2O_5 - MoO_3 mixed oxide catalysts is said to enhance the reactivity to the formation of the intermediate products of oxidation. In other words, they are believed to inhibit the further oxidation of intermediate compounds to the ultimate oxidation products, as well as check the direct complete oxidation of benzene. Thus, additives like titanium dioxide (63), sodium salts (69), phosphorus pentoxide (65), potassium salts (70), nickel nitrate (31) and lithium oxide (32) have been studied in conjunction with the mixed oxide catalysts of vanadium and molybdenum.

Inert materials like silica (79), alundum (68, 43) pumice (10,26), metallic aluminium (34), alumina (31, 71), quartz (67), fused corundum (40), silica gel (66) have been used as catalyst supports. However, it has been reported (66) that carriers like silica gel with high porosity have a deleterious effect on the conversion of benzene to maleic anhydride. On the other hand, carriers with low porosity (like quartz) are also not suitable, as the oxide coatings tend to peel off, especially in a fluidized bed, due to insufficient adhesion to the surface. Generally the best results are reported to be obtainable with carriers of medium porosity

like alundum (66).

Regarding the total oxides (molybdenum oxide plus vanadium oxide) required for the reaction, about 25% (on the carrier) has been found to be the best proportion by a few investigators (2,64,89). On the other hand, there are also patents (31,32,41) which claim about 15% total oxides to be the most suitable.

With respect to the size of the catalyst to be used in a fixed bed reactor, a range of about -3 +6 mesh (70,72) is considered to be the most favourable.

1.4 MODE OF BENZENE OXIDATION

A few references are available in the literature on the stepwise oxidation of benzene to the principal products of oxidation in the vapour phase.

The fact that Weiss and Downs (21,23,80) were able to isolate phenol in the products of reaction suggests a hydroxylation mechanism similar to that postulated in the case of vapour phase catalysis (3) in which the formation of monohydroxylated derivative is the first step. The hydroxyl group in phenol activates the para and ortho positions, so that the introduction of the second hydroxyl group would be expected to yield quinol (1 : 4 $C_6H_4(OH)_2$) and catechol (1:2$C_6H_4(OH)_2$) respectively, with a preponderance of the former. Quinol

was oxidized further to quinone. However the amount of quinone formed was very little.

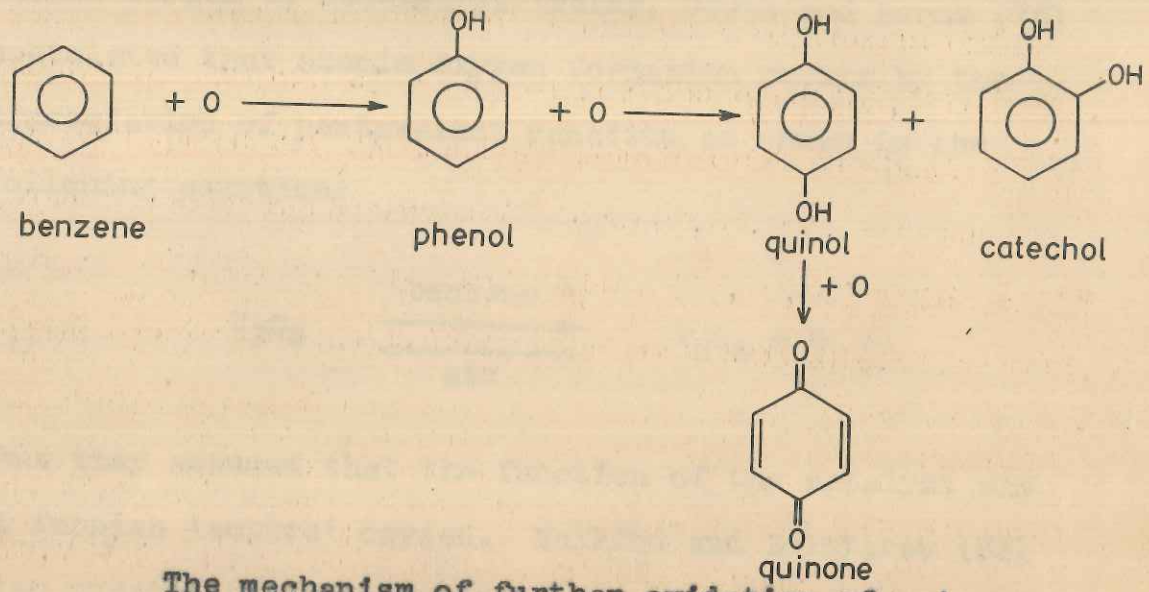

The mechanism of further oxidation of quinone to maleic anhydride is speculative, as none of the intermediate compounds in this step has been isolated. However the possibility of further hydroxylation of the quinone, and the formation of a polyketone due to rearrangement, may not be ruled out.

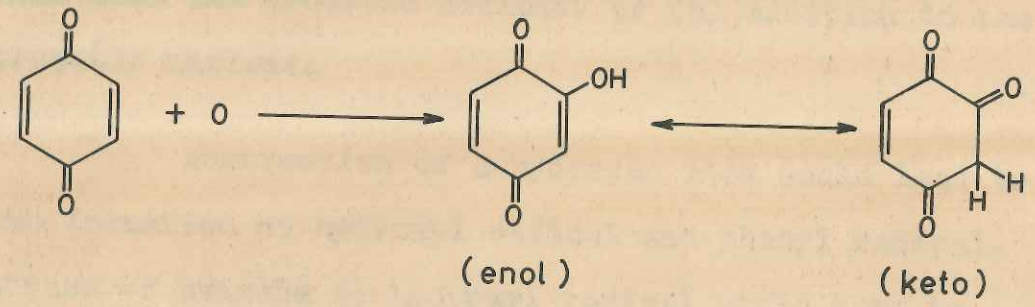

Further oxidation of this product results in ring rupture and formation of maleic anhydride

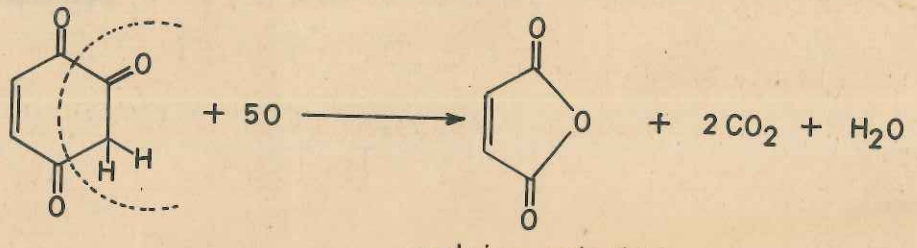

For the formation of phenol from benzene, atomic oxygen is necessary. Weiss, Downs and Burns (78) postulated that atomic oxygen formation occurs by the dissociation of pentavalent vanadium as shown in the following equation:

$$V_2O_5 \underset{\text{air}}{\overset{\text{benzene}}{\rightleftharpoons}} V_2O_4 + O$$

Thus they assumed that the function of the catalyst was to furnish 'active' oxygen. Zalkind and Zolotarev (83) also support the hydroxylation mechanism.

Recently Boocock and Cretonovic (8) have made an exhaustive study of benzene attack by atomic oxygen. According to them two modes of attack of atomic oxygen on benzene are possible : (a) abstraction of a hydrogen atom from the aromatic nucleus, or (b) addition to the aromatic nucleus.

Abstraction of a hydrogen atom would lead to the formation of hydroxyl radical and phenyl radical. Attack of benzene by hydroxyl radical would then be expected, with the subsequent production of phenol and diphenyl by radical association, according to the following scheme.

$$C_6H_6 + O \longrightarrow C_6H_5\cdot + OH\cdot$$

$$C_6H_6 + OH\cdot \longrightarrow C_6H_5\cdot + H_2O$$

$$C_6H_5\cdot + OH\cdot \longrightarrow C_6H_5OH$$

$$C_6H_5\cdot + C_6H_5\cdot \longrightarrow C_6H_5 - C_6H_5$$

Alternatively, as with the olefines and cycloolefines, the oxygen atom may add directly to benzene molecule, which presents a large number of possibilites, as shown below:

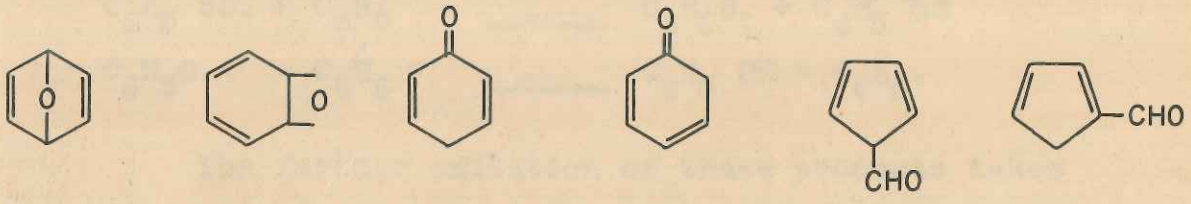

I II III IV V VI

However, none of these compounds is reported in the literature, although some derivatives are known. This is probably because I, II, III and IV isomerize quickly to the stable structure of phenol, whilst V and VI are undoubtedly prone to a variety of condensations, polymerizations and decompositions.

Norrish and Taylor (52) have carried out the complete oxidation (combustion) of benzene at a high temperature (685°C.) without a catalyst, but at long residence times reaching up to two hours. According to them, in the pyrolysis of benzene, small amounts of oxygen may catalyse the reaction leading to the formation of

biphenyl (here oxidation is not involved). Thus :

$$C_6H_6 + (O_2) \longrightarrow C_6H_5 + (HO_2).$$
$$2C_6H_5. \longrightarrow C_6H_5 - C_6H_5$$
$$H. + C_6H_6 \longrightarrow C_6H_5. + H_2$$

During combustion (oxidation),

$$C_6H_6 + O_2 \longrightarrow C_6H_5. + HO_2.$$
$$C_6H_5. + O_2 \longrightarrow C_6H_5\ OO.$$
$$C_6H_5\ OO. + C_6H_6 \longrightarrow C_6H_5O. + C_6H_5\ OH$$
$$C_6H_5O. + C_6H_6 \longrightarrow C_6H_5\ OH + C_6H_5.$$

The further oxidation of these products takes place in a similar manner.

1.5 KINETIC MODELS

Numerous references pertaining to process studies on the oxidation of benzene are available (17,23, 46), but only a few of them relate to the kinetics of the oxidation process, wherein rate equations have been given which can be used in reactor design. As pointed out earlier, the reaction proceeds through a number of intermediate steps, including the formation of phenol, hydroquinone and benzoquinone. Traces of formaldehyde and diphenyl have also been reported among the products. However, for the kinetic analysis of the reaction, the following scheme has normally been employed (17,34,40).

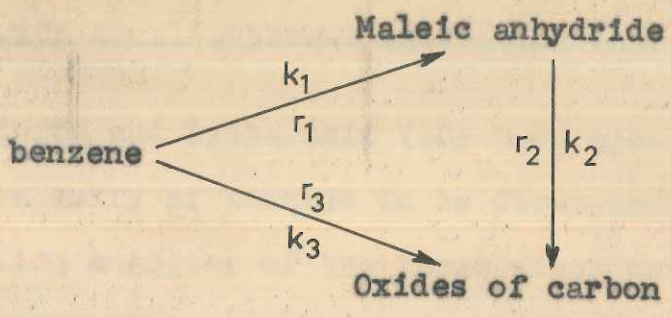

Hammar (34) has studied the oxidation of benzene over a number of catalysts consisting of V_2O_5 and MoO_3 on metallic aluminium. He has interpreted the data according to the above scheme. The rate of the first step is said to be very fast, being limited only by the mass transfer rate. The fact that the activation energy for this step was of the order of 25 kcal. per gm-mole, which is inconsistent with mass transfer control, has been explained by assuming that the active area of the catalyst available for the reaction is itself temperature dependent.

The rate of total combustion of benzene (r_3) was found to be almost independent of mass transfer, the rate determining step being either re-adsorption of maleic anhydride or surface reaction. However it is difficult to visualise the readsorption of maleic anhydride as a possible controlling step since maleic anhydride is not involved in the direct total combustion of benzene to carbon dioxide and water.

The three kinetic steps involved in the reaction were found by Hammar (34) to be uninhibited first-order

reactions with equal apparent activation energies.

Ioffe and Lyubarskii (40) have also found the oxidation velocity of benzene to be first-order, but the activation energies of the three steps were found to be unequal. At benzene concentrations > 10 percent oxidation was found to be independent of oxygen concentration in the gas phase.

According to Bretton (9), initially the benzene is adsorbed over the catalyst surface with the abstraction of hydrogen to form a radical. Then the oxygen from the gas phase strikes over it and the chemical reaction proceeds through the formation and destruction of peroxy radicals.

Hayashi et al (36) have applied the Hinshelwood (steady-state) reaction mechanism to the oxidation of benzene, assuming :

(i) oxygen is the only reactant adsorbed on the catalyst surface,

(ii) the rate of desorption of oxygen from the catalyst is negligible,

(iii) for reaction to occur, organic reactant in the gas phase must strike an adsorbed oxygen, and

(iv) a steady state is established in which the rate of removal of oxygen by chemical reaction equals the rate of adsorption of oxygen.

Equating the rate of adsorption of oxygen to the rate of chemical reaction, the final form of the equation developed, expressed in terms of partial pressure, was

$$r = \frac{k_a k_r p_B p_o}{k_a p_o + n\, k_r p_B}$$

Mars and van Krevelen (47) have proposed a similar model for the oxidation of naphthalene. According to them the oxidation scheme is represented by the following two steps :

(I) naphthalene + oxidized catalyst --→ products + reduced catalyst

(II) reduced catalyst + oxygen --→ oxidized catalyst

The final rate equation developed by equating these two steps is identical in form with the Hinshelwood equation developed by Hayashi et al (36).

Recently Dmuchovsky et al (18) have studied the kinetics of the catalytic oxidation of benzene.

According to them also benzene is oxidized in two independent paths, one leading to maleic anhydride, which may be further oxidized and the other leading to the final products of oxidation as indicated in the scheme. A first-order rate law holds good up to 75 percent of the reaction range. This has been found to be true at various temperatures in the range 319°-377°C. The apparent activation energies for the two paths of oxidation of benzene are quite considerable and almost the same; whereas that required for the oxidative decomposition of maleic anhydride is found to be lower. It has been proposed that in the rate limiting step, benzene reacts with molecular oxygen either in a 1:2 or 1:4 fashion to yield activated complexes possessing considerable mobility.

1.6 PROBLEM OUTLINE

The detailed review of the existing literature on the oxidation of benzene reported in the foregoing sections brings out the following salient features of this process:

(i) Vanadium and molybdenum mixed-oxides are apparently the most suitable catalysts.

(ii) The suitability of any particular catalyst composition has been established more from process data than from any rational interpretation of the kinetic

parameters of the reaction for various catalysts.

(iii) First-order kinetic equations have been proposed for all the three principal steps involved.

(iv) A solitary attempt has been made to postulate a model for the total oxidation of benzene according to the reaction,

$$\text{Benzene} + nO_2 \longrightarrow \text{Products}$$

In this steady-state model it has been assumed that at equilibrium,

rate of adsorption of oxygen = rate of reaction of surface oxygen

(v) Apparently no attempt has been made to postulate models for the three principal steps involved in benzene oxidation.

(vi) The possibility of mass transfer being the controlling step at elevated temperatures has been suggested; but the magnitude of the activation energy is inconsistent with mass transfer control.

Thus, although considerable work has been done on benzene oxidation, there are still several aspects of the process which require elucidation and analysis. The present investigation was undertaken with the following principal objectives :

(1) To establish the first-order rate constants and then to suggest a suitable catalyst composition, using

V_2O_5 and MoO_3 mixtures, on the basis of a comparative assessment of the kinetic parameters for different catalyst compositions, the object being to obtain a high selectivity to maleic anhydride.

(2) To examine the Hinshelwood steady-state model for the total oxidation of benzene and to apply this model to the catalysts selected.

(3) To establish plausible models (based on the Hougen-Watson approach) for each of the three significant steps involved in the oxidation of benzene.

(4) To examine the role of pore diffusion for the selected catalysts and also the effect of external mass transfer (if any).

References

1. Acad. Vep. populare Ponune, Baza Cercetari stunt. Timisora, Studu Cercertari stunt. Ser. Chim. 6, 135-44 (1959); Chem. Abst., 55, 7005g (1961).

2. Bhattacharya, S.K. and Venkataraman, N., J. Appl. Chem. (London), 8, 728-37 (1958).

3. Bibb and Lucas, Ind. Eng. Chem., 21, 635 (1929).

4. BIOS Final Report No. 1650.

5. BIOS Final Report No. 739.

6. Bissot, T.C. and Benson, K.A., Ind. Eng. Chem., Prod. Res. Develop., 2, 57 (1963).

7. Bludworth, J.E. and Pearson, P.C. (Celanese Corporation of India), U.S. Patent, 2,462,938, Mar. 1, 1949; Chem. Abst., 43, 5034c (1949).

8. Boocock, G. and Cvetanovic, R.J., Can. J. Chem., 39, 2436 (1961).

9. Bretton, R.H., Wan, S.U. and Dodge, B.F., Ind. Eng. Chem., 44, 594 (1952).

10. British Patent 948,057, Jan. 29, 1964; Chem. Abst., 60, 11903a (1964).

11. Church, J.M. and Bitha, P., Ind. Eng. Chem. Prod. Res. Develop., 2, 61 (1963).

12. CIOS File No. XXVII - 85.

13. Clark, C.K. and Hawkins, J.E., Ind. Eng. Chem., 33, 1177 (1941).

14. Clark, C.K. and Hawkins, J.E., Proc. Florida Acad. Sci., 4 (1939); 116 (1940); Chem. Abst., 35, 98 (1941).

15. Consortium fur elektrochemisch Industrie G.m.b.H., Brit. Patent, 790,559; Chem. Abst., 52, 15572c (1958).

16. Discussions Faraday Soc. No. 14, 160 (1953); Chem. Abst., 48, 10626h (1954).

17. Dixon, J.K. and Longfield, J.E., "Catalysis", (P.H. Emmett, ed.); Vol. VII, Chap. 3, Reinhold Publishing Corporation, New York (1960).

18. Dmuchovsky, B., Freeks, M.C., Pierron, E.D., Munch, R.H. and Zienty, F.B., J. Catalysis, 4, (22), 291 (1965).

19. Downs, C.R. J. Soc. Chem. Ind., 45T, 188-93 (1926).

20. Downs, C.R., Ind. Eng. Chem. 26, 17-20 (1934).

21. Downs, C.R., J. Soc. Chem. Ind., 46T, 383-86 (1927).

22. Drossbach, O., German Patent 724,758, July 23, 1942; Chem. Abst., 37, 5736 (1943).

23. Egloff, G., Berkman, S. and Morrell, J.C., "Catalysis Inorganic and Organic", pp.280-81, 533-48, 800-2, Reinhold Publishing Corp., New York (1940).

24. Esso Research & Engineering Co., German Patent 943,293, May 17, 1956; Chem. Abst., 53, 13113 (1959).

25. Faith, W.L., Keyes, D.B. and Clark, R.L., "Industrial Chemicals", 2nd Ed., pp.305-8, 500-4, Wiley, New York (1957).

26. Fakuda, T., J. Chem. Soc. Japan, Ind. Chem. Sect., 54, 111-13 (1951).

27. Falqui, M.T., Rand. Seminar. Fac. Sec. Univ. Cagliari, 23, 194 (1953); Chem. Abst., 49, 5157 (1955).

28. Faster, H.B. (National Aniline & Chemical Co.), U.S. Patent 2,114,798, April 19, 1938; Chem. Abst., 32, 4609 (1938).

29. Fedele Carello, Italian Patent, 461,821, Feb. 15, 1951; Chem. Abst., 46, 2842i (1952).

30. French Patent 1,340,392; Chem. Abst., 60, 6785 (1964).

31. French Patent 1,332,127; Chem. Abst., 59, 9807 (1963).

32. French Patent 1,262,809, Sept. 22, 1961; Chem. Abst., 56, 9975c (1962).

33. Gulati, I.B. and Bhattacharya, S.K., J. Sci. Ind. Research (India), 12B, 450 (1953); Chem. & Industry 1425 (1954).

34. Hammar, C.G.B., Svensk Kem. Tid., 64, 165-76 (1952); Chem. Abst., 46, 8945d (1952).

35. Hartig, M.J.P. (to E.I. du Pont de Nemours & Co.), U.S. Patent 2,625,519, Jan. 13, 1953 and U.S. Patent 2,691,660, Oct. 12, 1954; Chem. Abst., 47, 11226b (1953).

36. Hayashi, R., Hudgins, R.R. and Graydon, W.F., Can. J. Chem. Eng., 41, 220 (1963).

37. Hosaka, Y., J. Chem. Soc. Japan, Ind. Chem. Sect., 57, 197 (1954); Chem. Abst., 49, 11578i (1955).

38. Hurd, C.D. and Glass, H.G., J. Am. Chem. Soc., 61, 3490 (1939).

39. Ioffe, I.I., Ezhkova, Z.I. and Lyubarskii, A.G., Russ. J. Phys. Chem., 35, 1160 (1961).

40. Ioffe, I.I. and Lyubarskii, L.G., Kinetikai Kataliz, 3, 261-70 (1962); Chem. Abst., 58, 55g (1963).

41. Japanese Patent 14,213, Sept. 28, 1960; Chem. Abst., 55, 15356c (1961).

42. Kalnins, P., Hillers, S. and Tarvid, M., Latvijas, P.S.R., Zinatnu Akad., Vestis, 443 (1951); Chem. Abst., 48, 9994g (1954).

43. Kerr, R.O., Decker, W.R. and Dorsett, C.M., U.S. Patent 3,074,969, Jan. 22, 1963; Chem. Abst., 58, 11223c (1963).

44. Kiprianov, G.I. and Shostak, F.T., J. Appl. Chem. (U.S.S.R.), 11, 471 (1938); Chem. Abst., 32, 5788 (1938).

45. Krantz, K.W. (to E.I. du Pont de Nemours & Co.), U.S. Patent 2,605,238, July 29, 1952; Chem. Abst., 47, 4013e (1953).

46. Marek, L.F. and Hahn, D.A., "Catalytic Oxidation of Organic Compounds in the Vapour Phase", pp.365-403, The Chemical Catalog Co., Inc., New York (1932).

47. Mars, P. and van Krvelen, D.W., Chem. Eng. Sci., 3, 41 (1954), Special Supplement.

48. Meszaros, L. and Foldeak, S., Szegedienesis Acta Phys., et Chem. (N.S.) 4, 144 (1958); Chem. Abst., 53, 15040d (1959).

49. Naboru Nagameguri and Mototaro Matsumoto, Japanese Patent 10,665; Chem. Abst., 52, 1557 (1958).

50. Nair, C.S.B., Bhatnagar, J.N. and Basu, A.N., J. Sci. Ind. Research (India), 13B, 220 (1954).

51. Nielson, E.R. (to the Quaker Oats Co.), U.S. Patent 2,421,428 June 3, 1947; Chem. Abst., 41, 5551d (1947).

52. Norrish, R.G.W. and Taylor, G.W., Proc. Roy. Soc. (London), 234A, 160-77 (1956).

53. Novella, E.C., David, R.L. and Sanchez Lazano, V., Anales real soc. espan. fcs. of quim (Madrid), 52B, 63 (1956); Chem. Abst., 50, 13860g (1956).

54. Pigulevsku, V.V. and Yarzhemskaya, E.Y., J. Gen. Chem. (U.S.S.R.), 5, 1620 (1935); Chem. Abst., 30, 1978 (1936).

55. Plastics, 26, No. 283, 7 (1961).

56. Products Intermedios, S.L.E., Spanish Patent 193,998, July 31, 1951; Chem. Abst., 46, 19195f (1952).

57. Reid, J.C. (to Atlantic Refining Co.), U.S. Patent 2,773,838, Dec. 11, 1956; Chem. Abst., 51, 7408 (1957).

58. Research & Industry, 4, 3; 123; 149 (1959).

59. Sherwood, P.W., Petroleum Processing, 11, 82 (1956).

60. Skinner, W.A. and Tieszen, D., Ind. Eng. Chem., 53, 557 (1961).

61. Solomin, A.V., Suvorov, B.V. and Rafikov, S.R., Zhur. Obshchei Khim., 28, 133 (1958); Chem. Abst., 52, 12782h (1958).

62. Suvorov, B.V., Rafikov, S.R., et al., Dokalady Akad. Nank S.S.S.R., 88, 79 (1953); Chem. Abst., 48, 1977g (1954).

63. Takikawa, S., J. Soc. Chem. Ind. (Japan), 48, 31-9 (1945); Chem. Abst., 42, 6324 (1948).

64. Thampy, R.T. and Suri, I.K., Indian Patent 58756, June 4, 1958.

65. Trehan, B.S. and Thampy, R.T., Indian Patent 74,450, Nov. 3, 1962.

66. Trehan, B.S., Suri, I.K. and Thampy, R.T., J. Sci. Ind. Res., 18B, 147-51 (1959).

67. Trehan, B.S., Thampy, R.T. and Kuloor, N.R., Indian Patent 69164.

68. Trehan, B.S., Suri, I.K. and Thampy, R.T., Paintindia, 7, (1), 47-9 (1957).

69. U.S. Patent 2,777,860, Jan. 15, 1957; Chem. Abst., 51, 8131d (1957).

70. U.S. Patent 3,074,969, Jan. 22, 1963; Chem. Abst., 58, 11223c (1963).

71. U.S. Patent 2,967,185, Jan. 3, 1961; Chem. Abst., 55, 9727b (1961).

72. U.S. Patent 2,674,582; Chem. Abst., 48, 8258 (1954).

73. Ushakova, V.P., Korneichuk, G.P. and Roiter, V.A., Ukrain Khim. Zhur, 23, 310 (1957); Chem. Abst., 52, 4757hi (1958).

74. Vande Velde, A.J.J., Natuurw. Tijdschr., 20, 124 (1938); Chem. Abst., 32, 7900 (1938).

75. Weiss, J.M. U.S. Patent 2,209,908, 1941; Chem. Abst., 35, 135 (1941).

76. Weiss, J.M. and Downs, C.R., J. Am. Chem. Soc., 44, 1118 (1922).

77. Weiss, J.M. and Downs, C.R., Ind. Eng. Chem., 12, 228 (1920).

78. Weiss, J.M., Downs, C.R. and Burns, R.M., Ind. Eng. Chem., 15, 965-67 (1923).

79. Weiss, J.M., U.S. Patent 2,154,079, Apr. 11, 1939; Chem. Abst., 33, 5411 (1939).

80. Weiss, J.M. and Downs, C.R., J. Am. Chem. Soc., 45, 1003, 2341 (1923).

81. Winslow, N.M. and Heise, G.W. (to National Carbon Co.), U.S. Patent 2,427,433, Sept. 16, 19470 Chem. Abst., 42, 461 (1948).

82. Yabuta, T. and Simose, R., Inst. Phys. Chem. Res. (Tokyo), 8, 197-205 (1929); Chem. Abst., 23, 3441 (1929).

83. Zalkind, Y.S. and Zolotarev, S.J., J. Appl. Chem. (U.S.S.R.), 6, 781-4 (1933); Chem. Abst., 28, 4039 (1934); Chem. Abst., 30, 1978 (1936).

CHAPTER-2

EXPERIMENTAL

Chapter 2

EXPERIMENTAL

2.1 EXPERIMENTAL SET-UP

2.1.1 General

A diagrammatic sketch of the reactor assembly is shown in Figure 2.1. Metered primary air was fed through benzene vaporizer (A) where it was saturated with benzene, and met a stream of metered secondary air in mixing bulb (F). The mixed stream was then passed through preheater (B), which prevented the condensation of organic vapour to reactor (E). The preheater was heated by a fluidized bed of bauxite. The product stream was passed through a train of condensers cooled by ice-salt mixture, and finally through caustic bulbs where carbon dioxide was absorbed.

2.1.2 Vaporizer

As shown in Figure 2.2 the vaporizer consisted essentially of a narrow graduated tube (300 mm. long x 6 mm. diameter) with a stop cock at one end and a bulb at the other. A bead at the neck of the bulb prevented liquid benzene being carried away.

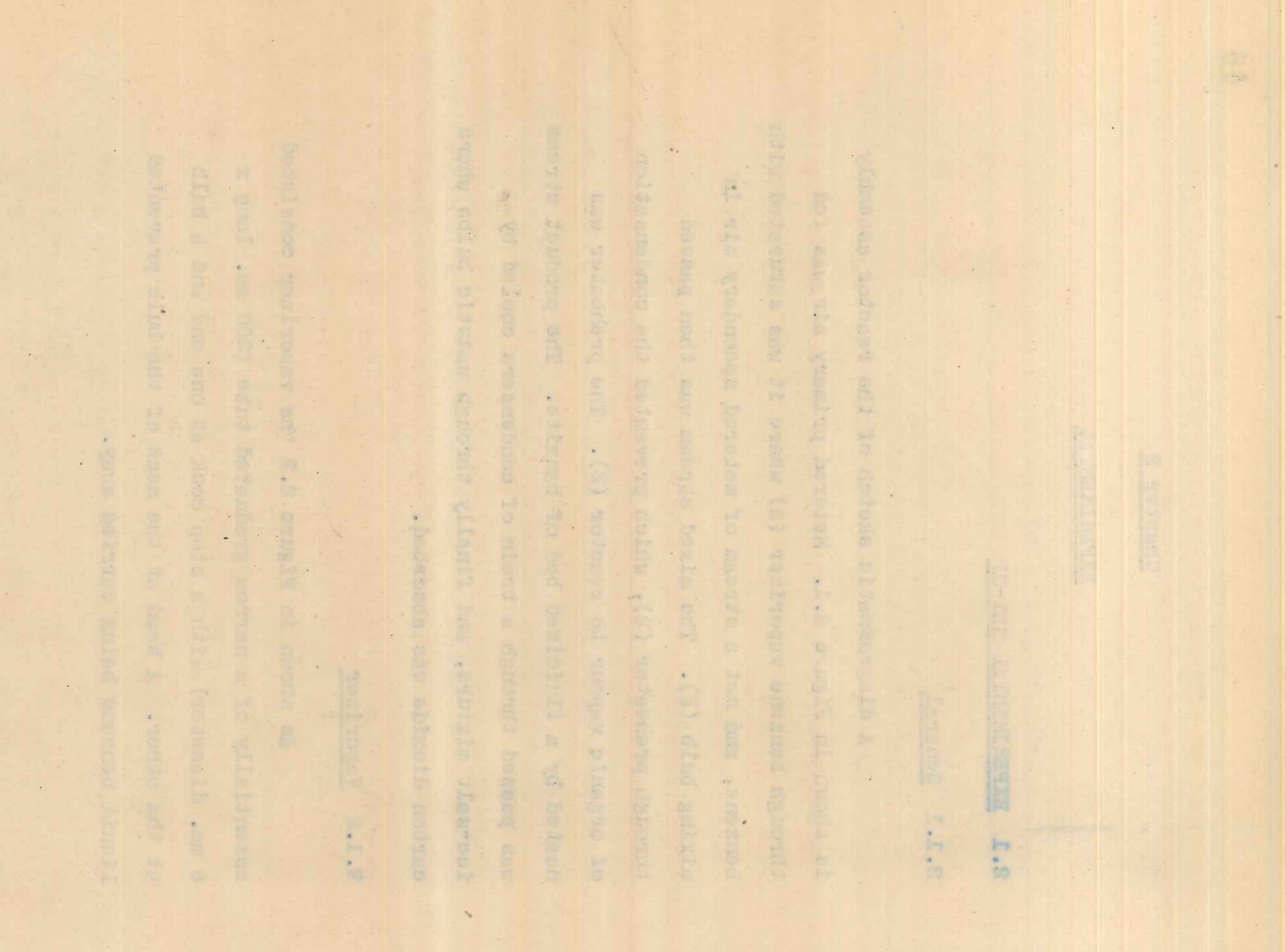

FIG. 2·1. EXPERIMENTAL SET-UP

2.1.3 Reactor

In the present study an integral type of reactor was used to get the kinetic data. Although a few studies have been carried out using a fluidized bed reactor for obtaining the kinetic data (in view of the high exothermicity of the reaction) (1), it must be emphasized that the use of a fluidized bed reactor is not warranted in any kinetic investigation, except where with appropriate stirring arrangements and baffles the fluidized bed could be made to approach a fully mixed reactor. In the reactor chosen for the present study, the diameter was small enough (25 mm.) to ensure plug flow conditions. A top-to-bottom feed was preferred to a bottom-to-top feed, since at high feed rates the top layers of the catalyst would tend to fluidize in the latter case. The reactor consisted of a 25 mm. diameter tube with a sintered disc at the bottom. The catalyst used was heated by a fluidized bed of bauxite. The advantages of such an arrangement are three-fold:

(a) Initially when the reactor bed is at a temperature lower than the desired one, the fluidized bed acts as a heating medium.

(b) During the reaction, when the temperature in the bed shoots up due to the exothermicity of the reaction, it serves as a coolant.

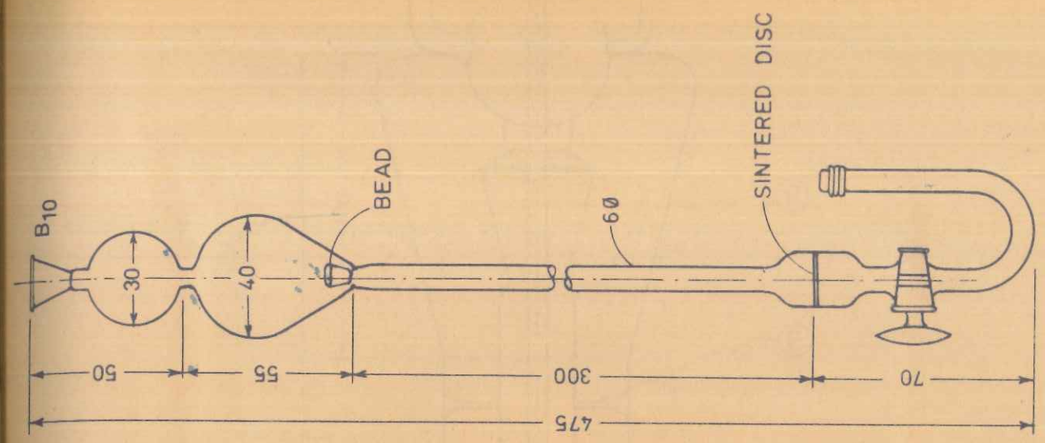

FIG. 2.2 VAPORIZER DETAILS

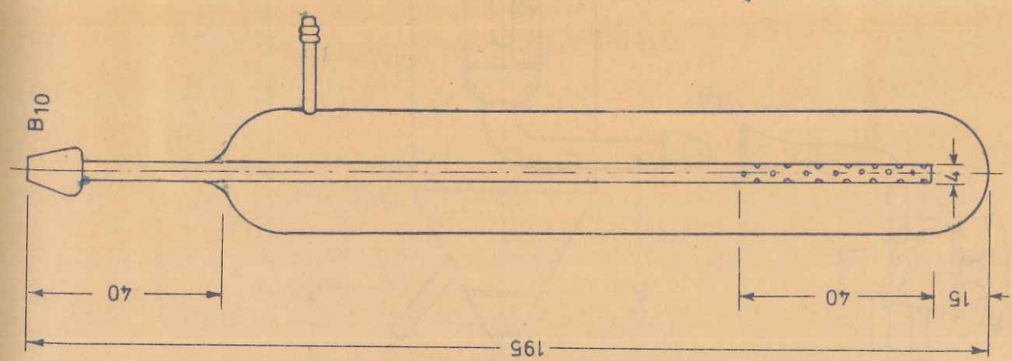

FIG. 2.4. CONDENSER DETAILS

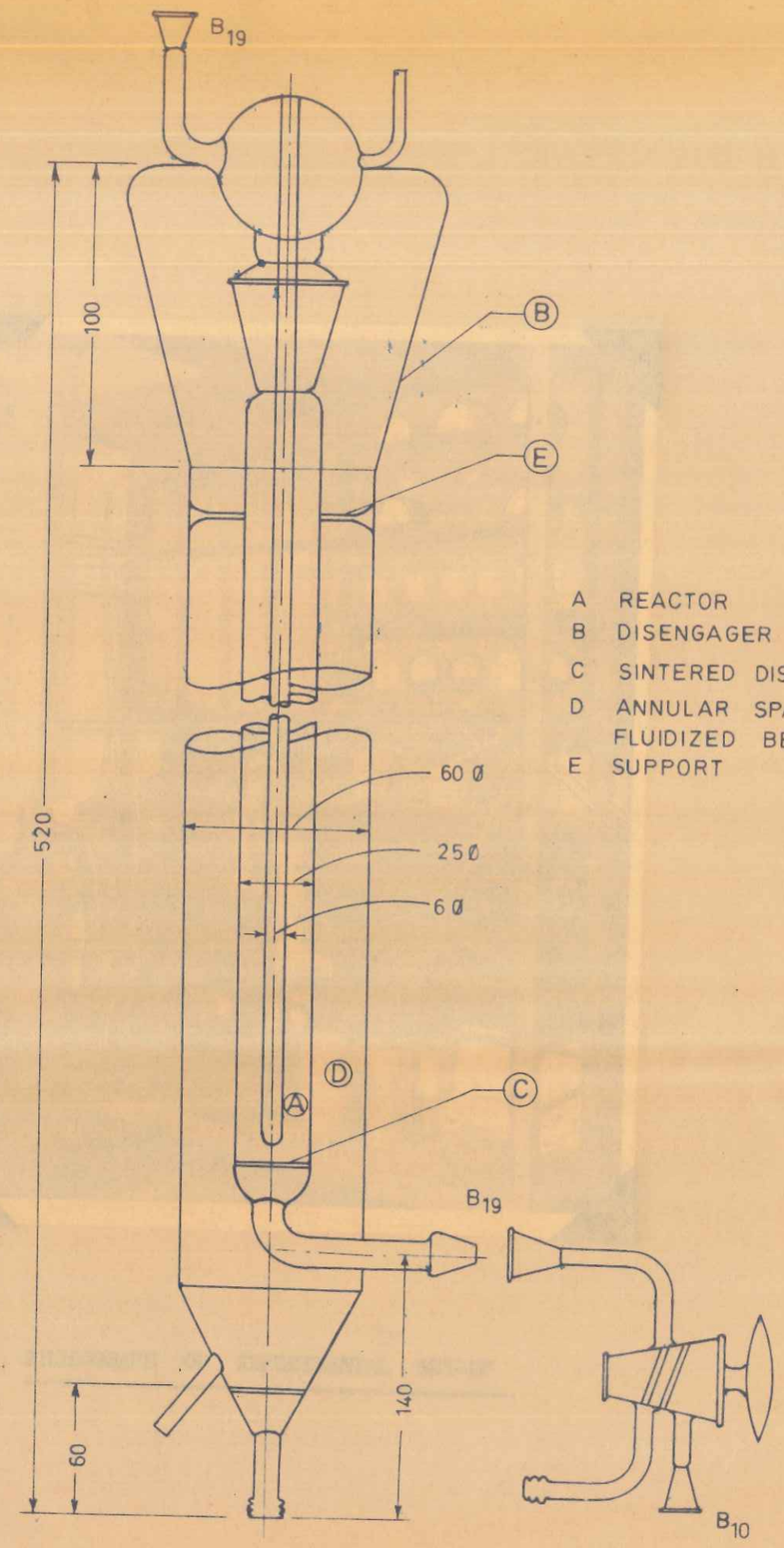

A REACTOR
B DISENGAGER
C SINTERED DISC
D ANNULAR SPACE FOR FLUIDIZED BED
E SUPPORT

FIG. 2·3. REACTOR DETAILS

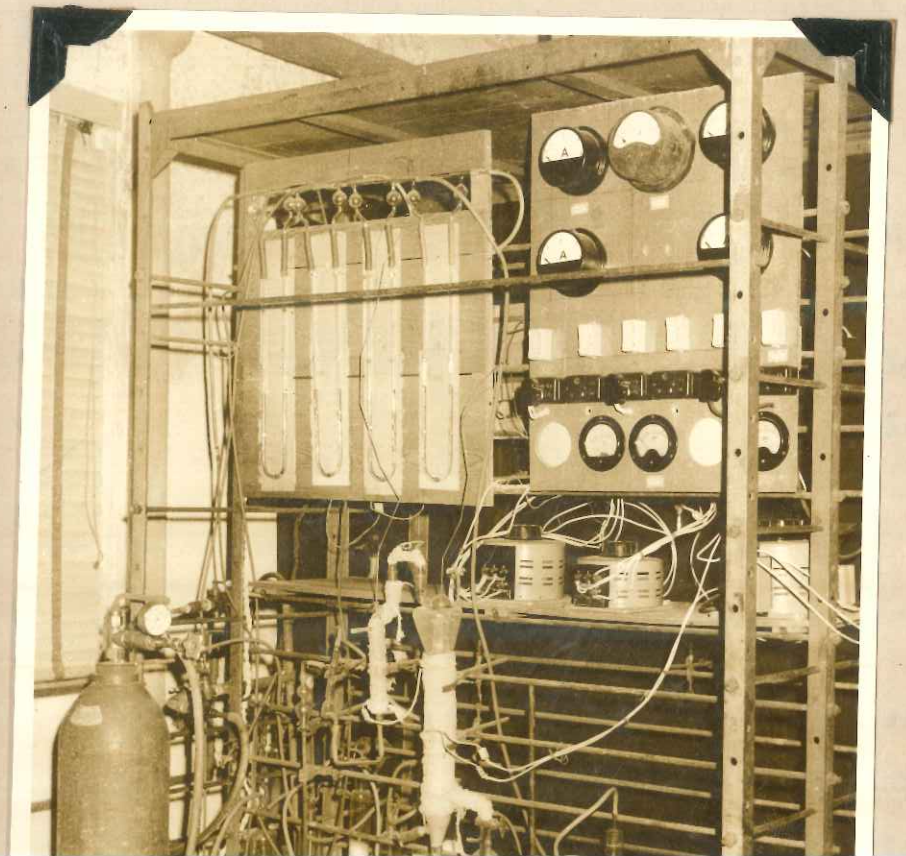

(c) It helps to maintain near isothermal conditions in the bed by quick dissipation of heat in the catalyst bed.

The other details of the reactor are shown in Figure 2.3.

2.1.4 Condenser

The details of the condenser are indicated in Figure 2.4. This consisted of a narrow 4 mm. tube connection, partly sintered at the lower portion and having a jacketed tube (25 mm. diameter) with an outlet.

2.2 CATALYST

2.2.1 General

A comprehensive review has been presented by Egloff (3) of the catalysts used for the oxidation of benzene and also of the various methods of catalyst preparation (cf Section 3, Chapter 1). In general any catalyst required for a reaction can be prepared by the coprecipitation or coating technique. The coprecipitation technique is generally followed for hydrogenation catalysts, as in the case of reduction of nitrobenzene to aniline, for which the required copper catalyst is prepared by precipitating the copper hydroxide in the presence of the carrier.

The coating technique consists in evaporating

the soluble salt solution of the required metal in the presence of the carrier, such that a uniform coating of the metallic salt is formed over the carrier. Generally for oxidation catalysts the coating technique is followed.

For the vapour phase oxidation of benzene, vanadium-molybdenum mixed oxide catalysts are commonly used. These are generally prepared by the coating technique.

For benzene oxidation the metallic salts generally recommended are ammonium meta vanadate and ammonium molybdate. Ammonium molybdate is freely soluble in water, where as the meta vanadate is sparingly soluble. Hence ammonium meta vanadate is dissolved in an acid medium. The acid medium may be a mineral acid like hydrochloric acid (12) or an organic acid like oxalic acid (13). The advantagesof oxalic acid are said to be three-fold: (1) the solubility of ammonium meta vanadate in water is greatly increased, thus eliminating the necessity for the evaporation of large quantities of water; (2) the activity of the catalyst is increased; and (3) the catalyst is said to dry to a "glass-like, greenish, amorphous mass" firmly attached to the catalyst support. Another advantage of oxalic acid over hydrochloric acid is that, unlike the latter, it does not evolve acidic fumes during catalyst preparation and activation. Hence

the catalysts studied have generally been prepared in oxalic acid medium. (Hydrochloric acid medium was used in certain cases to see whether it made any difference in product formation, but no marked effect was observed.)

A typical method of catalyst preparation containing 14% total oxidescontent in the ratio of V_2O_5: MoO_3 = 7.2:6.8 (approx 1:1) over silica gel is given below.

2.2.2 Catalyst preparation

9.255 parts of ammonium meta vanadate (NH_4VO_3; m.wt. 117) and 8.343 parts of ammonium molybdate ($(NH_4)_6 Mo_7O_{24}.4H_2O$; m.wt. 1235.95) were dissolved in 250 parts of hot 10% oxalic acid solution (10 gm. of oxalic acid in 100 ml. distilled water). To this solution 100 parts of silica gel (size -5 +12 B.S. standard) were added. The whole was evaporated to dryness with stirring over a water bath. This mass was then heated at 120-150°C. in a furnace for an hour, and the clusters formed in the mass were broken up and activated in a muffle at 400°C. for 8 hours. This was sieved to the required size.

The catalyst was then charged into the reactor and activated with air at 400°C. for 1½ hours, and for one hour more in the presence of air containing about 1% benzene vapour.

Several catalysts were prepared in accordance with the method outlined above, details of which are given in Table - 2.1. The compositions of these catalysts have been chosen to provide a near optimum value based on rate studies discussed in Section 3.7, Chapter 3 . As pointed out in Chapter 3 surface area and pore volume have been determined for two of the catalysts which have been found to be satisfactory (Table - 3.6). The BET method was used for surface area determination and the pore volume was determined by the usual displacement technique.

2.3 ANALYTICAL TECHNIQUES

The products of the oxidation of benzene consist of both solid and gaseous components. They include maleic anhydride, oxides of carbon, water vapour and a little of benzoquinone. Other products mentioned, in particular by Weiss and Downs (14), include phenol, diphenyl and formaldehyde. However, none of these latter products was detected in the product obtained. Diphenyl is formed generally only at temperatures as high as 650°C. (11). The absence of phenol was assumed because of the $FeCl_3$ colour test being negative.

2.3.1 Estimation of maleic anhydride

The methods stated in the literature for the estimation of maleic anhydride include polarographic

Table - 2.1

Catalysts prepared

Serial number	Catalyst number	Total oxides content, %	Ratio of V_2O_5 to MoO_3	Particle size B.S.S. mesh
1	1	14	1:0	- 5 +12
2	2	14	1:1	- 5 +12
3	3	14	1:2	- 5 +12
4	3A	14	1:2	-12 +22
5	3B	14	1:2	-22 +36
6	3C	14	1:2	-36 +60
7	4	25	1:1	- 5 +12
8	5	35	1:1	- 5 +12

estimation (4,5), potentiometric titration (9) and gravimetric estimation (6), apart from the usual alkali titration (2).

In the present work maleic anhydride was estimated by titration against standard alkali using phenolphthalein as indicator.

2.3.2 Estimation of benzoquinone

Benzoquinone in the presence of maleic anhydride (acid) can be estimated by potentiometric titration (10). A method analogous to this was followed in the present work. The solution containing benzoquinone was reacted with I^- in an acid medium. The liberated I_2 was then titrated against $S_2O_3^{--}$ by an indirect titration.

2.3.3 Estimation of carbon dioxide

Carbon dioxide was estimated by the conventional method of absorbing it in caustic bulbs and finding the difference in weight.

2.3.4 Estimation of carbon monoxide

The estimation of carbon monoxide generally consists in oxidizing it to carbon dioxide and estimating it as given above.

Hopcalite (7,8) is said to be an ideal catalyst

capable of oxidizing carbon monoxide to carbon dioxide even at room temperature. Due to the non-availability of hopcalite catalyst, copper oxide at elevated temperature was used. However the results were not at all consistent. Hence the tail gas containing carbon monoxide was analysed in the conventional Orsat apparatus by absorbing it in ammonical cuprous chloride solution.

2.3.5 Estimation of water

No chemical methods were adopted for the estimation of water, and the water formed was calculated from material balance.

2.4 PROCEDURE

The required quantity of the catalyst was charged into the reactor. Then the preheater and the reactor heaters were switched on, and the secondary air was also started. When the required temperature was attained, the primary air was turned on through the vaporizer. As the level of the manometer controlling the primary air was kept constant, the air rate passing through the vaporizer was constant; and hence the rate of benzene fed also remained steady.

Till steady-state conditions were reached, the product vapours from the reactor were vented out through

a bypass. When steady-state was reached, the primary air was stopped for a while, the level of benzene in the vaporizer noted down, the primary air restarted, and the three-way stop-cock turned on to the train of condensers previously adjusted to the required conditions. The duration of a run under steady conditions varied from 15 to 30 minutes, depending on the quantity and the ratio of air and benzene used. At the end of the run, the primary air was switched off first, then the three-way cock turned to the bypass. The level of benzene in the vaporizer was noted down, the difference in levels giving the quantity of benzene fed, and the manometer reading the quantity of air fed.

Whenever the bed height was changed, additional catalyst quantities were always taken from the same lot.

References

1. Badrinarayana, M.C., Ph.D. Thesis on oxidation of benzene submitted to the Indian Institute of Science, Bangalore.

2. Bhattacharya, S.K. and Venkataraman, N., J. Appl. Chem. (London), 8, 728-37 (1958).

3. Egloff, G., Berkman, S. and Morrell, J.C., "Catalysis - Inorganic and Organic," pp.280,800, Reinhold Publishing Corp., New York (1940).

4. Elcing, P.J., et al., J. Am. Chem. Soc., 71, 3616 (1949).

5. Elcing, P.J., Martin, A.J. and Rosenthal, I., Anal. Chem., 25, 1082 (1953).

6. Faith, W.L. and Shaible, A.M., J. Am. Chem. Soc., 60, 52 (1938).

7. Lamb, A.B., Bray, W.C. and Fraser, J.C.W., Ind. Eng. Chem., 12, 213 (1920).

8. Lamb, A.B., J. Am. Chem. Soc., 44, 738 (1922).

9. "Maleic Anhydride," Bulletin issued by Monsanto Chemicals (India).

10. Malyskev, A.I. and Ioffe, I.I., Zhur. Anal. Khim, 13, 374 (1958); Chem. Abst., 53, 133a (1959).

11. U.S. Patent 1,322,983 (1919); (Marek, L.F. and Hahn, D.A., "The Catalytic Oxidation of Organic Compounds in the Vapour Phase," The Chemical Catalog Co., NY (1932) pp.367

12. U.S. Patent 2,967,185, Jan. 3, 1961, Chem. Abst., 55, 9727 (1961).

13. U.S.S.R. Patent 131,353, Sept. 10, 1960, Chem. Abst., 55, 6733 (1961).

14. Weiss, J.M. and Downs, C.R., Ind. Eng. Chem., 12, 228 (1920); J. Soc. Chem. Ind., 45T, 188 (1926).

CHAPTER-3

INITIAL TREATMENT OF DATA

Chapter 3

INITIAL TREATMENT OF DATA

3.1 ORGANISATION OF EXPERIMENTS

Any kinetic study entails the determination of conversions under different conditions. The principal variables studied and the ranges of these variables are given below:

Partial pressure of benzene	: 0.61×10^{-2} to 1.83×10^{-2} atm.
Temperature	: 310-400°C.
Molar ratio of benzene to air	: 1:50 to 1:140
Contact time (W/F)	: 60-400 gm.hr./gm-mole
Catalyst size	: -5 +12 to -36 +60 B.S.S. mesh

(The contact time is here defined as the ratio, W/F, where W is the weight of the catalyst in gm. and F is the hourly molar feed rate of benzene.)

W/F is normally varied either by changing the weight of the catalyst (W) or by changing the feed rate (F), although the latter is more common. Nevertheless in this case, as very high molar ratios of benzene to air were used (and a small quantity of catalyst was taken to ensure isothermal conditions), from the practical point

of view the feed rate could not be varied over a wide range. Hence the entire range of W/F values was covered by changing both W and F in an appropriate manner. The rate of benzene feed varied from 4 to 7.5 gm./hr. and the weight of the catalyst from 5 to 25 gm. Moreover, the catalyst for the kinetic runs was taken from a single stock prepared according to the method outlined in Chapter 2, thus avoiding discrepancies in the results due to variations in catalyst activity. Although there was no significant deactivation up to 60 hours, the catalyst in the reactor never exceeded 20 hours of usage in order to ensure the total absence of catalyst deactivation.

3.2 EXPERIMENTAL DATA

In order to establish the complete kinetics of this reaction and to propose plausible reaction models, over 300 experimental runs were carried out by a systematic variation of the significant variables listed earlier. The results of all these runs have been expressed in terms of the partial pressures of the products of reaction, viz, unreacted benzene and oxygen, maleic anhydride, carbon dioxide and water. Several tests showed that carbon monoxide and benzoquinone were formed in negligible quantities. Accordingly these have not been included in the partial pressure calculations. The

results of the experimental runs are presented in Appendix - A, Tables - A.1 to A.13. These runs cover the experimental programme listed in Table - 3.1.

Each of the Tables - A.1 to A.13 includes the results of the variation of residence time (W/F) and the molar ratio of benzene to air, both these factors together giving a considerable spread in the partial pressure values at any given temperature. These partial pressure values are necessary for formulating rate equations. At the same time the values of reaction rates also must be available, for which plots of conversion vs W/F are required. Thus Appendix - A, Tables - A.14 to A.29 give the derived values of x_M and x_C as functions of W/F for different ratios and temperatures.

Since the rates are normally derived by graphical differentiation or by differentiation of the analytical equations set up for the x - W/F curves, such curves were prepared for all ratios and temperatures listed in Table - 3.1. Representative plots at a few experimental conditions are shown in Figures B.1 to B.8 in Appendix - B. The rates were determined by graphical differentiation of these plots.

3.3 PRELIMINARY EVALUATION OF EXTERNAL MASS TRANSFER

In all kinetic studies it should be ensured

Table - 3.1

Summary of experimental data collected (with references to tables in Appendix - A)

Serial number	Catalyst number	Total oxides content %	Ratio of V_2O_5 to MoO_3	Particle size B.S.S. mesh	Temperatures studied °C.	Table reference (of Appendix - A)
1	1	14	1:0	- 5 +12	400	A.1, A.14.
2	2	14	1:1	- 5 +12	310, 330, 350, 375, 400	A.2, A.3, A.4, A.5, A.6, A.15, A.16, A.17, A.18, A.19.
3	3	14	1:2	- 5 +12	310, 330, 350, 375, 400	A.7, A.8, A.9, A.10, A.11, A.20, A.21, A.22, A.23, A.24.
4	3A	14	1:2	-12 +22	350	A.25.
5	3B	14	1:2	-22 +36	350	A.26.
6	3C	14	1:2	-36 +60	350	A.27.
7	4	25	1:1	- 5 +12	400	A.12, A.28.
8	5	35	1:1	- 5 +12	400	A.13, A.29.

that external film diffusion and pore diffusion are eliminated as far as possible. The gas film resistance can be overcome by operating at a high velocity and the resistance to pore diffusion by a proper choice of the catalyst size.

Hougen et al. (7) have developed charts by which the partial pressure difference between the flowing fluid and the exterior surface of catalyst particles in a packed bed can be evaluated as a function of a modified Reynolds number (Re) of the stream, a rate number (R") and the Schmidt number (Sc). Here,

$$Re = \frac{G}{a_v \mu}$$

$$R'' = \frac{r}{a_m G_m}$$

$$Sc = \frac{\mu}{\rho D}$$

In the present study due to practical difficulties, the velocity of air was confined to the range, G = 50 to 145 lb./hr.ft.^{2} (corresponding to Reynolds number 2 to 5). For the experimental condition the rate number was estimated to be about 1.0×10^{-4} and the Schmidt number 0.7. Using these values in the above mentioned chart the partial pressure gradient ($\Delta p/p$) worked out to be about 0.001. This indicates that

the mass transfer coefficient is quite high and that external diffusion offers negligible resistance.

This should however be regarded only as indicative of the absence of mass transfer, since these charts may not be very reliable at low Reynolds numbers, and also diffusional falsification of reaction rates can occur under several conditions. Thus it was assumed, to start with, that mass transfer effects were absent and the data analysed subsequently (Chapter 5) to determine the exact controlling regimes in benzene oxidation.

It is also necessary to obtain rate data in the absence of pore diffusion. In the present study this was included in the mechanistic evaluation of the reaction and is discussed in Chapter 5.

3.4 DETERMINATION OF FIRST-ORDER CONSTANTS

3.4.1 General

Prior to the postulation of plausible kinetic models, it is essential to estimate the independent rates of the three reactions taking place. This may be done by developing empirical rate equations (which should be first-order equations according to the literature, in this case), determining the reaction velocity constants for all the steps from the corresponding integrated equations and then calculating the rates of individual steps at different residence times.

3.4.2 Determination of rate constants

For the kinetic analysis of the reaction, the

following scheme has been chosen (Chapter 1, page 38)

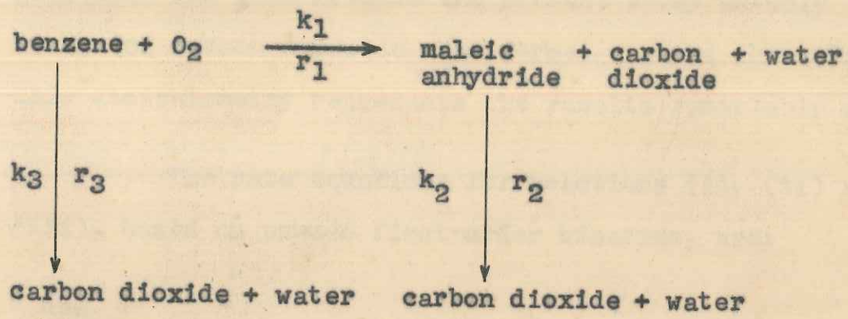

The reaction scheme presented may be stoichiometrically represented as follows:

$$C_6H_6 + 9/2O_2 \xrightarrow{k_1} C_4H_2O_3 + 2CO_2 + 2H_2O \quad \text{(i)}$$

$$C_4H_2O_3 + 3O_2 \xrightarrow{k_2} 4CO_2 + H_2O \quad \text{(ii)}$$

$$C_6H_6 + 15/2O_2 \xrightarrow{k_3} 6CO_2 + 3H_2O \quad \text{(iii)}$$

Dmuchovsky et al. (3) have assumed a slightly different stoichiometry since their data were better represented (for their catalyst) by that stoichiometry, which is,

$$C_6H_6 + 4O_2 \xrightarrow{k_1} C_4H_2O_3 + CO + CO_2 + 2H_2O \quad \text{(iv)}$$

$$C_4H_2O_3 + 5/2O_2 \xrightarrow{k_2} 3CO_2 + CO + H_2O \quad \text{(v)}$$

$$C_6H_6 + 13/2O_2 \xrightarrow{k_3} 4CO_2 + 2CO + 3H_2O \quad \text{(vi)}$$

But the stoichiometry represented by reactions (i), (ii) and (iii) has been used in the present study as only traces of carbon monoxide were formed, and as shown later this stoichiometry represents the results remarkably well.

The rate equations for reactions (i), (ii) and (iii), based on pseudo first-order kinetics, are:

$$-\frac{dp_B}{d(W/F)} = (k_1 + k_3)\, p_B \qquad .. \quad 3.1$$

$$\frac{dp_M}{d(W/F)} = k_1 p_B - k_2 p_M \qquad .. \quad 3.2$$

$$\frac{dp_C}{d(W/F)} = (2k_1 + 6k_3)\, p_B + 4k_2 p_M \qquad .. \quad 3.3$$

Equations (3.1), (3.2) and (3.3), on integration, give:

$$p_B = p_{Bo}\; e^{-(k_1 + k_3)\,(W/F)} \qquad .. \quad 3.4$$

$$p_M = \frac{k_1 p_{Bo}}{k_2 - (k_1 + k_3)} \left[e^{-(k_1 + k_3)\,(W/F)} - e^{-k_2 (W/F)} \right] .. \quad 3.5$$

$$p_C = \frac{p_{Bo}}{k_1 + k_3} \left[-2k_1 - 6k_3 - \frac{4k_1 k_2}{k_2 - (k_1 + k_3)} \right] \left[e^{-(k_1 + k_3)\,(W/F)} - 1 \right] + \frac{4k_1 p_{Bo}}{k_2 - (k_1 + k_3)} \left[e^{-k_2 (W/F)} - 1 \right] \qquad .. \quad 3.6$$

The value of $(k_1 + k_3)$, which represents the velocity constant for the total disappearance of benzene, can be determined from the slope of the line obtained by plotting $\log \frac{p_{Bo}}{p_B}$ vs. W/F, in accordance with Equation (3.4). Such plots were prepared for all the catalysts and at all the different temperatures studied using the raw experimental data given in Appendix - A, Tables - A.1 to A.13. These plots appear in Appendix - B, Figures B.9 to B.16. It can be seen that the first order law holds good for the overall depletion rate of benzene up to 75 percent of the residence time (W/F) covered. Similar conclusions have also been drawn by other investigators working with different catalysts.

From a knowledge of the values of $(k_1 + k_3)$ as outlined above, the individual values of k_1, k_2 and k_3 can be ascertained by one or more of the following methods.

(a) Equation (3.5) can be recast into a more convenient form by multiplying both sides of the equation by

$$1/p_{Bo}\left[\exp.(-(k_1 + k_3)(W/F)) - \exp.(-k_2(W/F))\right]$$

From the experimental molar ratios (p_m/p_B) at two different residence times, together with the experimentally determined constant $(k_1 + k_3)$, the value of k_2 can be found. k_1 and k_3 can then be evaluated from simple

algebraic procedures.

(b) $\frac{dp_M}{d(W/F)}$ can be evaluated for different values of W/F by finding the slopes of the curve of p_m vs. W/F, and then k_1 and k_2 can be calculated from Equation (3.2).

(c) Equation (3.2) can be rewritten for the initial condition, i.e. at W/F = 0, as

$$\left(\frac{dp_M}{d(W/F)}\right)_0 = k_1 p_{Bo} \qquad .. \quad 3.7$$

From the value of $\left(\frac{dp_M}{d(W/F)}\right)_o$ obtained from the plot mentioned in method (b), the value of k_1 can be directly determined.

It has been found that k_1, k_2 and k_3 calculated by the different methods listed above agree closely. These values of k_1, k_2 and k_3 for different catalysts are listed in Tables - 3.2* and 3.3 together with the activation energies. (Two other constants, k_{1S} and k_M, are also included in the table, and will be discussed in a subsequent section.)

3.5 TEMPERATURE DEPENDENCE OF FIRST ORDER RATE CONSTANTS

The effect of temperature on the rate constants has been studied in the range 310-400°C. In order to present the relationship in the form of the well known

* This table contains all the kinetic constants for the two catalysts finally chosen (Section 3.7, Chapter 3, Page 70).

TABLE - 3.2

RATE AND ADSORPTION CONSTANTS FOR THE THREE SIGNIFICANT REACTIONS INVOLVED IN BENZENE OXIDATION

	CATALYST–2					CATALYST–3				
Temperature °C.	k_1 $X10^3$	k_2 $X10^3$	k_3 $X10^3$	k_{1s} $X10^2$	K_M $X10^{-3}$	k_1 $X10^3$	k_2 $X10^3$	k_3 $X10^3$	k_{1s} $X10^2$	K_M $X10^{-3}$
310	0·403	0·846	0·132	3·80	2·21	0·368	0·776	0·126	3·94	3·400
330	0·675	1·430	0·225	6·21	1·10	0·696	1·447	0·229	6·66	1·100
350	1·141	2·468	0·396	16·00	0·75	1·358	2·806	0·453	14·45	0·700
375	1·292	2·593	0·409	—	—	1·455	2·982	0·477	—	—
400	1·361	2·716	0·444	—	—	1·513	3·113	0·519	—	—
E for temp. range 310–350 °C. kcal./gm-mole.	19·060	19·550	20·270	23·97	21·17	23·730	23·750	23·860	24·16	26·430
E for temp. range 350–400 °C. kcal./gm-mole.	2·920	1·600	1·910	—	—	1·800	1·730	2·270	—	—

Table - 3.3

Rate constants for different catalyst compositions at 400°C.

Catalyst number	$k_1 x 10^3$	$k_2 x 10^3$	$k_3 x 10^3$
1	1.35	3.15	0.58
2	1.36	2.71	0.44
3	1.51	3.11	0.52
4	2.14	4.76	1.20
5	2.15	4.97	1.32

Arrhenius equation, plots of log k vs. 1/T were prepared (Figures 3.1 and 3.2). In this case each plot gave two lines of different slopes. In the high temperature region (350-400°C.), the activation energy was of the order of 2 kcal./gm-mole, where as in the lower temperature region (310-350°C.) the activation energy was 20±2 kcal./gm-mole. Moreover, it may be seen from Table - 3.2 that the activation energies for all the three steps are equal, as reported by Hammar (4).

The significance of the two activation energies is discussed in Chapter 5.

3.6 ACCURACY OF ESTIMATED CONSTANTS

The accuracy of the estimated constant has been checked as follows:

(i) Using the rate constants in Tables - 3.2 and 3.3 the total benzene disappearance (Equation (3.4)) and the expected conversion to maleic anhydride (Equation (3.5)) have been calculated and found to be in accordance with the experimental results, as shown in Figures B.17 to B.23 of Appendix - B. The average deviation is about 8%. The experimental points in these figures were plotted from the conversion data given in Appendix - A, Tables - A.14 to A.27.

(ii) The time required for reaching the maximum

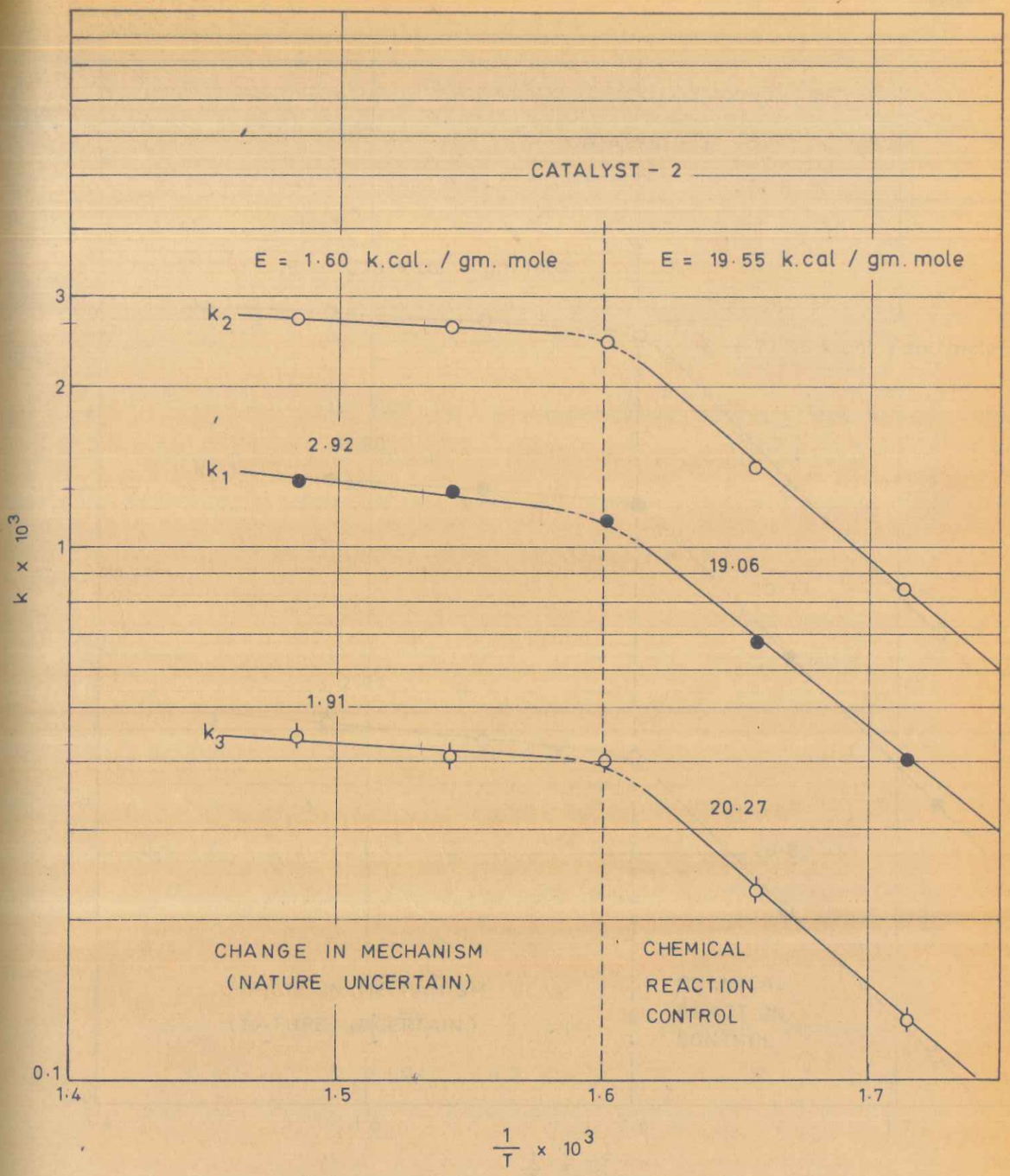

FIG. 3·1. IDENTIFICATION OF CONTROLLING REGIMES FROM ARRHENIUS PLOTS FOR CATALYST - 2

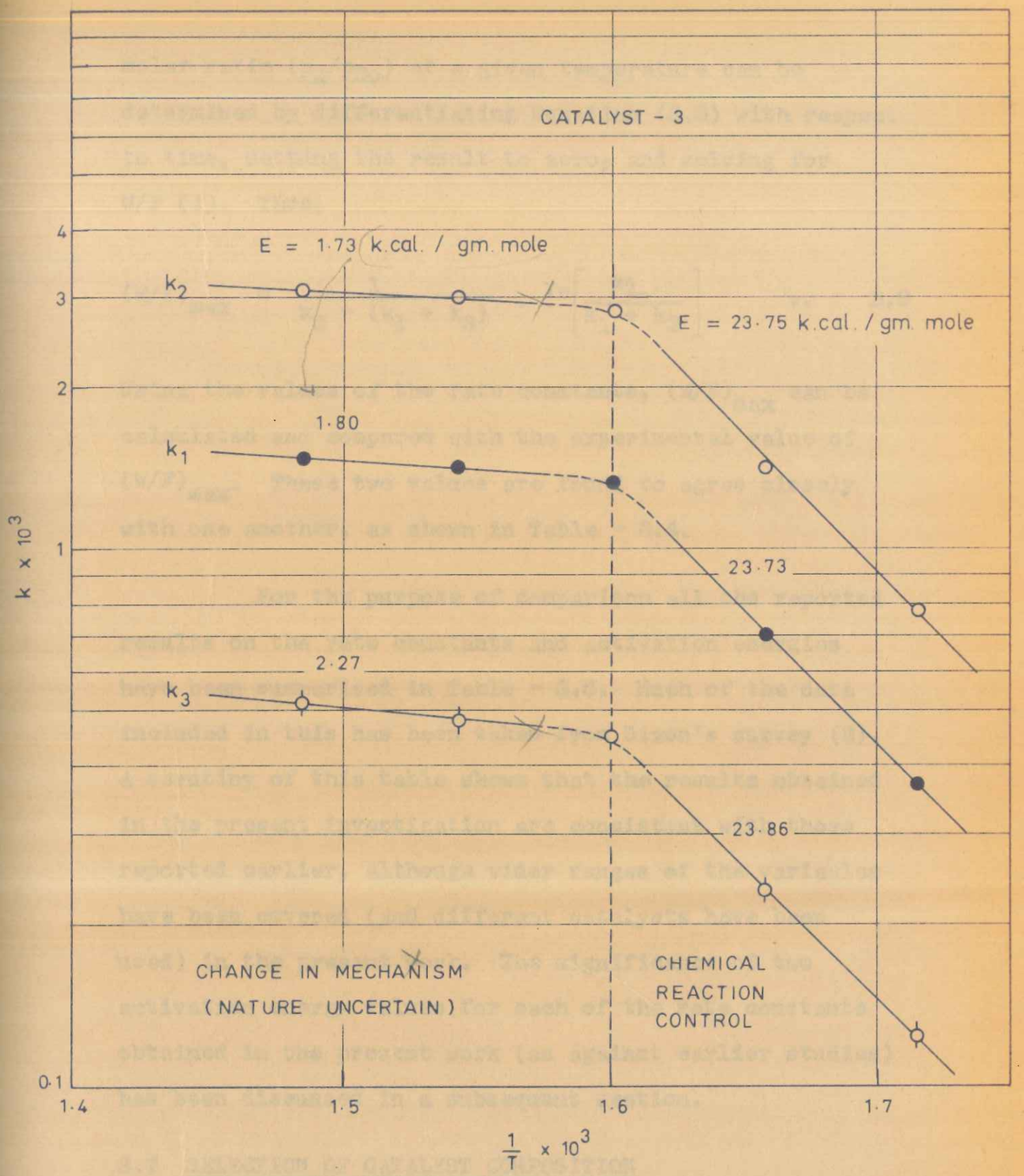

FIG. 3·2. IDENTIFICATION OF CONTROLLING REGIMES FROM ARRHENIUS PLOTS FOR CATALYST-3

molar ratio (p_M/p_{Bo}) at a given temperature can be determined by differentiating Equation (3.5) with respect to time, setting the result to zero, and solving for W/F (1). Thus,

$$(W/F)_{max} = \frac{1}{k_2 - (k_1 + k_3)} \ln\left[\frac{k_1}{k_1 + k_3}\right] \quad .. \quad 3.8$$

Using the values of the rate constants, $(W/F)_{max}$ can be calculated and compared with the experimental value of $(W/F)_{max}$. These two values are found to agree closely with one another, as shown in Table - 3.4.

For the purpose of comparison all the reported results on the rate constants and activation energies have been summarised in Table - 3.5. Much of the data included in this has been taken from Dixon's survey (2). A scrutiny of this table shows that the results obtained in the present investigation are consistent with those reported earlier, although wider ranges of the variables have been covered (and different catalysts have been used) in the present work. The significance of two activation energy values for each of the rate constants obtained in the present work (as against earlier studies) has been discussed in a subsequent section.

3.7 SELECTION OF CATALYST COMPOSITION

The optimum catalyst is one which yields a high

Table - 3.4

Test of rate constants by evaluation of $(W/F)_{max}$ from Equation (3.8)

Catalyst number	Temperature °C.	$(W/F)_{max}$ Exptl.	$(W/F)_{max}$ Calc.	Error, %
1	400	255	292	-14.5
2	310	-	-	-
2	330	-	-	-
2	350	313	320	- 2.2
2	375	300	309	- 3.0
2	400	305	312	- 2.3
3	310	-	-	-
3	330	-	-	-
3	350	260	290	-11.5
3	375	265	270	- 5.7
3	400	260	273	- 5.0
4	400	305	313	- 2.6
5	400	290	315	- 8.6

TABLE - 3·5 .

SUMMARY OF KINETIC DATA ON BENZENE OXIDATION

AUTHOR	HAMMAR	STEGER	MARS AND VAN KREVELEN	HOLSEN	DMUCHOVSKY et al.	PRESENT WORK
CATALYST	$V_2O_5 \cdot MoO_3$ on aluminium	$Ag_2O \cdot V_2O_5 \cdot MoO_3 \cdot Al_2O_3$ on SiC	$V_2O_5 \cdot K_2SO_4$ on SiO_2	V_2O_5 on Al_2O_3	$V_2O_5 \cdot MoO_3$ promoted with Ni Na-salts on carborundum	$V_2O_5 \cdot MoO_3$ on silica gel
Temperature range (°C.)	375 - 400	450 - 530	375	325 - 450	319 - 377	310 - 400
Range of partial pressures (mm. Hg.)						
a) Benzene	2·5 - 5·0	~ 10 - 20	< 6 > 6	7 - 14	~ 8·75	4·5 - 14
b) Oxygen	150	~ 170	< 200 > 300	150	~ 150	~ 150
Kinetic order						
a) with respect to benzene	~ 1	1	1 < 1	~ 1	1	1
b) with respect to oxygen	-	< 1	-	-	-	-
Contact time range (sec.)	-	-	-	-	up to 0·5	up to 0·4
Dependence of rate on mass transfer	Yes	No	-	-	-	Yes (in higher temp. range)
Activation energy (kcal./gm-mole)	28 ± 4	15	-	19-20	~ 30	22 ± 2 (in lower temp. range)
Ratio, $k_1/(k_1 + k_3)$	0·75 ± 0·03	0·7	-	0·7	-	~ 0·75
Ratio, k_2/k_1	0·2 - 0·5	0·1	-	2-10	-	2
Model proposed	-	-	-	-	-	Adsorption controlled

proportion (with reference to the total benzene converted) of the desired product and is relatively cheaper than other catalysts. Here the catalyst selection was made by comparing the rate constant values. Thus the catalyst composition which gives a high $k_1/(k_1 + k_3)$ value (indicating a high yield of maleic anhydride) and a low k_2/k_1 value (indicating low decomposition of maleic anhydride) may be considered suitable.

The catalyst parameters studied were the ratio of molybdenum oxide to vanadium oxide and the total concentration of these two oxides on silica gel. It was established from preliminary runs that pure molybdenum oxide gives negligible conversion to maleic anhydride, while pure vanadium oxide leads to a considerable wastage of benzene as oxides of carbon (i.e. low selectivity to maleic anhydride). Thus, with these two limiting values of catalyst composition being unsuitable, three different ratios of molybdenum and vanadium oxides were tried, and the total concentration of the two oxides was also varied. The rate constants, k_1, k_2 and k_3, were determined at 400°C. for each of the catalyst compositions selected, and the results are presented in Tables - 3.2 and 3.3.

Plots of $k_1/(k_1 + k_3)$ and k_2/k_1 as functions of the total oxides content at a fixed ratio of the oxides (vanadium oxide : molybdenum oxide = 1:1) are

shown in Figure 3.3. The experimental results on which this figure is based are given in Appendix - A, Tables - A.1 to A.13. From this plot it is clear that approximately 14% total oxides content is superior to the other compositions tried.

In a subsequent series of runs, the oxides content was fixed at 14% and the ratio of these oxides varied. The experimental data for this series is also given in Tables - A.1 to A.13 of Appendix - A. The variation of $k_1/(k_1 + k_3)$ and k_2/k_1 with total oxides content is shown graphically in Figure 3.4, from which it may be concluded that a ratio of (1:1) is perhaps the most suitable in the oxidation of benzene.

From the discussion presented above it appears that the following composition of the catalyst would be nearly optimum for benzene oxidation.

Catalyst number	- 2
Carrier	- silica gel
(V_2O_5 + MoO_3) content	- 14%
V_2O_5 : MoO_3	- 1:1

Catalyst - 3 in which the total concentration of the oxides is the same as in catalyst - 2 but the ratio of vanadium oxide to molybdenum oxide is 1:2

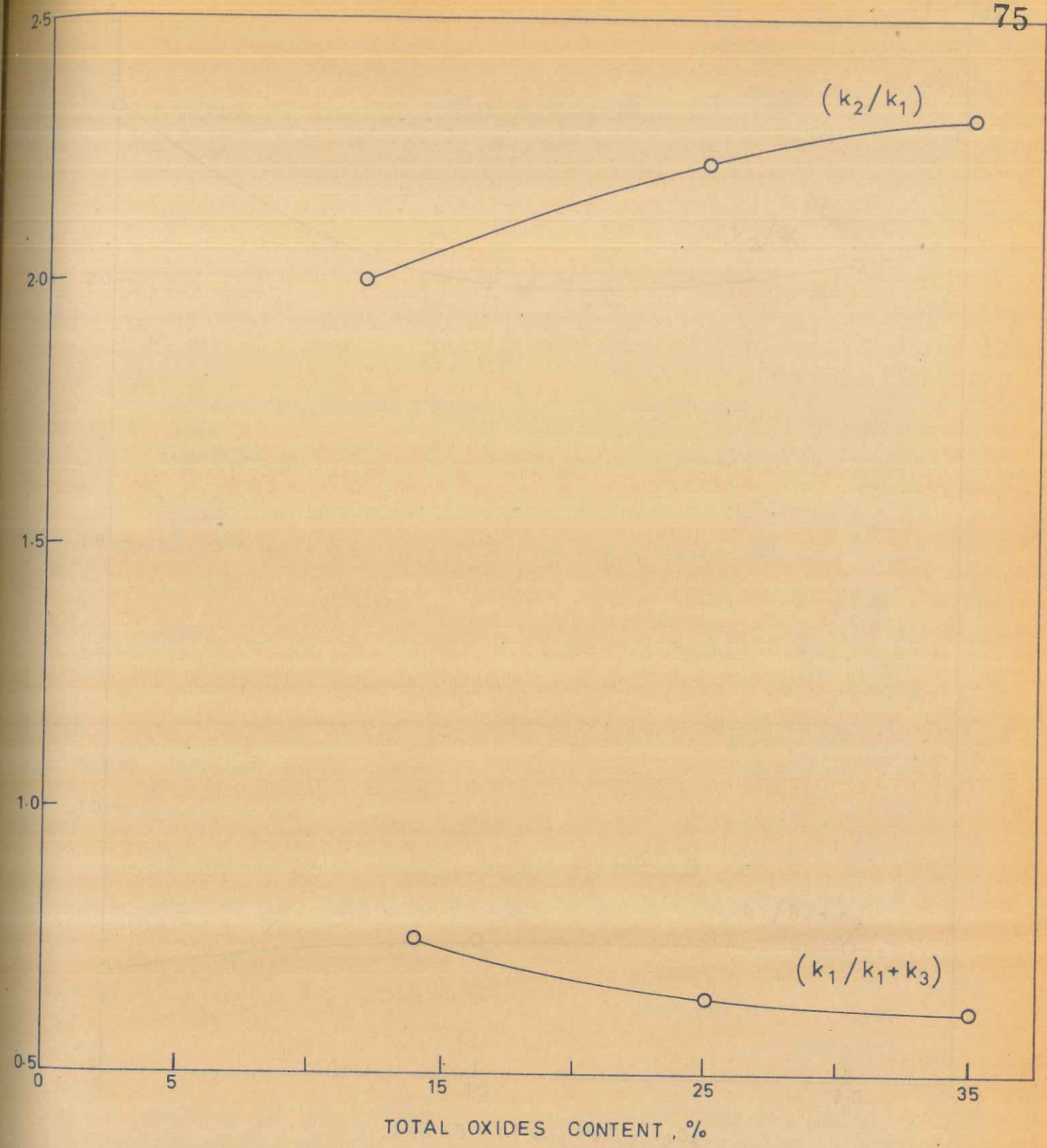

FIG. 3·3. EFFECT OF TOTAL OXIDES CONTENT ON SELECTIVITY

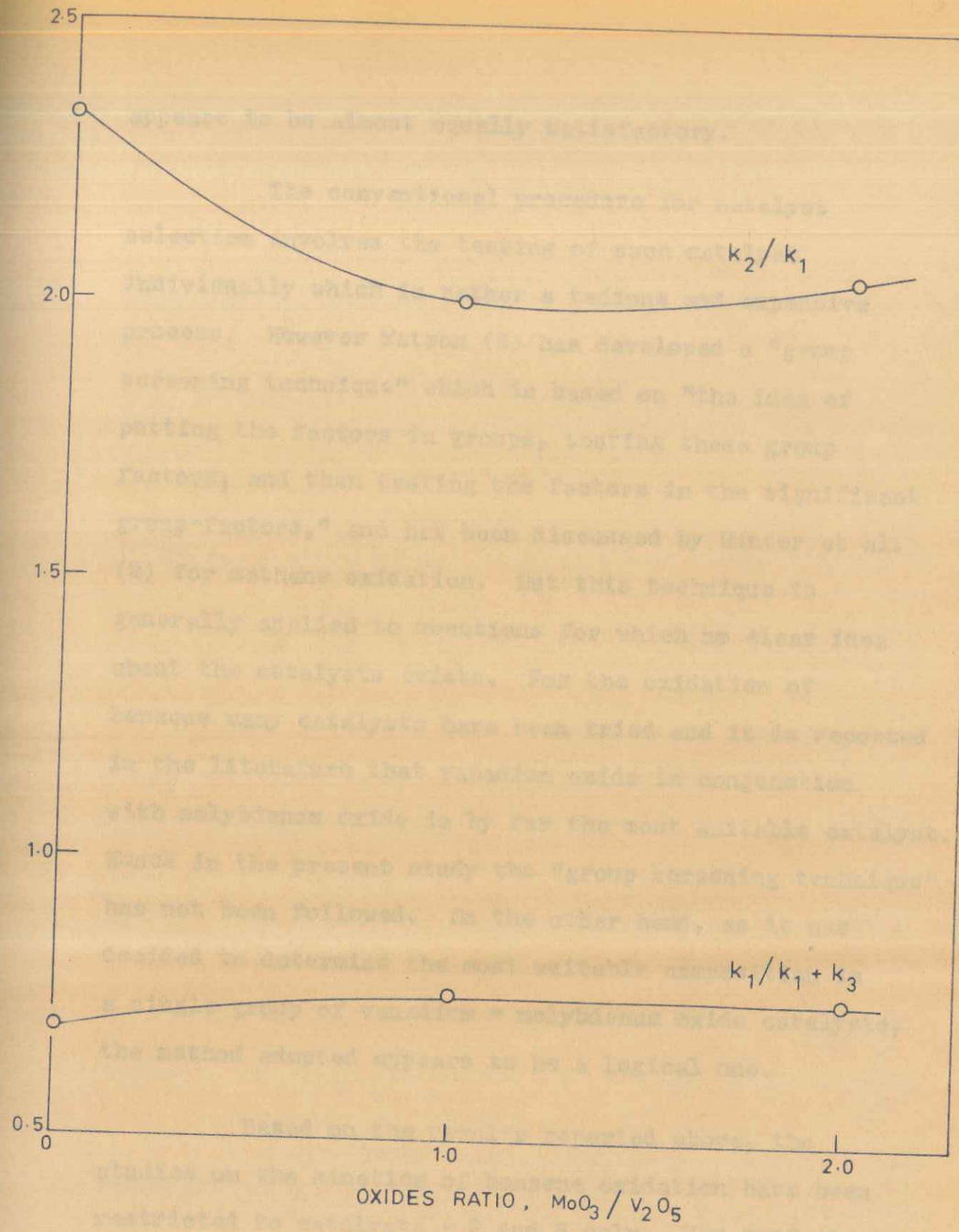

FIG. 3.4. EFFECT OF OXIDES RATIO ($MoO_3 : V_2O_5$) ON SELECTIVITY

appears to be almost equally satisfactory.

The conventional procedure for catalyst selection involves the testing of each catalyst individually which is rather a tedious and expensive process. However Watson (6) has developed a "group screening technique" which is based on "the idea of putting the factors in groups, testing these group factors, and then testing the factors in the significant group-factors," and has been discussed by Hunter et al. (5) for methane oxidation. But this technique is generally applied to reactions for which no clear idea about the catalysts exists. For the oxidation of benzene many catalysts have been tried and it is reported in the literature that vanadium oxide in conjunction with molybdenum oxide is by far the most suitable catalyst. Hence in the present study the "group screening technique" has not been followed. On the other hand, as it was decided to determine the most suitable composition in a single group of vanadium - molybdenum oxide catalysts, the method adopted appears to be a logical one.

Based on the results reported above, the studies on the kinetics of benzene oxidation have been restricted to catalysts - 2 and 3 only. The surface areas and the pore volumes of these catalysts were determined by the B.E.T. method and displacement technique respectively, and these values are included in Table - 3.6.

Table - 3.6

Properties of the catalysts selected for kinetic analysis

Catalyst number	Surface area sq.m./gm.	Pore volume ml./ml.
2	144	0.38
3	256	0.41

References

1. Benson, S.W., "The Foundations of Chemical Kinetics," pp.35, McGraw Hill, New York (1960).

2. Dixon, J.K. and Longfield, J.E., "Catalysis," (P.H. Emmett, ed.); Vol. VII, Chap. 3, Reinhold Publishing Corporation, New York (1960).

3. Dmuchovsky, B., Freeks, M.C., Pierron, E.D., Munch, R.H. and Zienty, F.B., J. Catalysis, 4, (2), 291 (1965).

4. Hammar, C.G.B., Svensk Kem. Tid., 64, 165-76 (1952); Chem. Abst., 46, 8945 (1952).

5. Hunter, W.G. and Mezaki, R., Ind. Eng. Chem., 56, 38 (1964).

6. Watson, G.S., Technometrics, 3, 371 (1961).

7. Yoshida, F., Ramaswami, D. and Hougen, O.A., Am. Inst. Chem. Eng., Convention, Washington, D.C., December 1960.

CHAPTER-4

PLAUSIBLE MODELS

Chapter 4

PLAUSIBLE MODELS

4.1 GENERAL

Two methods of approach are possible for postulating models for the oxidation of benzene (any hydrocarbon). In the first method it is assumed that only two steps are important, and that at steady state the rates of these two steps are equal (i.e. rate of adsorption of oxygen or benzene is equal to rate of reaction on the surface). In the second method the reaction is assumed to be controlled by the slowest step in a series of possible steps which occur during the catalytic reaction. All other steps are so fast as to have reached equilibrium.

While an attempt has been made in the past to postulate a model in accordance with the first method, apparently no attempt has been made to delineate the controlling steps in the three principal reactions occurring during the oxidation of benzene. Furthermore, these models (due to Hinshelwood) are only concerned with the oxidation of benzene as a whole, and not with the individual steps involved in the overall process. The Hinshelwood models are briefly analysed below, after which plausible controlling step models are developed for all the reactions.

4.2 HINSHELWOOD MODELS

Hayashi et al (6) have applied the Hinshelwood reaction mechanism to the oxidation of benzene, assuming:

(i) oxygen is the only reactant adsorbed on the catalyst surface,

(ii) the rate of desorption of oxygen from the catalyst surface is negligible,

(iii) for reaction to occur, organic reactant in the gas phase must strike an adsorbed oxygen,

(iv) a steady state is established in which the rate of removal of oxygen by chemical reaction equals the rate of adsorption of oxygen.

Equating the rate of adsorption of oxygen to the rate of chemical reaction, the final form of the equation developed (expressed in terms of partial pressures) was

$$r = \frac{k_a k_r p_B p_O}{k_a p_O + n k_r p_B} \qquad .. \quad (4.1)$$

Mars and van Krevelen (16) proposed a similar model for the oxidation of naphthalene. They represented the oxidation scheme according to the following two steps:

(I) naphthalene + oxidized catalyst ⟶
products + reduced catalyst

(II) reduced catalyst + oxygen ⟶
oxidized catalyst

The rate equation developed by them can be shown to be identical in form with Equation (4.1), based on the Hinshelwood model.

4.2.1. Applicability of the Hinshelwood model

If the Hinshelwood mechanism were to hold good, the adsorption constant k_a should have the same value for all hydrocarbon oxidations at the same temperature for a given catalyst, since they all would have one common step -- adsorption of oxygen on the catalyst surface. However, it may be noted from Table - 4.1 that the value of the adsorption constant depends on the hydrocarbon used (6). This would indicate that the mechanism suggested by Hayashi et al (6) and Mars and van Krevelen (16) is not of general applicability. Moreover, the present data also do not uphold the mechanism, as shown below:

Equation (4.1) may be rewritten in the form

$$\frac{p_B p_O}{r} = \frac{p_O}{k_r} + \frac{1}{k_a} n p_B \quad \ldots \quad (4.2)$$

Table - 4.1

Reported specific adsorption constants at 324°C.(6)

Catalyst number	Hydrocarbon used	$k_a \times 10^5$
11	Benzene	0.511
	Toluene	3.270
	Naphthalene	4.550
12	Benzene	0.650
	Toluene	4.340
	Naphthalene	6.010

Thus, a plot of $\frac{p_B p_O}{r}$ vs. np_B should give a straight line with slope = $1/k_a$ and intercept = p_O/k_r, considering p_O to be nearly constant.

However, in the present work, the above plot yields a curve and not a straight line as expected, indicating that the data do not uphold this mechanism (oxygen adsorption). This was found to be true at all the temperatures for both the catalysts. Representative plots are shown in Figures 4.1 and 4.2.

4.2.2 Proposed (modified Hinshelwood) model

According to Bretton (3), initially the hydrocarbon is adsorbed over the catalyst surface with the abstraction of hydrogen to form a radical. Then the oxygen from the gas phase strikes over it and the chemical reaction proceeds through the formation and destruction of peroxy radicals.

Based on Bretton's postulates (3), a rate equation similar to that suggested by Hayashi et al (6) and Mars and van Krevelen (4) (for naphthalene) can be developed with the following assumptions:

(i) benzene is the only reactant adsorbed on the catalyst surface,

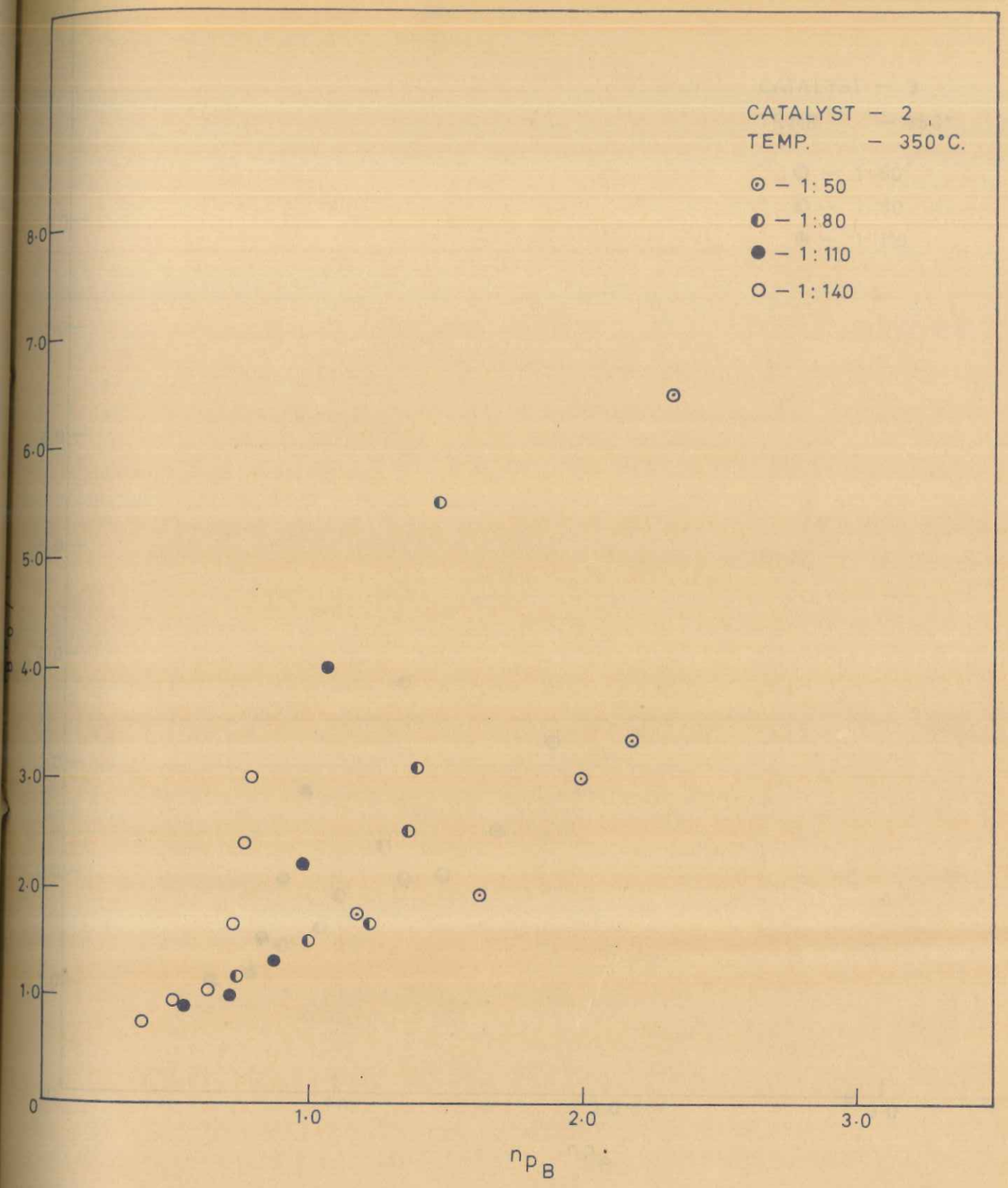

FIG. 4·1. HINSHELWOOD MODEL PLOT – OXYGEN ADSORBED

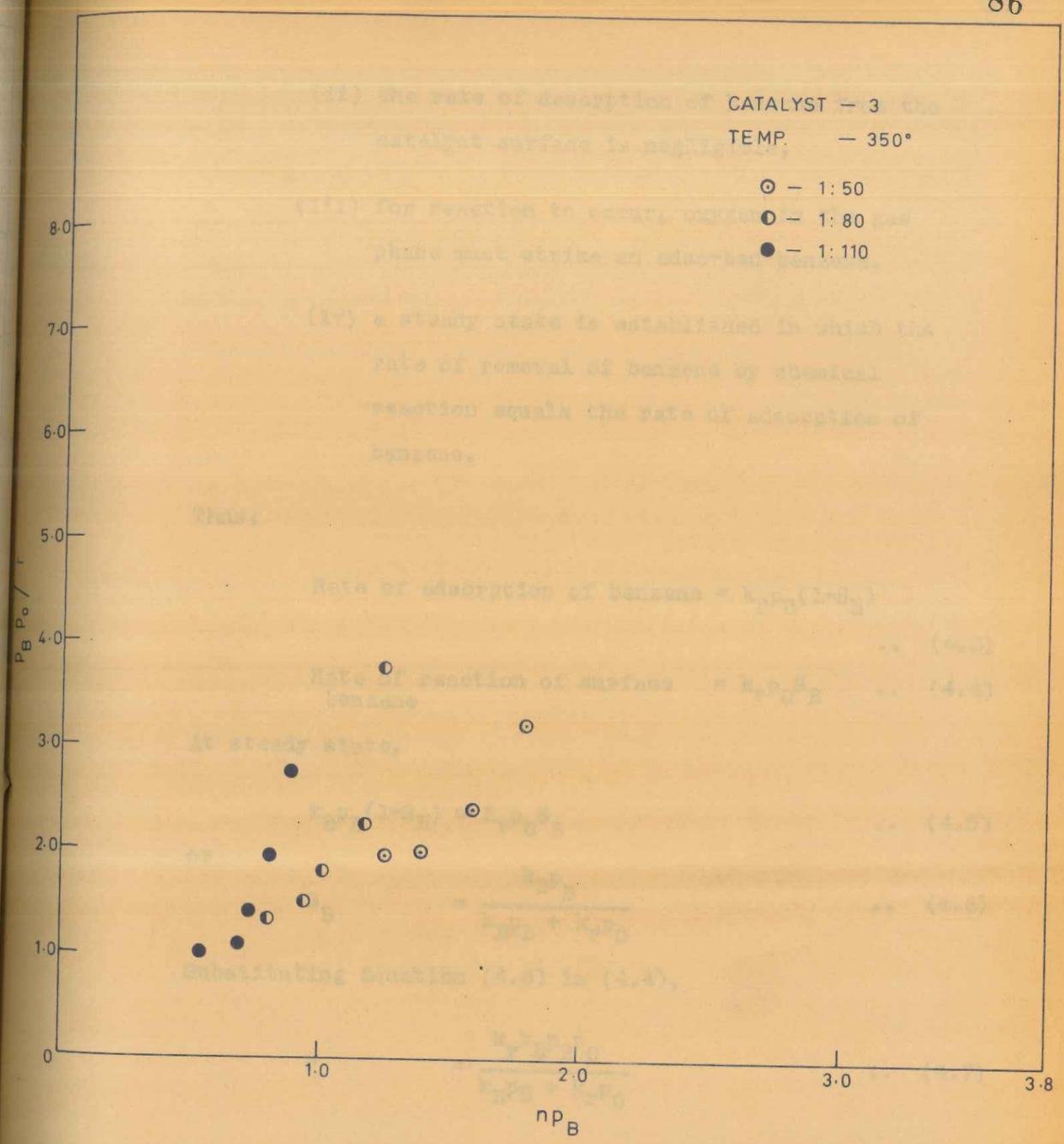

FIG. 4.2. HINSHELWOOD MODEL PLOT - OXYGEN ADSORBED

(ii) the rate of desorption of benzene from the catalyst surface is negligible,

(iii) for reaction to occur, oxygen in the gas phase must strike an adsorbed benzene,

(iv) a steady state is established in which the rate of removal of benzene by chemical reaction equals the rate of adsorption of benzene.

Thus:

$$\text{Rate of adsorption of benzene} = k_B p_B (1-S_B) \quad .. \quad (4.3)$$

$$\text{Rate of reaction of surface benzene} = k_r p_O S_B \quad .. \quad (4.4)$$

At steady state,

$$k_B p_B (1-S_B) = k_r p_O S_B \quad .. \quad (4.5)$$

or

$$S_B = \frac{k_B p_B}{k_B p_B + k_r p_O} \quad .. \quad (4.6)$$

Substituting Equation (4.6) in (4.4),

$$r = \frac{k_r k_B p_B p_O}{k_B p_B + k_r p_O} \quad .. \quad (4.7)$$

It should be recognised that the total reaction rate, r, corresponds to the sum of the first and third steps of the reaction scheme used, i.e., $r = (r_1 + r_3)$

(rate of total benzene conversion).

4.2.3 Test of proposed model

Equation (4.6) may be rewritten as,

$$\frac{p_B p_O}{r} = \frac{1}{k_r} p_B + \frac{p_O}{k_B} \quad .. \quad (4.8)$$

A plot of $\frac{p_B p_O}{r}$ vs. p_B should give a straight line with $1/k_r$ as slope and p_O/k_B as intercept, considering p_O to be nearly constant.

However in the present case, the above plot yields a straight line for the initial conditions only (i.e., W/F = 0), the corresponding equation being

$$\left(\frac{p_B p_O}{r}\right)_o = \frac{1}{k_{ro}} p_{Bo} + \frac{p_O}{k_B} \quad .. \quad (4.9)$$

Plots of this equation are presented in Figures 4.3 to 4.8 for both the catalysts. When data point outside the initial conditions are included a straight line is not obtained, as can be seen from the representative plots shown in Figures 4.9 and 4.10.

The fact that the proposed model holds good for the initial conditions, and fails completely as the conversion rises, could be due to a change in the order of the reaction with the formation of oxidation products.

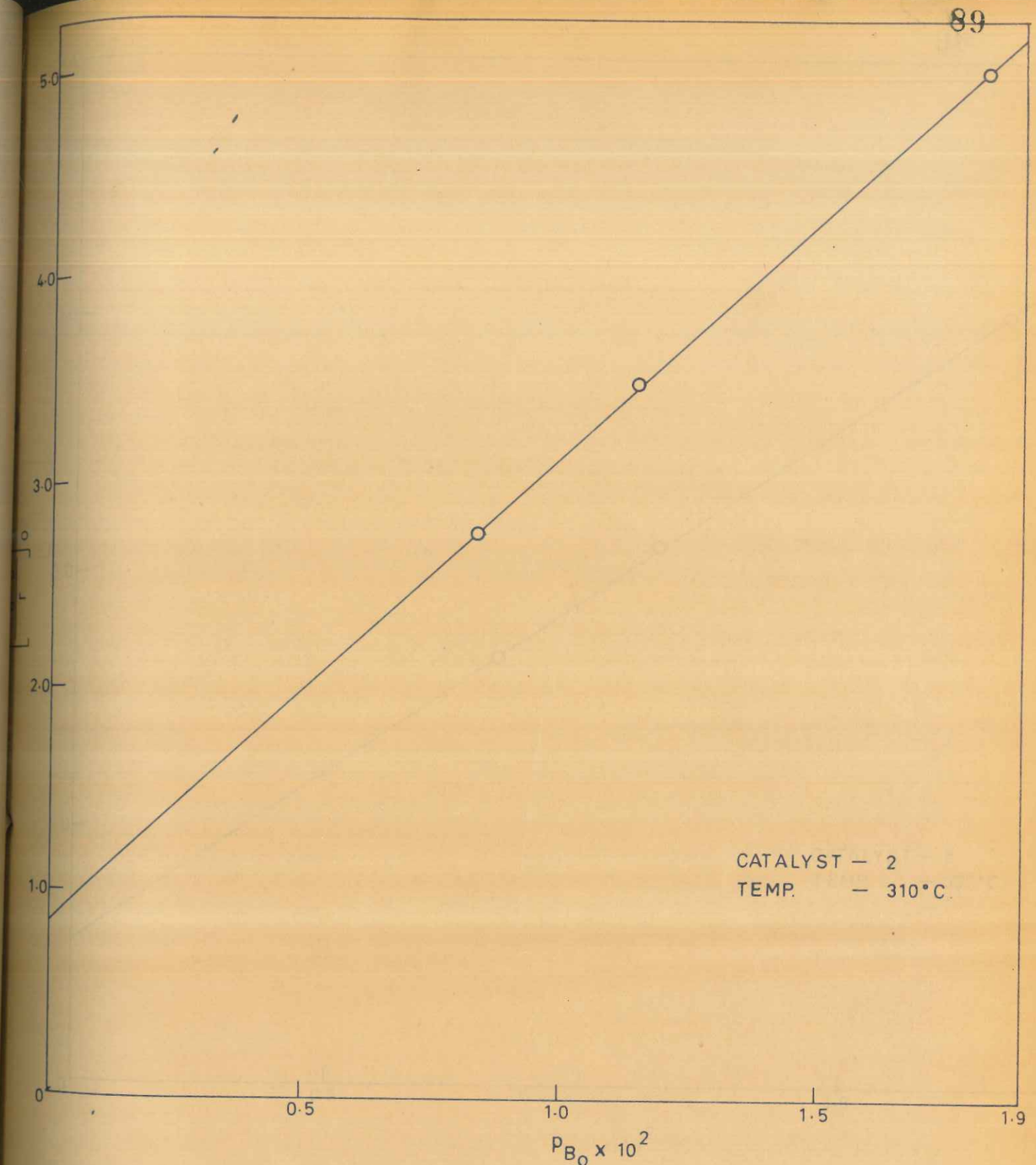

FIG. 4.3. PLOT OF EQUATION (4·9) (for initial condition) FOR THE MODIFIED HINSHELWOOD MODEL - BENZENE ADSORBED

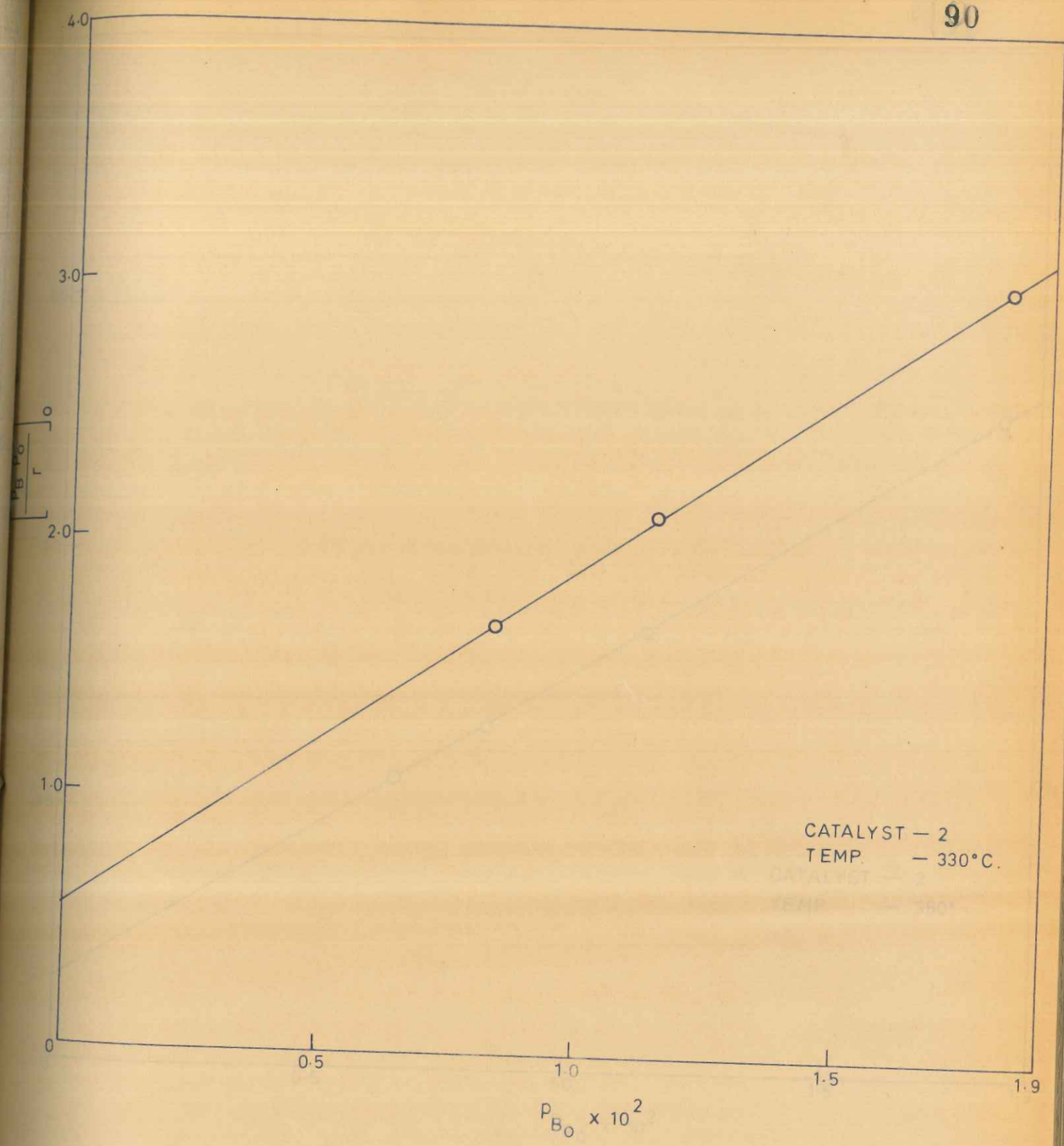

FIG. 4.4. PLOT OF EQUATION (4.9) (for initial condition) FOR THE MODIFIED HINSHELWOOD MODEL - BENZENE ADSORBED

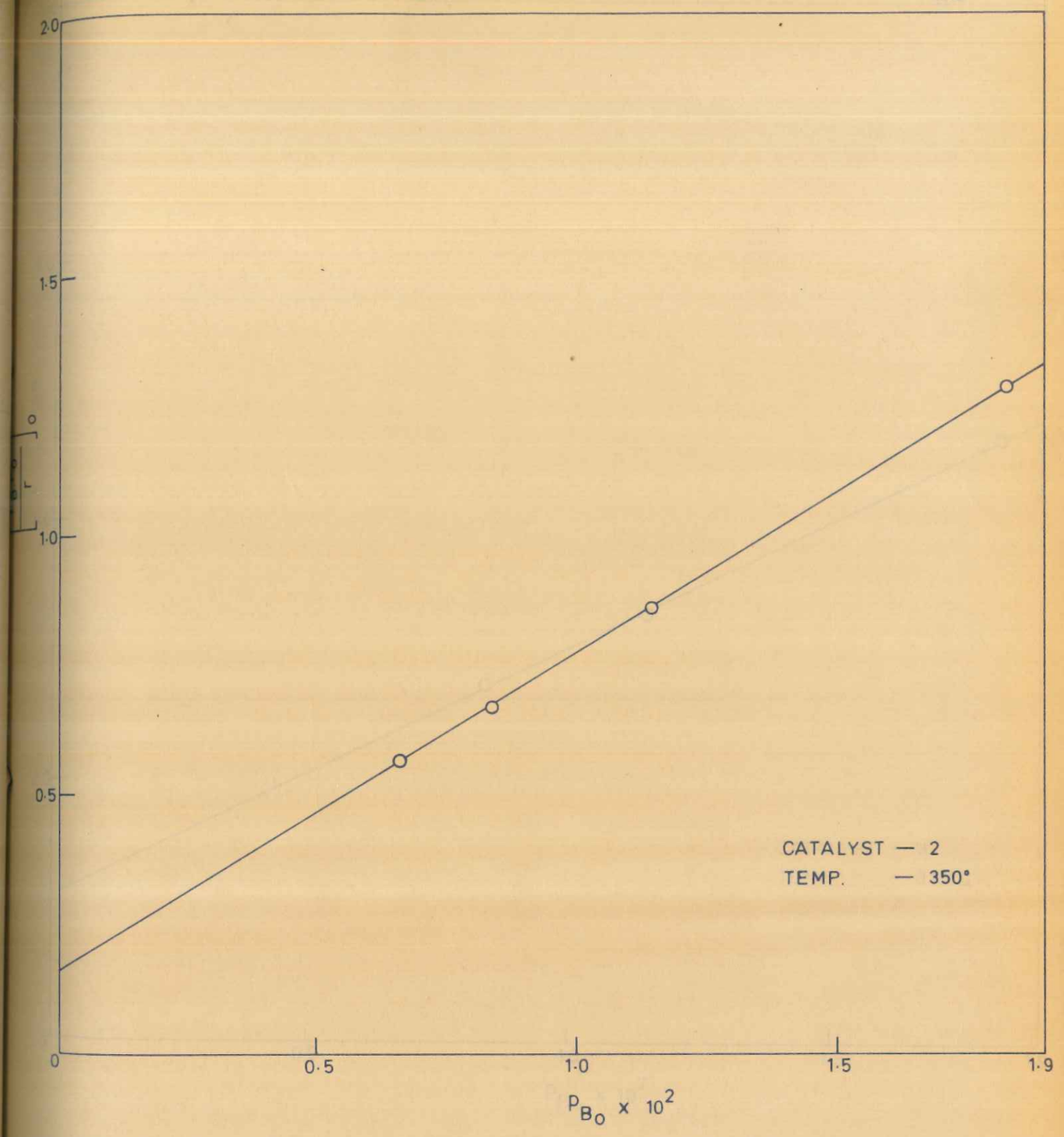

FIG. 4.5. PLOT OF EQUATION (4.9) (for initial condition) FOR THE MODIFIED HINSHELWOOD MODEL - BENZENE ADSORBED

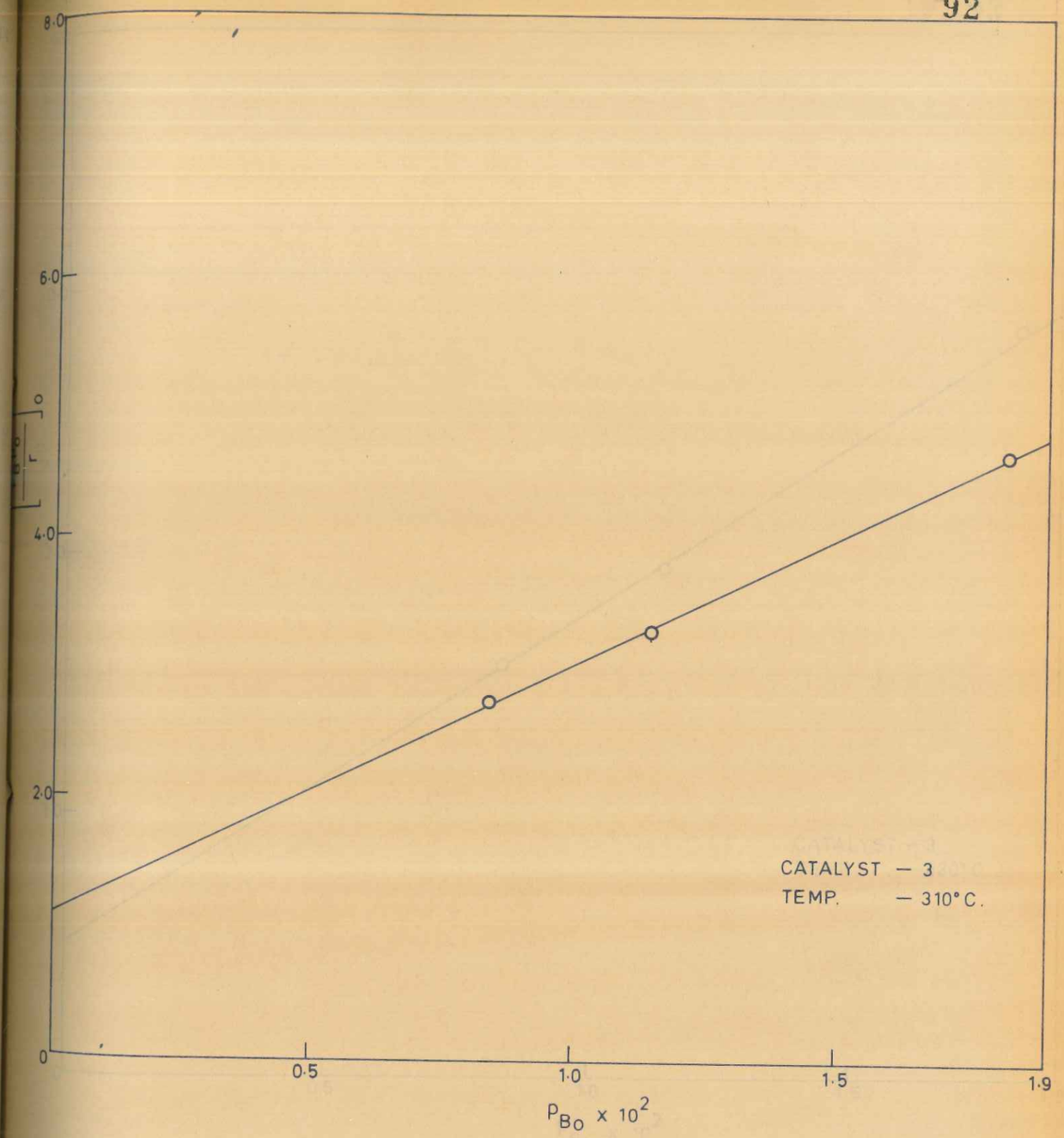

FIG. 4·6. PLOT OF EQUATION (4·9) (for initial condition) FOR THE MODIFIED HINSHELWOOD MODEL - BENZENE ADSORBED

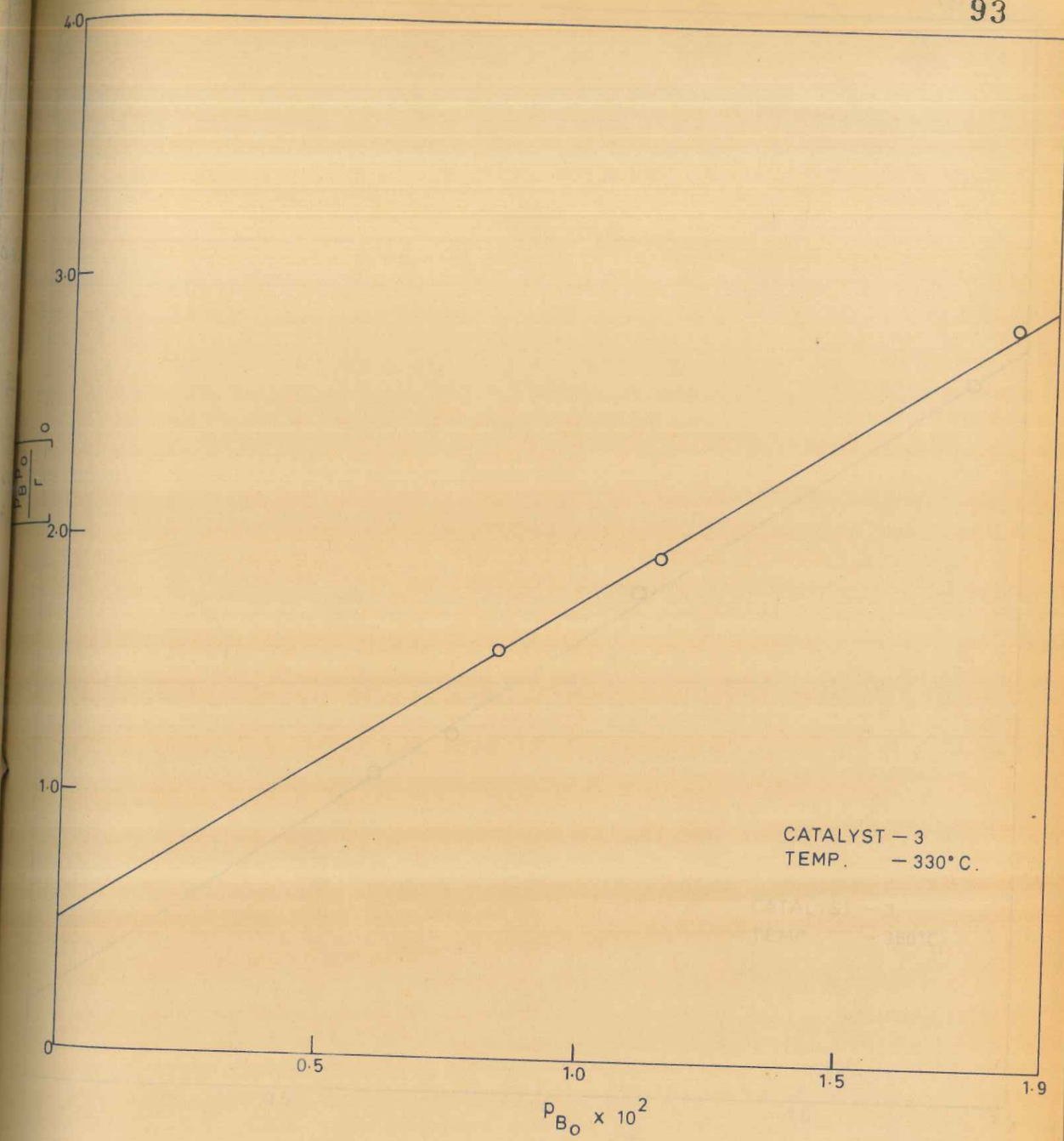

FIG. 4·7. PLOT OF EQUATION (4·9) (for initial condition) FOR THE MODIFIED HINSHELWOOD MODEL- BENZENE ADSORBED

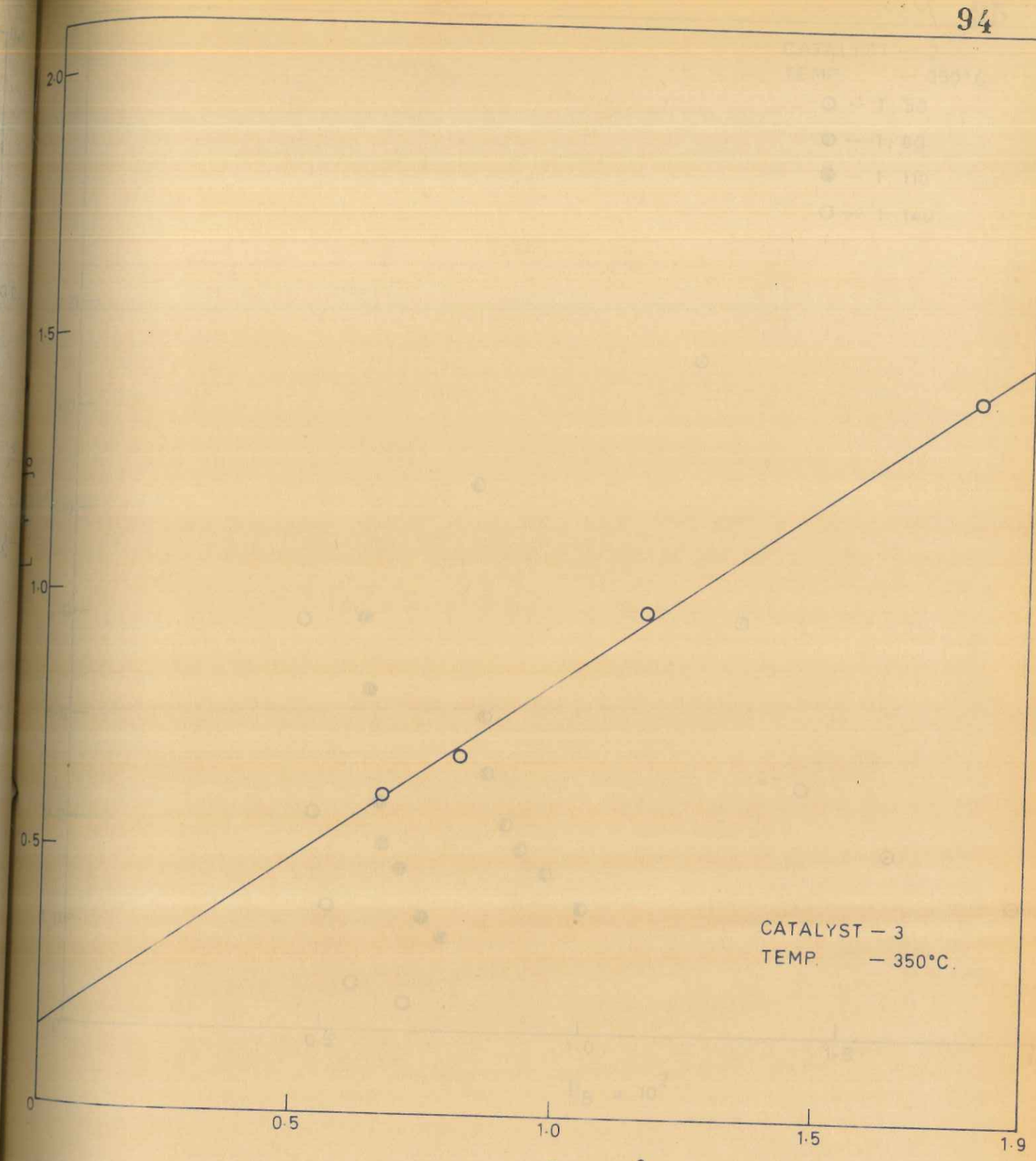

FIG. 4·8. PLOT OF EQUATION (4·9) (for initial condition) FOR THE MODIFIED HINSHELWOOD MODEL - BENZENE ADSORBED

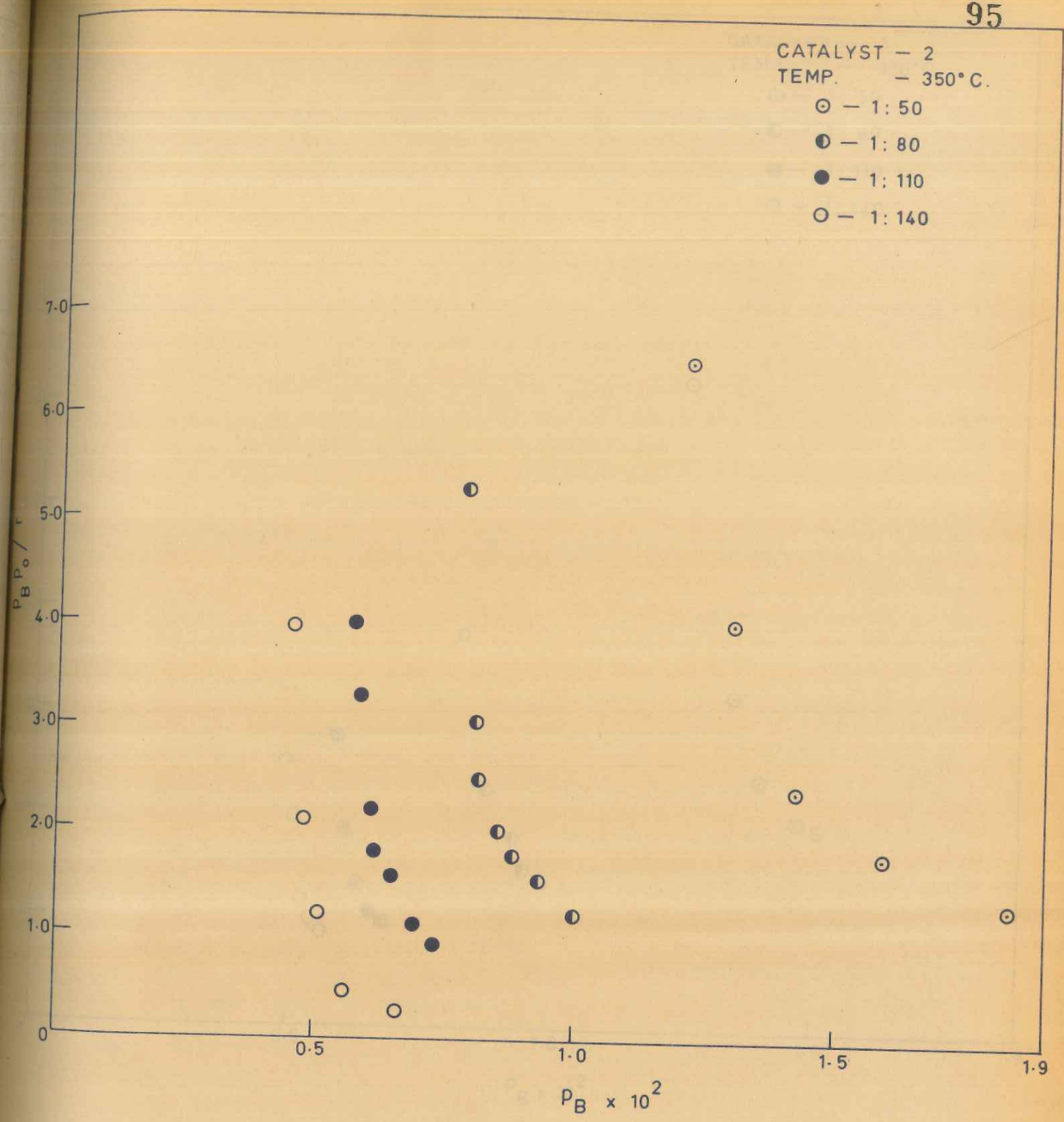

FIG. 4·9. PLOT OF EQUATION (4·8) FOR ALL CONDITIONS FOR THE MODIFIED HINSHELWOOD MODEL — BENZENE ADSORBED

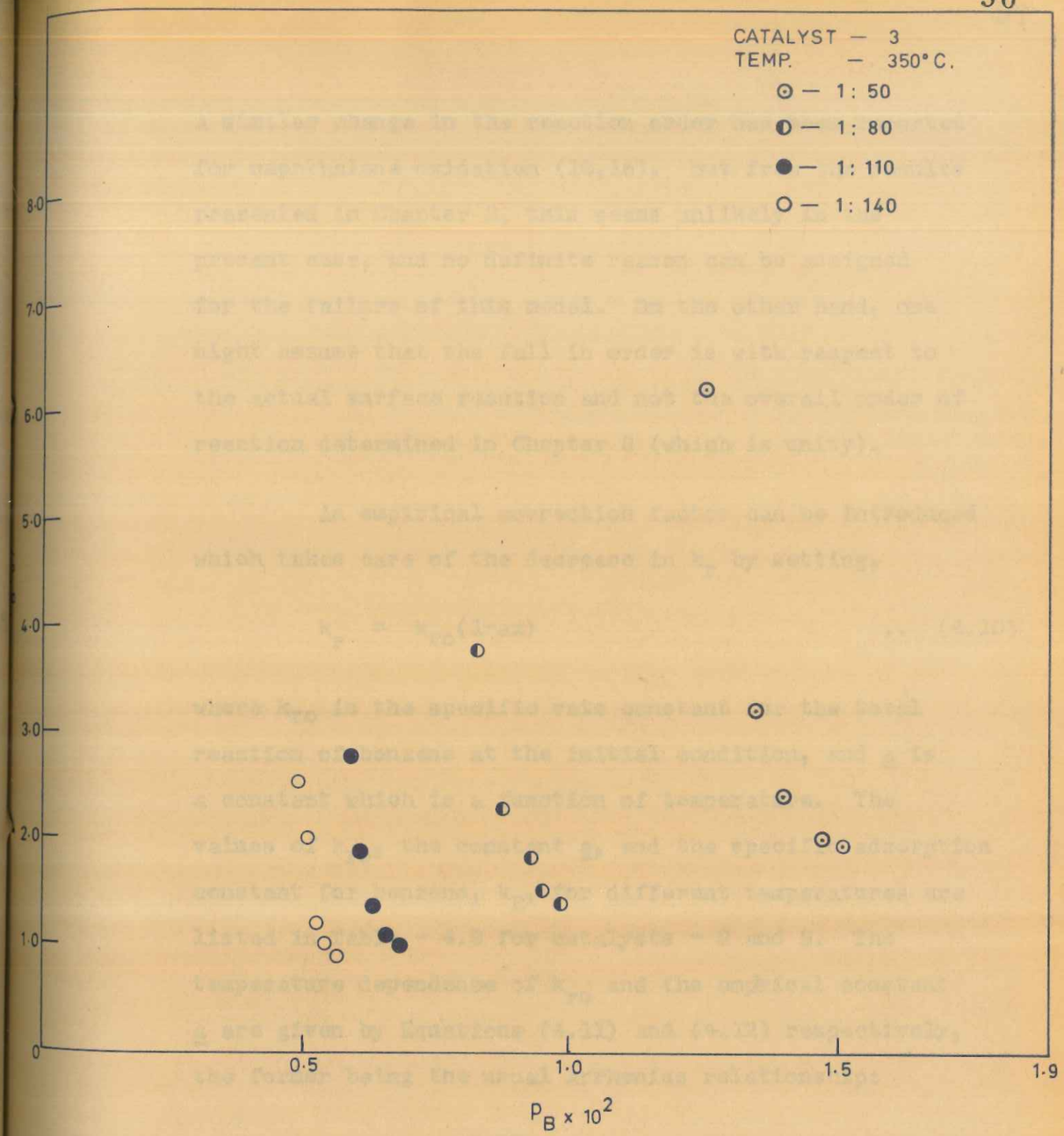

FIG. 4·10. PLOT OF EQUATION (4·8) FOR ALL CONDITIONS FOR THE MODIFIED HINSHELWOOD MODEL — BENZENE ADSORBED

A similar change in the reaction order has been reported for naphthalene oxidation (10,16). But from the results presented in Chapter 3, this seems unlikely in the present case, and no definite reason can be assigned for the failure of this model. On the other hand, one might assume that the fall in order is with respect to the actual surface reaction and not the overall order of reaction determined in Chapter 3 (which is unity).

An empirical correction factor can be introduced which takes care of the decrease in k_r by setting,

$$k_r = k_{ro}(1-ax) \qquad .. \quad (4.10)$$

where k_{ro} is the specific rate constant for the total reaction of benzene at the initial condition, and a is a constant which is a function of temperature. The values of k_{ro}, the constant a, and the specific adsorption constant for benzene, k_B, for different temperatures are listed in Table - 4.2 for catalysts - 2 and 3. The temperature dependence of k_{ro} and the empirical constant a are given by Equations (4.11) and (4.12) respectively, the former being the usual Arrhenius relationship:

$$k_{ro} = A\, e^{-E/RT} \qquad .. \quad (4.11)$$

and

$$a = \alpha\, T^{\beta} \qquad .. \quad (4.12)$$

Table - 4.2

Values of the specific rate constant k_{ro} (for the initial condition) and the specific adsorption constant k_B at different temperatures for the modified Hinshelwood model*

Catalyst number	Temperature °C.	$k_{ro} \times 10^2$	a	k_B
2	310	0.448	10.60	0.230
	330	0.741	4.76	0.345
	350	1.538	2.63	1.762
3	310	0.515	11.10	0.179
	330	0.781	4.77	0.387
	350	1.450	2.99	1.283

check with Table 3(2)

*As stated in the text, these are for total benzene disappearance.

The graphical representation of Equations (4.11) and (4.12) appears in Figures 4.11, 4.12 and 4.13, 4.14 respectively, and the values of the constants A, E, α and β are listed in Table - 4.3 for both the catalysts.

As in the case of the activation energies for the first-order rate equations developed in Chapter 3, two distinct regions of the activation energy values were observed. But Figures 4.11 and 4.12 show the results in the lower temperature range only (310-330°C.). The correlation for the higher temperature range (350-400°C.) was equally satisfactory and the corresponding values of A, E, α and β are also included in Table - 4.3.

Equations (4.8) and (4.10) were verified by back calculating the rates and comparing them with the observed values. The results for the low temperature range are shown in Figures 4.15 and 4.16. Representative data for the two catalysts appear in Tables - A.30 and A.31 of Appendix - A. The average error is 8-10%.

4.3 PROBABLE CONTROLLING MECHANISMS

4.3.1 General

Two methods of determining the controlling mechanisms are available. One is due to Hougen-Watson (9) and the other due to Balandin and his coworkers (1,2). Both

Table - 4.3

Constants of Equations (4.11) and (4.12) for the modified Hinshelwood model

Catalyst number	Constant	Temp. range 310 - 350°C.	Temp. range 350 - 400°C.
2	A	9.92×10^{5}	7.08×10^{-2}
	E	-22.39	-1.90
	α	6.24×10^{39}	6.24×10^{39}
	β	-14.02	-14.02
3	A	1.06×10^{5}	3.35×10^{-1}
	E	-19.73	-6.67
	α	6.84×10^{40}	6.84×10^{40}
	β	-14.39	-14.39

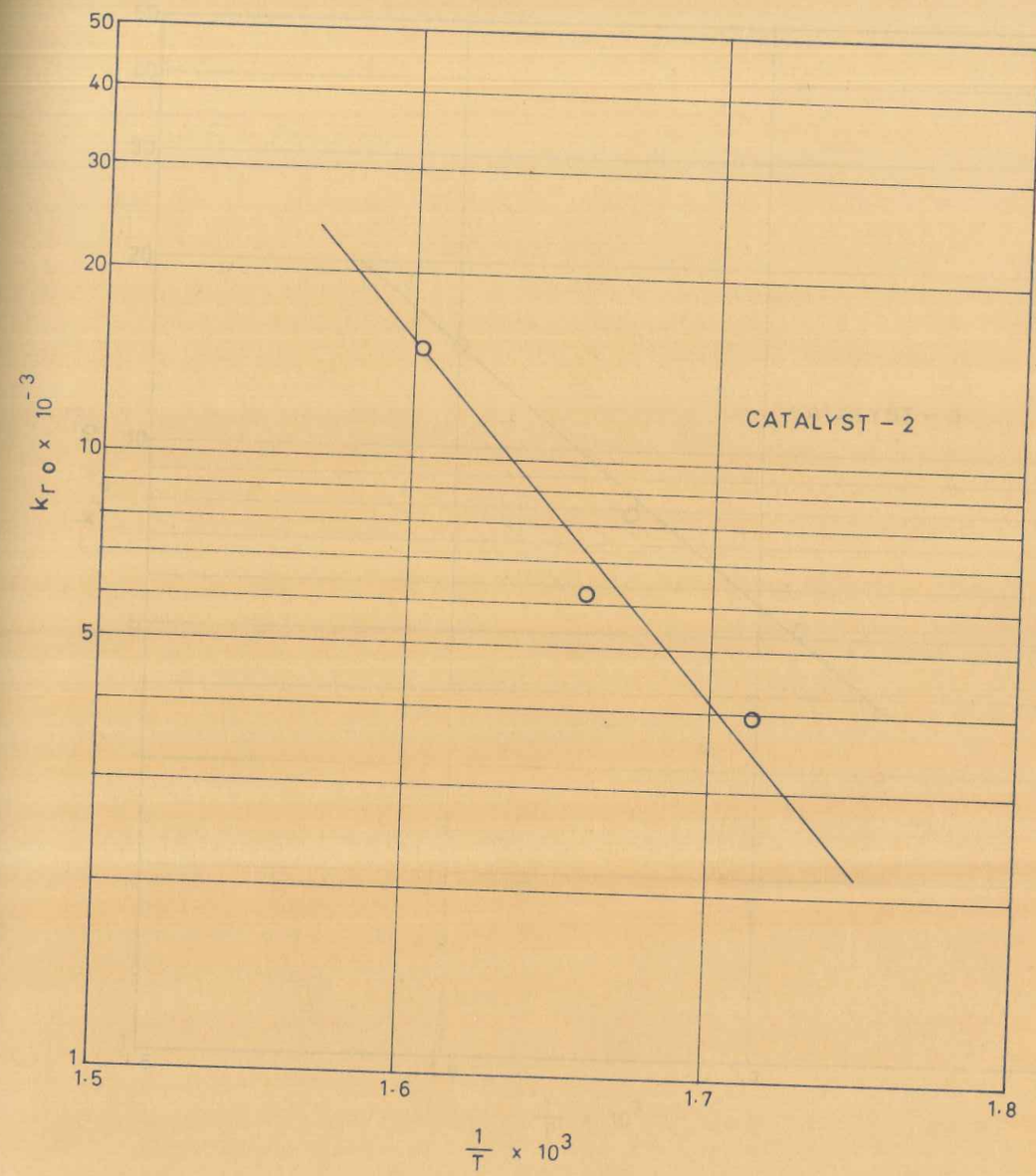

FIG 4.11. TEMPERATURE DEPENDENCE OF THE RATE CONSTANT k_{ro} AT INITIAL CONDITION FOR THE MODIFIED HINSHELWOOD MODEL

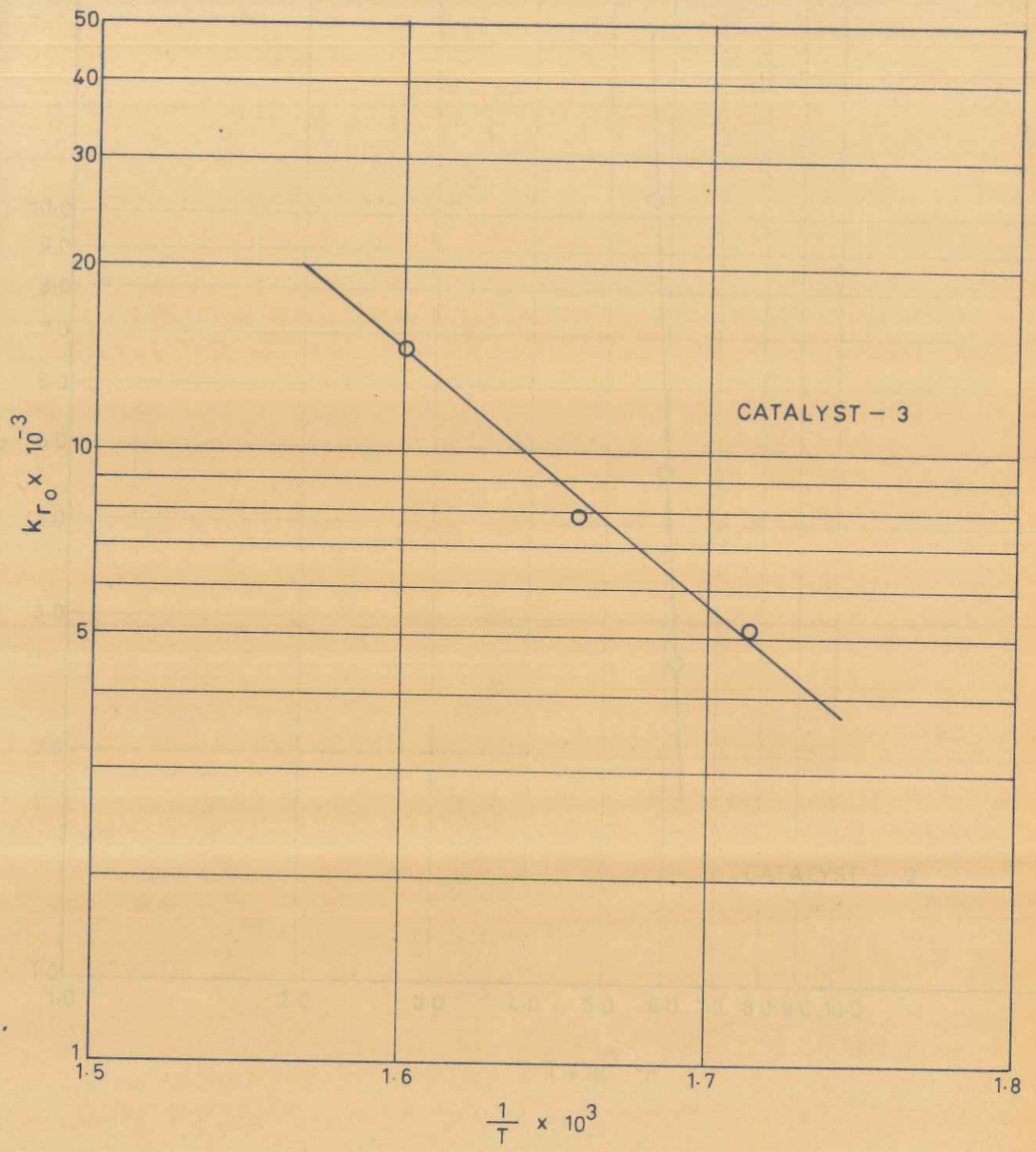

FIG. 4·12. TEMPERATURE DEPENDENCE OF THE RATE CONSTANT k_{r_o} AT INITIAL CONDITION FOR THE MODIFIED HINSHELWOOD MODEL

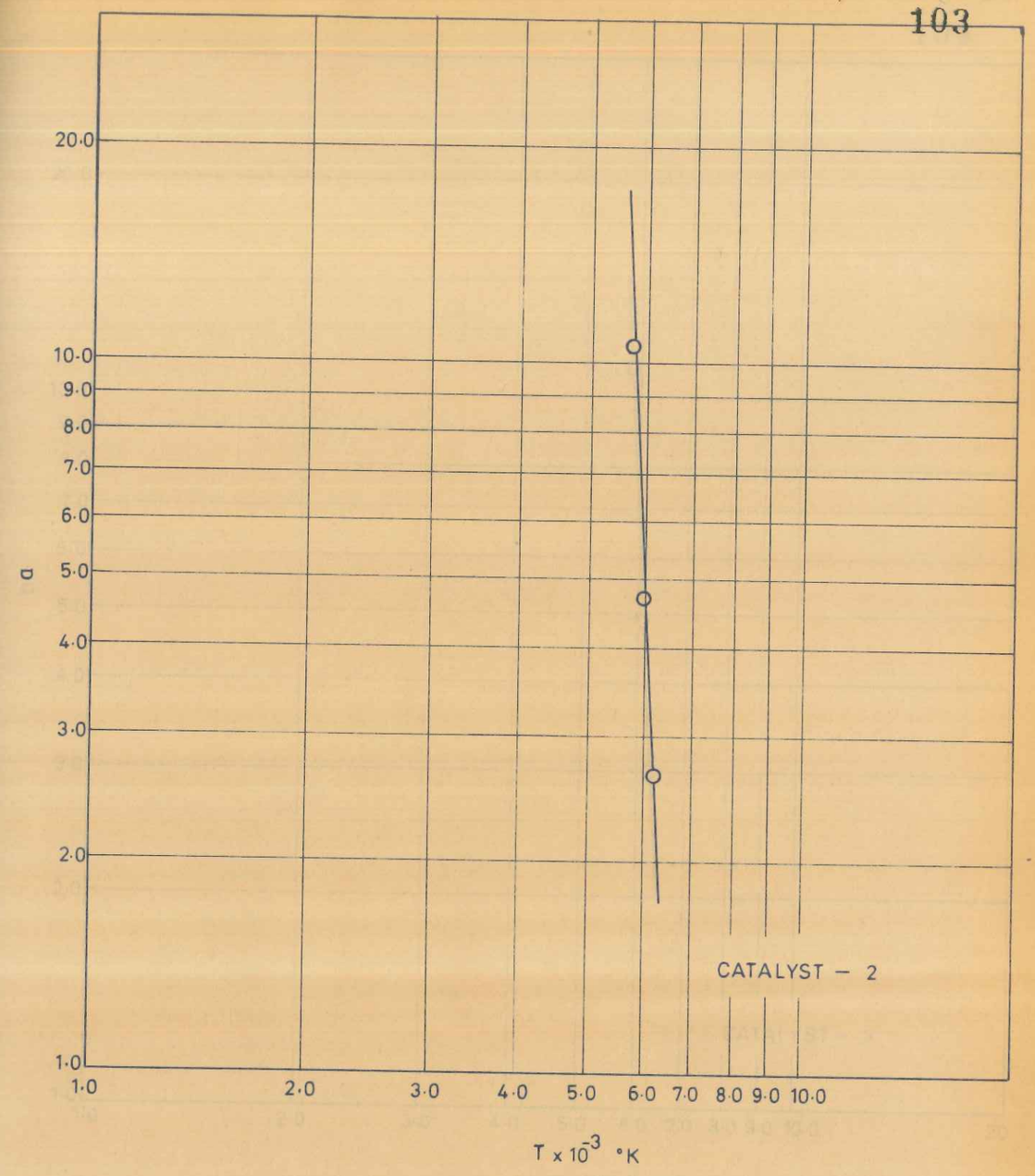

FIG. 4.13. EMPIRICAL CORRELATION OF CONSTANT 'a' WITH TEMPERATURE FOR THE MODIFIED HINSHELWOOD MODEL FOR CATALYST-2

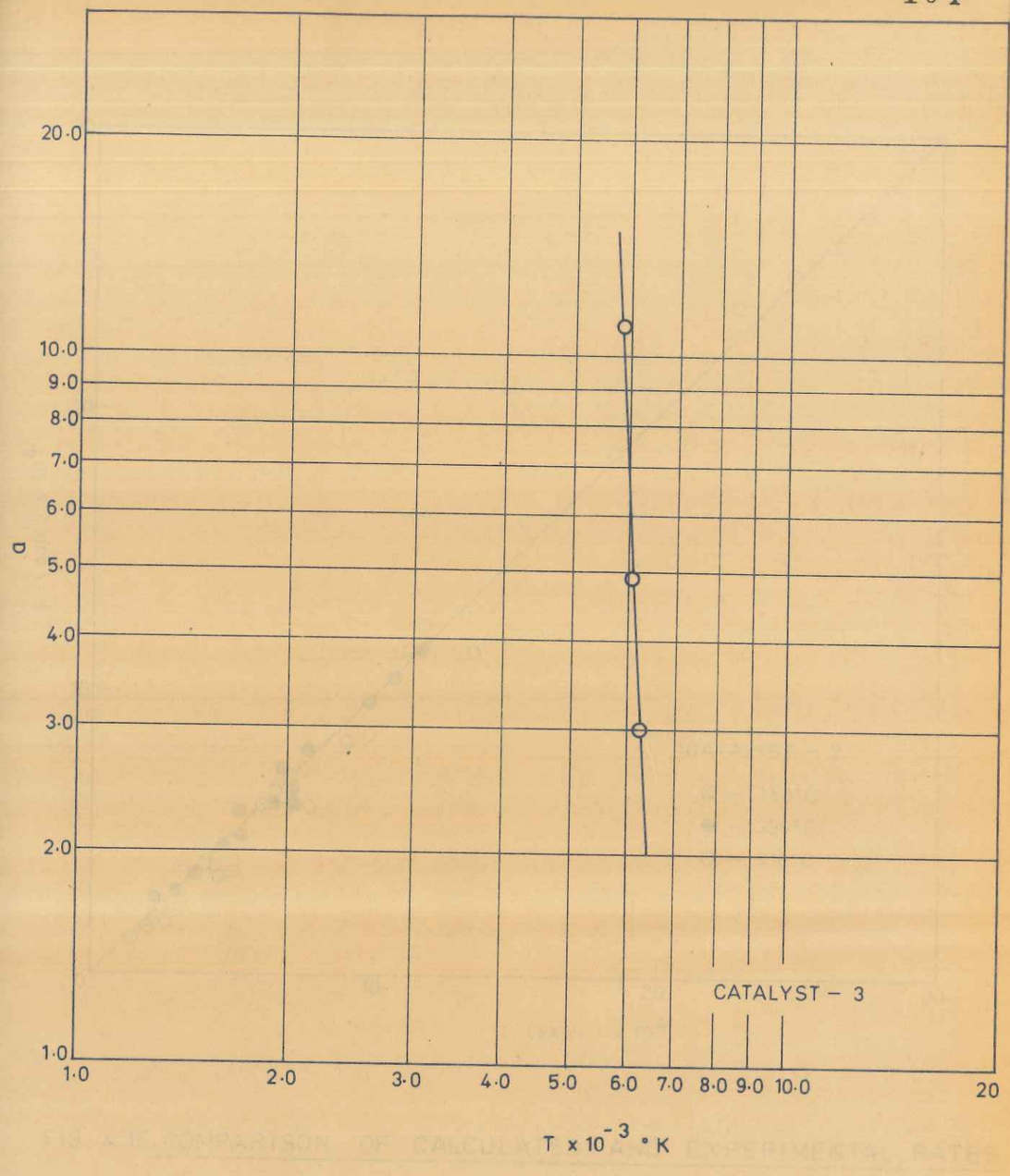

FIG. 4·14. EMPIRICAL CORRELATION OF CONSTANT 'a' WITH TEMPERATURE FOR MODIFIED HINSHELWOOD MODEL FOR CATALYST-3

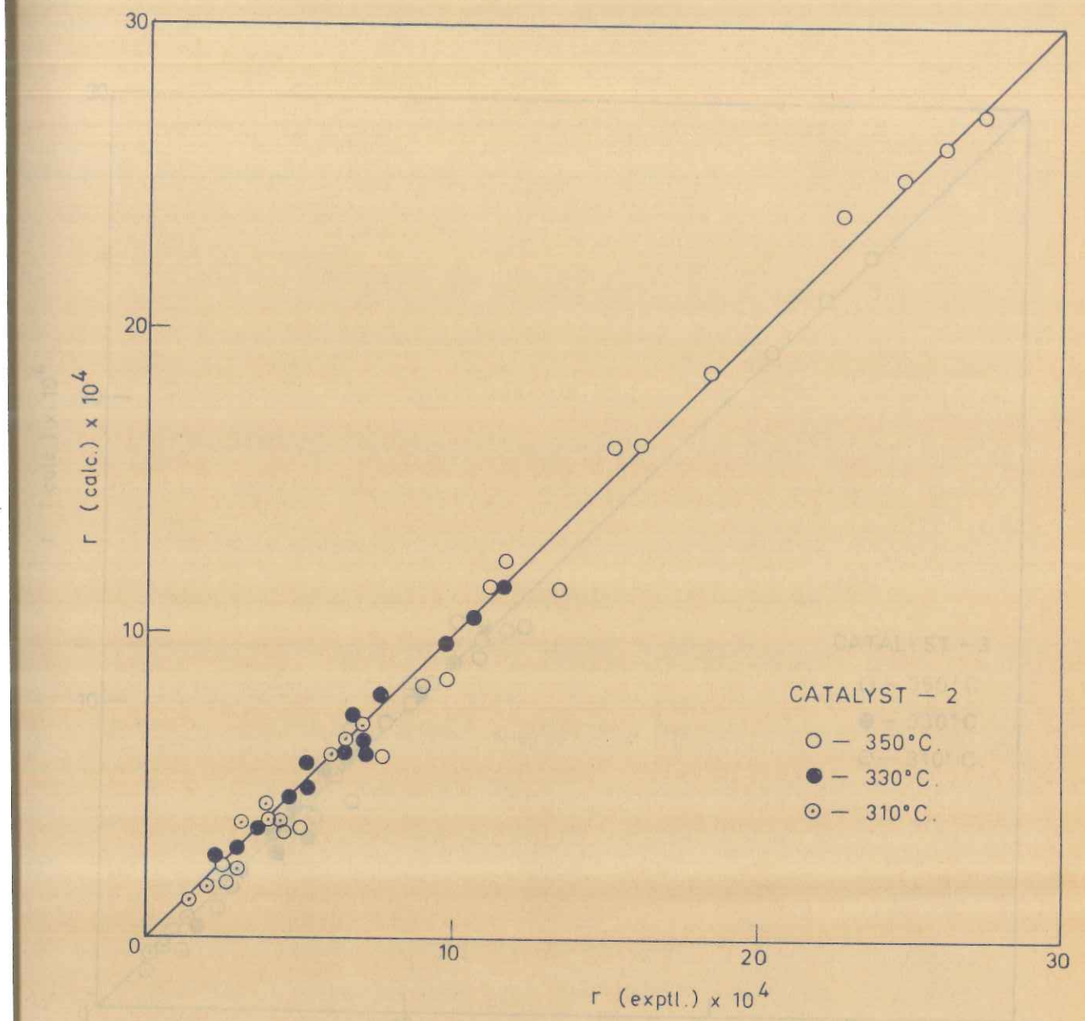

FIG. 4·15 COMPARISON OF CALCULATED AND EXPERIMENTAL RATES FOR THE MODIFIED HINSHELWOOD MODEL

[Equations (4·8) & (4·10)]

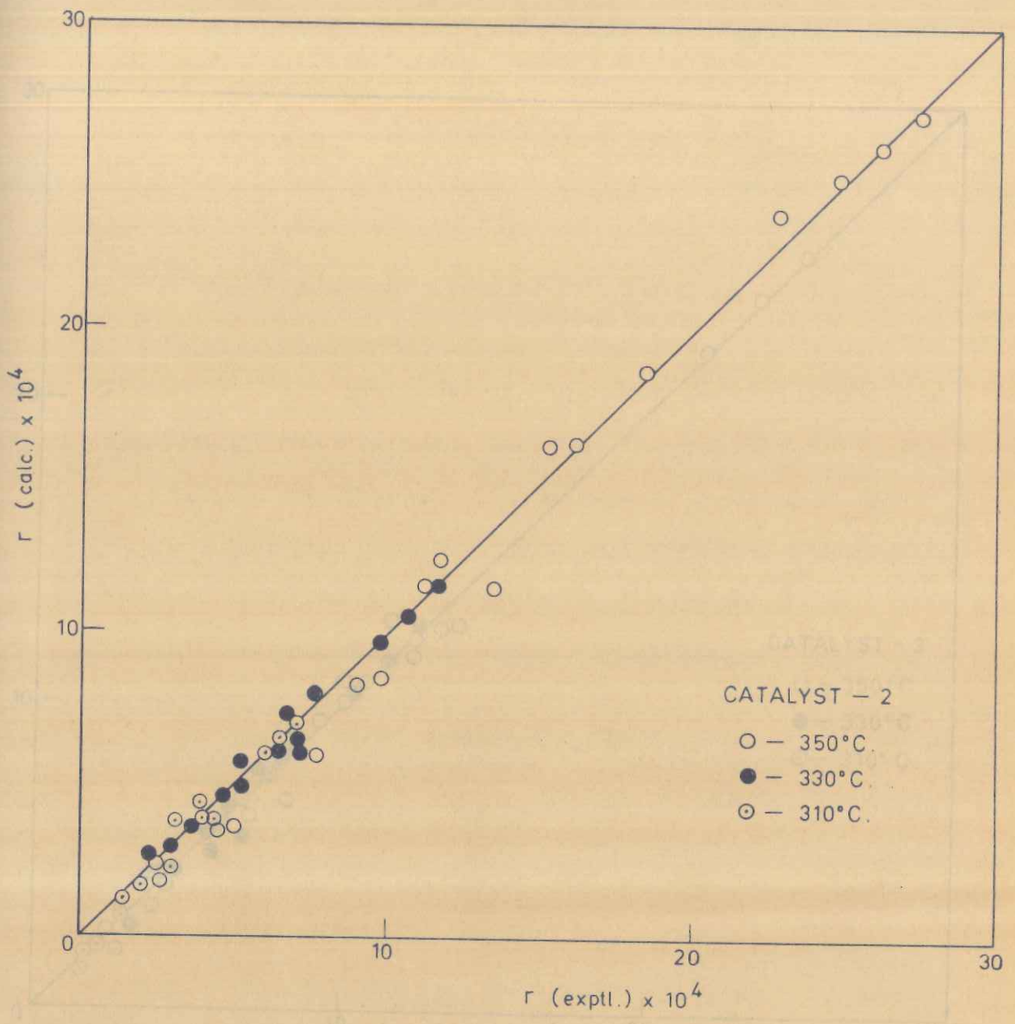

FIG. 4·15 COMPARISON OF CALCULATED AND EXPERIMENTAL RATES FOR THE MODIFIED HINSHELWOOD MODEL

[Equations (4·8) & (4·10)]

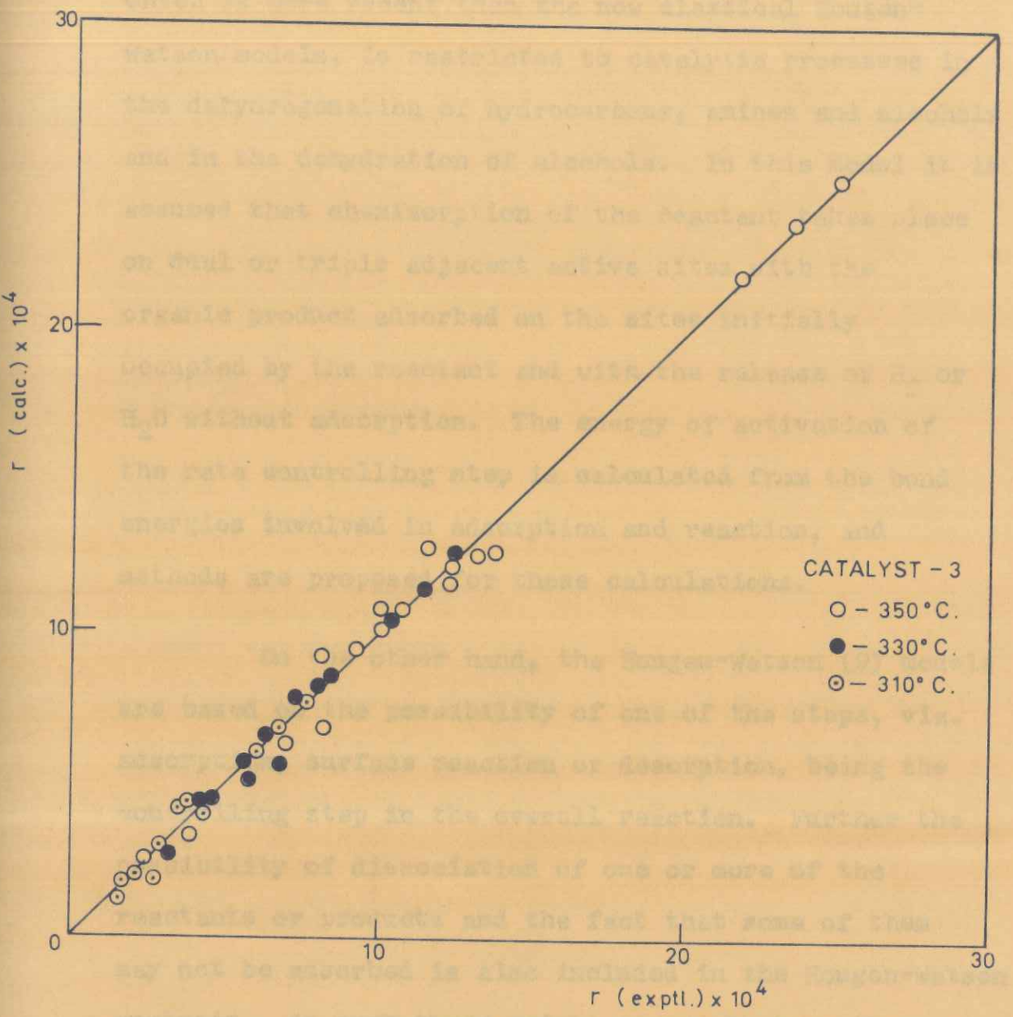

FIG. 4.16. COMPARISON OF CALCULATED AND EXPERIMENTAL RATES FOR THE MODIFIED HINSHELWOOD MODEL [Equations (4.8) & (4.10)]

these methods are based essentially on the Langmuir-Hinshelwood adsorption hypothesis. The Balandin model, which is more recent than the now classical Hougen-Watson models, is restricted to catalytic processes in the dehydrogenation of hydrocarbons, amines and alcohols and in the dehydration of alcohols. In this model it is assumed that chemisorption of the reactant takes place on dual or triple adjacent active sites with the organic product adsorbed on the sites initially occupied by the reactant and with the release of H_2 or H_2O without adsorption. The energy of activation of the rate controlling step is calculated from the bond energies involved in adsorption and reaction, and methods are proposed for these calculations.

On the other hand, the Hougen-Watson (9) models are based on the possibility of one of the steps, viz. adsorption, surface reaction or desorption, being the controlling step in the overall reaction. Further the possibility of dissociation of one or more of the reactants or products and the fact that some of them may not be adsorbed is also included in the Hougen-Watson analysis. As such these models appear to have the advantage of greater flexibility.

In the original Hougen-Watson method the rate and adsorption constants were determined by linearising the equation which, for a reaction involving two reactants

A and B (and for chemical reaction controlling), is usually of the form:

$$r = \Delta k p_A p_B \quad .. \quad (4.13)$$

where

$$\Delta = \frac{1}{(1 + \sum p_i K_i)^n} \quad .. \quad (4.14)$$

p_i = partial pressure of the i^{th} component,

and

K_i = adsorption constant constant of the i^{th} component.

The form of the denominator in the Δ expression would be different for adsorption and desorption models. The term, Δ , represents the effect of adsorption on the chemical reaction.

In their studies on the dehydrogenation of butane and butenes over chrome-alumina catalyst, Happel et al (5) have extended the theory of Horiuti (7) and showed that the term Δ can be regarded purely as an empirical function of the partial pressures. According to them the rate equation can be expressed as,

$$r = \Delta' k_s p_A^{1/\gamma} p_B^{1/\gamma} \quad .. \quad (4.15)$$

where

γ = stoichiometric number, which is defined as the number of times an elementary

step in a sequence occurs during a single occurrence of the overall reaction as represented by the overall chemical equation,

and

$$\Delta' = \frac{1}{(1 + \sum p_i^m K_i)^n} \qquad .. \quad (4.16)$$

If γ and m are both assumed to be unity, Equation (4.15) becomes identical with the Hougen-Watson equation for surface reaction. With this restriction the expression for Δ given in Equation (4.14) can be extended to several models, and based on a statistical analysis of the data a suitable model then selected.

The evaluation of γ is often quite difficult, and a procedure has been outlined by Horiuti et al (8) which assumes that γ for the overall reaction is the same as that for the controlling step in the series of elementary steps involved. Thus the exponent $1/\gamma$ in Equation (4.15) represents the reciprocal of the stoichiometric number of the rate controlling step. Considering a simple reaction of the type,

$$A + 2B \longrightarrow 3C, \qquad .. \quad (4.17)$$

the various elementary steps in accordance with the Hougen-Watson model and the corresponding values of stoichiometric numbers are given below:

step	stoichiometric number
A + 1 ⟶ Al (where 1 is an active site)	1
B + 1 ⟶ Bl	2
Al + Bl ⟶ Cl	3
Cl ⟶ C + 1	3

It can be seen that the rate controlling elementary step is probably the adsorption of A. But this can be stated with certainty only after fitting up model equations for different steps. Thus there is no need *a priori* to eliminate γ from the equations, and it should be possible to estimate γ along with the other constants involved in the Δ expression from suitable linear or non-linear procedures.

In the present reaction system the determination of γ by the simple method described for reaction (4.17) is not possible since the reaction is complex and several products are involved. Thus one could include γ in the usual Hougen-Watson equation and estimate its value as mentioned above, or assume it to be unity as has been done in the original Hougen-Watson method and which has been shown to be largely true by the successful application of these models. It is significant that a value of unity for γ gave reasonably satisfactory results for the dehydrogenation of butane and butenes over

chrome-alumina catalyst (5) (although from statistical methods a value of between 1 and 2 was found to be the best).

In the present study γ was assumed to be unity and the constants of the Hougen-Watson models estimated by the usual linearisation methods. In the last few years several non-linear methods of estimating the Hougen-Watson constants have been reported, principally by Lapidus (15) and Watson and collaborators (11,12,13,14). In these methods the restraint imposed by linearising the models is removed and more meaningful constants are obtained. However, since the non-linear methods are best applicable to integrated rate equations or to rate data obtained in a differential reactor, their use is not called for in the present case where the rates have been determined by an indirect procedure as follows.

The reaction rates for each of the three steps were calculated from the values of k_1, k_2 and k_3 given in Tables - 3.2 and 3.3 and from the partial pressures of benzene, oxygen, maleic anhydride, carbon dioxide and water at different residence times (Tables - A.1 to A.13 of Appendix - A). Then it was a matter of fitting the data in accordance with the linearised Hougen-Watson procedure. For the present complex reaction this method of obtaining individual rates was considered superior to

that based on a material balance of the rates of formation or disappearance of reaction components.

4.3.2 Controlling mechanism for the three reaction steps

Reaction step 1

The various mechanisms considered and the corresponding equations for surface reaction controlling are given below (in all these equations the possibility of a triple site mechanism was not considered and therefore it was throughout assumed that one or more of the reactants or products was not adsorbed):

(I) Surface reaction controlling; water not adsorbed.

(a) When reaction occurs between adsorbed benzene and adsorbed oxygen,

$$r_1 = \frac{k_{1s} p_B p_O}{(1 + K_B p_B + K_O p_O + K_M p_M + K_C p_C)^2} \quad .. \quad (4.18)$$

(b) When reaction occurs between adsorbed benzene and oxygen in the gas phase,

$$r_1 = \frac{k_{1s} p_B}{(1 + K_B p_B + K_M p_M + K_C p_C)^2} \quad .. \quad (4.19)$$

(c) When reaction occurs between benzene in gas phase and adsorbed oxygen,

$$r_1 = \frac{k_{1s}p_O}{(1 + K_O p_O + K_M p_M + K_C p_C)^2} \quad .. \quad (4.20)$$

(II) Surface reaction controlling; carbon dioxide not adsorbed.

(a) When reaction occurs between adsorbed benzene and adsorbed oxygen,

$$r_1 = \frac{k_{1s}p_B p_O}{(1 + K_B p_B + K_O p_O + K_M p_M + K_W p_W)^2} \quad .. \quad (4.21)$$

(b) When reaction occurs between adsorbed benzene and oxygen in gas phase,

$$r_1 = \frac{k_{1s}p_B}{(1 + K_B p_B + K_M p_M + K_W p_W)^2} \quad .. \quad (4.22)$$

(c) When reaction occurs between benzene in gas phase and adsorbed oxygen,

$$r_1 = \frac{k_{1s}p_O}{(1 + K_O p_O + K_M p_M + K_W p_W)^2} \quad .. \quad (4.23)$$

(III) Surface reaction controlling; maleic anhydride not

adsorbed.

(a) When reaction occurs between adsorbed benzene and adsorbed oxygen,

$$r_1 = \frac{k_{1s} p_B p_O}{(1 + K_B p_B + K_O p_O + K_C p_C + K_W p_W)^2} \quad .. \quad (4.24)$$

(b) When reaction occurs between adsorbed benzene and oxygen in gas phase,

$$r_1 = \frac{k_{1s} p_B}{(1 + K_B p_B + K_C p_C + K_W p_W)^2} \quad .. \quad (4.25)$$

(c) When reaction occurs between benzene in gas phase and adsorbed oxygen,

$$r_1 = \frac{k_{1s} p_O}{(1 + K_O p_O + K_C p_C + K_W p_W)^2} \quad .. \quad (4.26)$$

(IV) Surface reaction controlling; carbon dioxide and water not adsorbed.

(a) When reaction occurs between adsorbed benzene and adsorbed oxygen,

$$r_1 = \frac{k_{1s}p_B p_O}{(1 + K_B p_B + K_O p_O + K_M p_M)^2} \quad .. \quad (4.27)$$

(b) When reaction occurs between adsorbed benzene and oxygen in gas phase,

$$r_1 = \frac{k_{1s}p_B}{(1 + K_B p_B + K_M p_M)} \quad .. \quad (4.28)$$

(c) When reaction occurs between benzene in gas phase and adsorbed oxygen,

$$r_1 = \frac{k_{1s}p_O}{(1 + K_O p_O + K_M p_M)} \quad .. \quad (4.29)$$

(V) Surface reaction controlling; carbon dioxide and maleic anhydride not adsorbed.

(a) When reaction occurs between adsorbed benzene and adsorbed oxygen,

$$r_1 = \frac{k_{1s}p_B p_O}{(1 + K_B p_B + K_O p_O + K_W p_W)^2} \quad .. \quad (4.30)$$

(b) When reaction occurs between adsorbed benzene and oxygen in gas phase,

$$r_1 = \frac{k_{1s}p_B}{(1 + K_B p_B + K_W p_W)} \quad .. \quad (4.31)$$

(c) When reaction occurs between benzene in gas phase and adsorbed oxygen,

$$r_1 = \frac{k_{1s}p_O}{(1 + K_O p_O + K_W p_W)} \quad .. \quad (4.32)$$

(VI) Surface reaction controlling; maleic anhydride and water not adsorbed.

(a) When reaction occurs between adsorbed benzene and adsorbed oxygen,

$$r_1 = \frac{k_{1s}p_B p_O}{(1 + K_B p_B + K_O p_O + K_C p_C)^2} \quad .. \quad (4.33)$$

(b) When reaction occurs between adsorbed benzene and oxygen in gas phase,

$$r_1 = \frac{k_{1s}p_B}{(1 + K_B p_B + K_C p_C)} \quad .. \quad (4.34)$$

(c) When reaction occurs between benzene in gas phase and adsorbed oxygen,

$$r_1 = \frac{k_{1s}p_O}{(1 + K_O p_O + K_C p_C)} \qquad .. \quad (4.35)$$

None of these equations [(4.18) to (4.35)] yielded all positive constants.* Hence none of the mechanisms considered above would be plausible.

As a next step, similar equations were developed for adsorption of reactant controlling and desorption of product controlling, and their validity ascertained.

It was found that for reaction step 1, the acceptable model would be: adsorption of benzene controlling with carbon dioxide and water not adsorbed on the catalyst surface, the reaction occurring between adsorbed benzene and oxygen in the gas phase. The corresponding equation is given by,

$$r_1 = \frac{K_{1s}p_B}{(1 + K_M p_M)} \qquad .. \quad (4.36)$$

The adsorption mechanism also seems to be indicated by the initial rate plot in accordance with the method of Yang and Hougen (17). In this plot the initial rate is plotted as a function of total pressure or molar

* they were highly negative

ratio of the reactants in the feed. Representative plots of the initial rate as a function of molar ratio of benzene and air in the feed are shown in Figures 4.17 to 4.19. From the nature of these curves it appears that adsorption of one of the reactants might be the controlling step, a fact borne out by the least square analysis of the data described earlier.

Note: In the reaction models given above the constant appearing in the numerator (the so-called kinetic term) is expressed as a single constant, although it may contain an adsorption constant as in the original Hougen-Watson model. This has been done in accordance with the simplified procedure suggested by Corrigan (4).

Reaction step 2

An analysis similar to the one carried out for reaction step 1 was also made for this step. Based on this analysis the following model is proposed:

Adsorption of maleic anhydride controlling, with carbon dioxide and water not adsorbed and reaction occurring between adsorbed maleic anhydride and oxygen in the gas phase. The corresponding equation is

$$r_2 = k_{2s} p_M \qquad .. \quad (4.37)$$

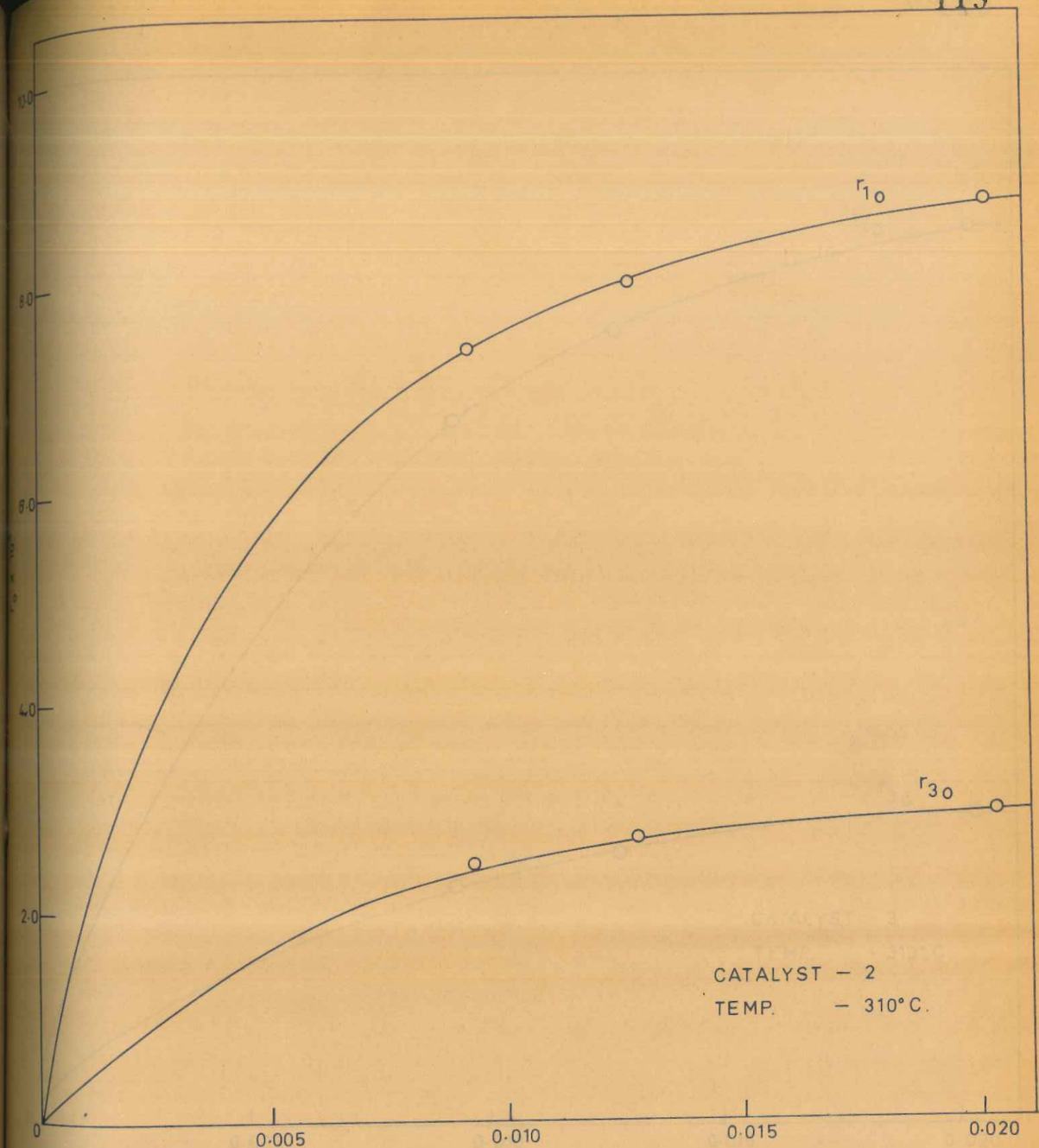

FIG. 4·17. INITIAL RATE PLOTS FOR REACTION STEPS (1) & (3) FOR CATALYST – 2

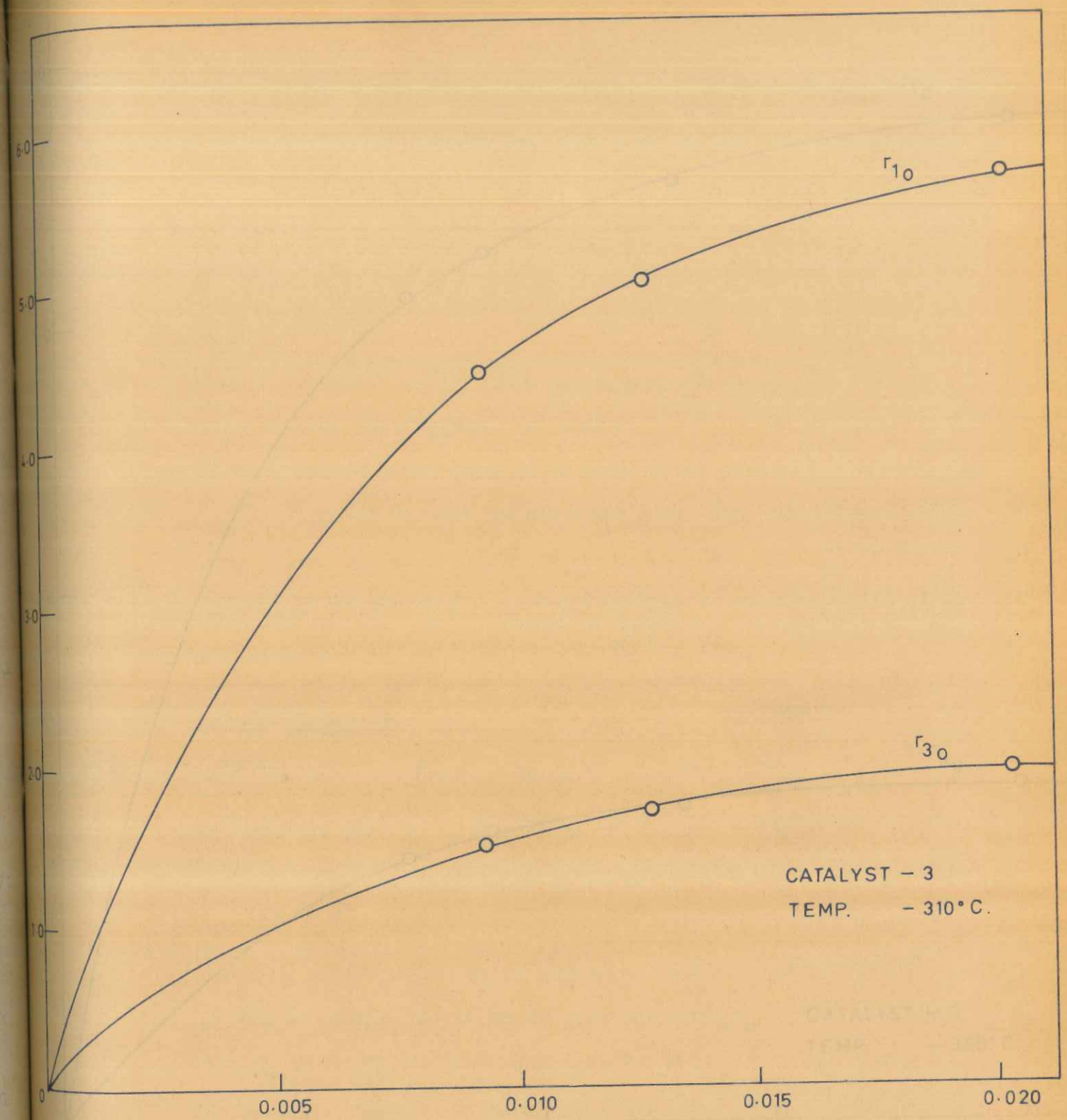

FIG. 4·18. INITIAL RATE PLOTS FOR REACTION STEPS 1 & 3 FOR CATALYST-3

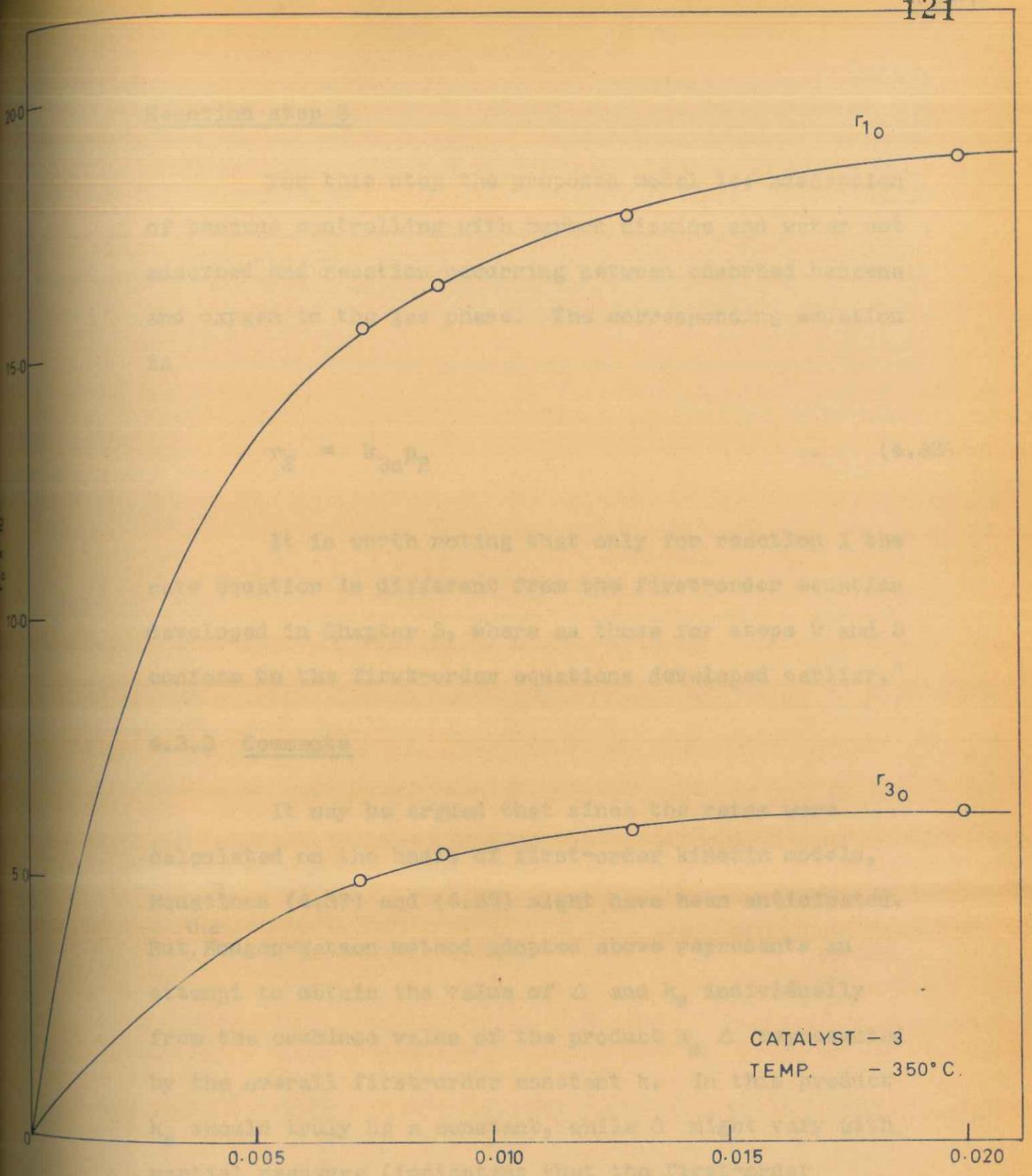

FIG. 4·19. INITIAL RATE PLOTS FOR REACTION STEPS (1) & (3)

FOR CATALYST - 3

Reaction step 3

For this step the proposed model is: adsorption of benzene controlling with carbon dioxide and water not adsorbed and reaction occurring between adsorbed benzene and oxygen in the gas phase. The corresponding equation is

$$r_3 = k_{3s} p_B \qquad .. \quad (4.38)$$

It is worth noting that only for reaction 1 the rate equation is different from the first-order equation developed in Chapter 3, where as those for steps 2 and 3 conform to the first-order equations developed earlier.*

4.3.3 Comments

It may be argued that since the rates were calculated on the basis of first-order kinetic models, Equations (4.37) and (4.38) might have been anticipated. But the Hougen-Watson method adopted above represents an attempt to obtain the value of Δ and k_s individually from the combined value of the product $k_s \Delta$ represented by the overall first-order constant k. In this product k_s should truly be a constant, while Δ might vary with partial pressure (indicating that the first-order constant may not truly be a constant, and that an average value has been obtained which has been assumed to be

* Proposed models are similar to the "splitting off" of olefines in the dealkylation of alkylbenzenes (CEP, 50, 35 (1954)).

constant within certain limits of error). The above analysis has shown that Δ is unity for reaction steps 2 and 3 and is a variable quantity for reaction step 1.

It is apparent from the controlling step models as well as the modified Hinshelwood model that benzene is adsorbed in preference to oxygen (which is probably weakly adsorbed if at all). Since the desorption of oxygen is generally rather a slow step, models based on hydrocarbon adsorption appear to be more plausible.

It has been postulated that water is not adsorbed on the catalyst. In the case of silica gel water is present in various forms. But it is unlikely that at the temperature involved (310-400°C.) it would be present in the adsorbed form, as it has been found that the loss in weight of silica gel is hardly 1-2% at the temperatures involved. Hence it is a reasonable conclusion that no water is present in silica gel at these temperatures (i.e. water is not adsorbed as proposed in the models).

4.3.4 Test of the models

Among the constants k_{1s}, k_{2s}, k_{3s} and K_M, the validity of k_{2s} and k_{3s} (which are identical with the first-order rate constants, k_2 and k_3) has already been confirmed in Chapter 3. The values of the constants, k_{1s} and K_M, are given in Table - 3.2, and the accuracy of

these constants has been tested by calculating the reaction rates using these constants and comparing with the experimental rate values, as shown in Figures 4.20 and 4.21. Representative data for the two catalysts appear in Tables - A.30 and A.31 of Appendix - A. The average error is 13-15%.

4.3.5 Temperature dependence of the constants

The temperature dependence of the adsorption constant, K_M, and the surface reaction constant, k_{ls}, can be expressed in the usual Arrhenius form. These plots are shown in Figures 4.22 and 4.23. These constants have been evaluated for the lower temperature range only since (as shown later) this range corresponds definitely to chemical reaction control. The constants in the high temperature range may not be meaningful and are therefore not included in the table (in spite of the evidence that high temperature range also may be chemically controlled).

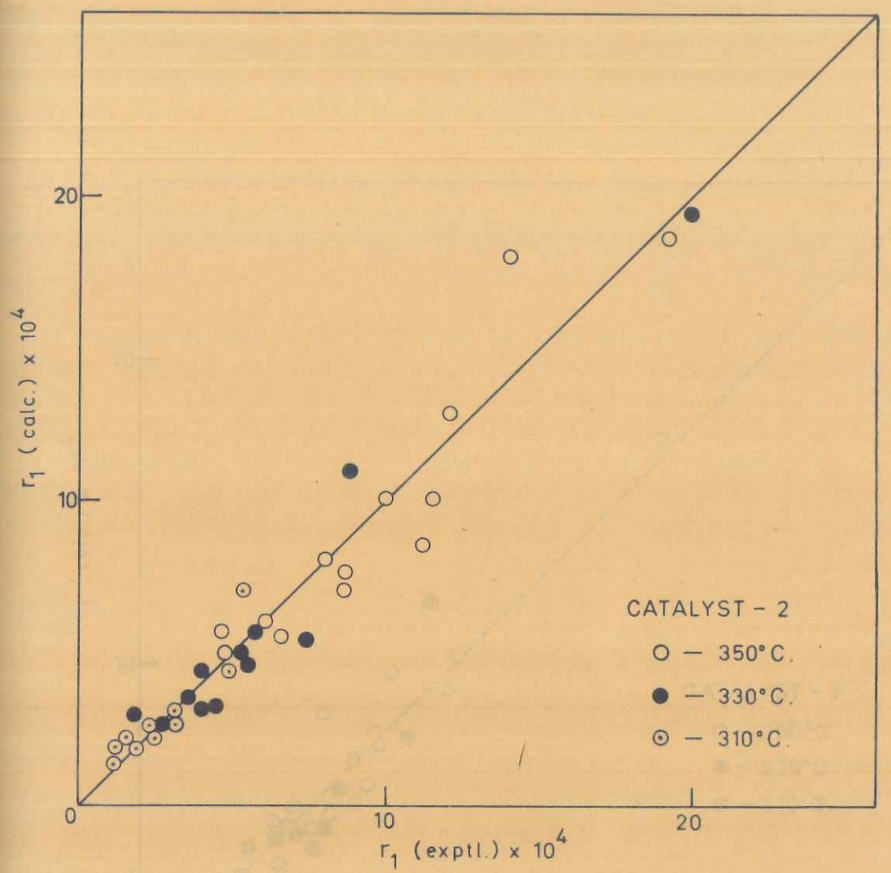

FIG. 4·20. COMPARISON OF CALCULATED AND EXPERIMENTAL RATES FOR HOUGEN-WATSON MODEL FOR MALEIC ANHYDRIDE FORMATION [Equation (4·36)]

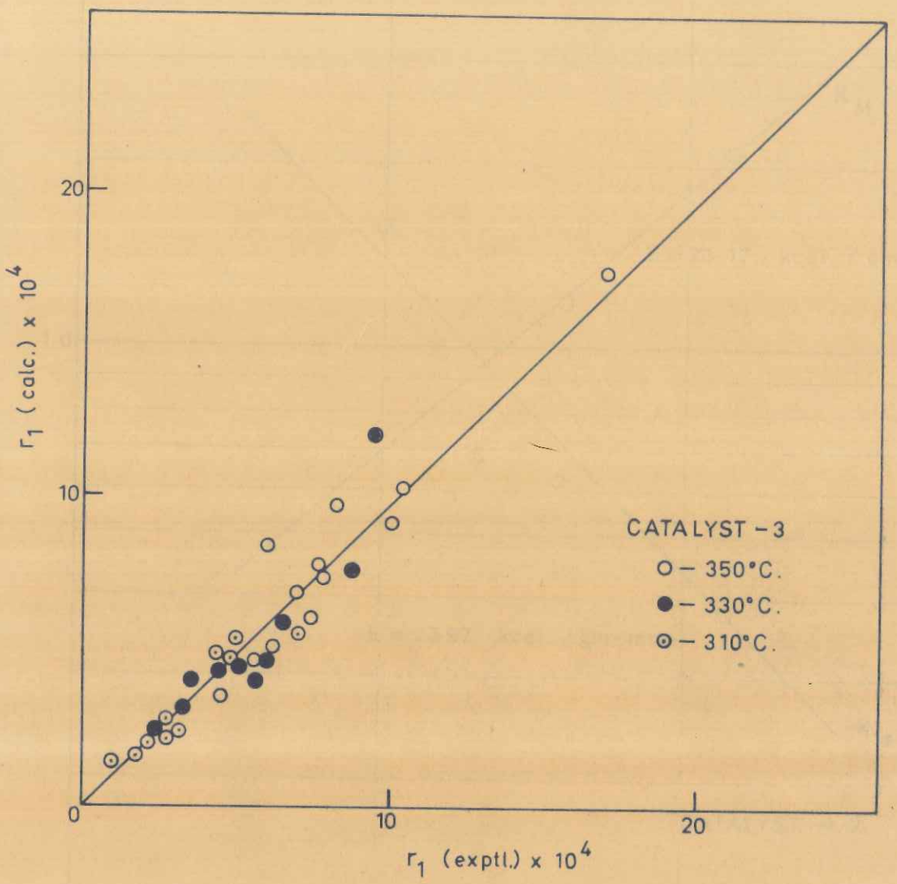

FIG. 4·21. COMPARISON OF CALCULATED AND EXPERIMENTAL RATES FOR THE HOUGEN-WATSON MODEL FOR MALEIC ANHYDRIDE FORMATION [Equation (4·36)]

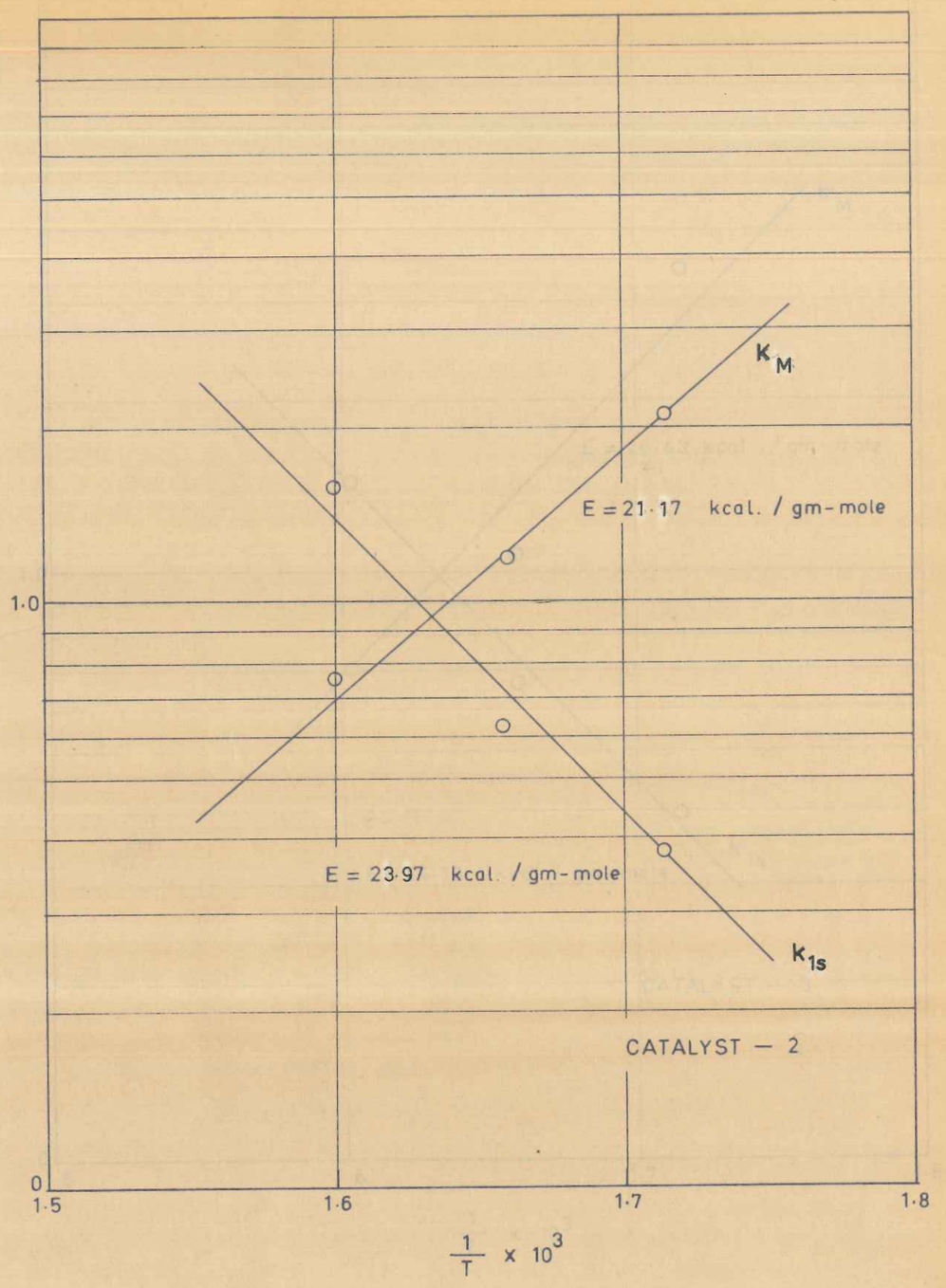

FIG. 4.22. TEMPERATURE DEPENDENCE OF THE RATE CONSTANT k_{1s} AND THE ADSORPTION CONSTANT K_M (maleic anhydride) FOR THE ADSORPTION CONTROL MODEL WITH CATALYST-2

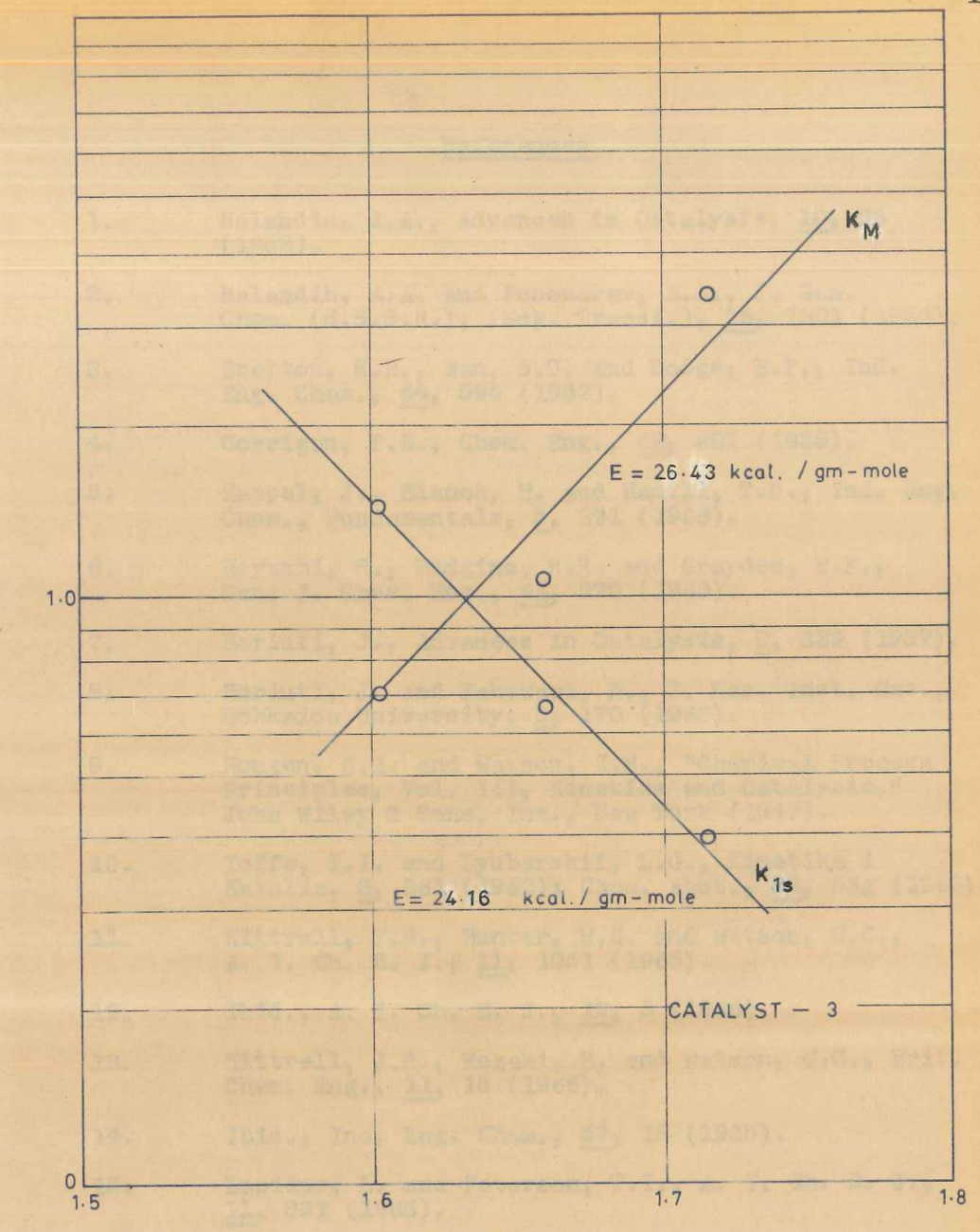

FIG. 4·23. TEMPERATURE DEPENDENCE OF THE RATE CONSTANT k_{1s} AND THE ADSORPTION CONSTANT K_M (maleic anhydride) FOR ADSORPTION CONTROL MODEL WITH CATALYST-3

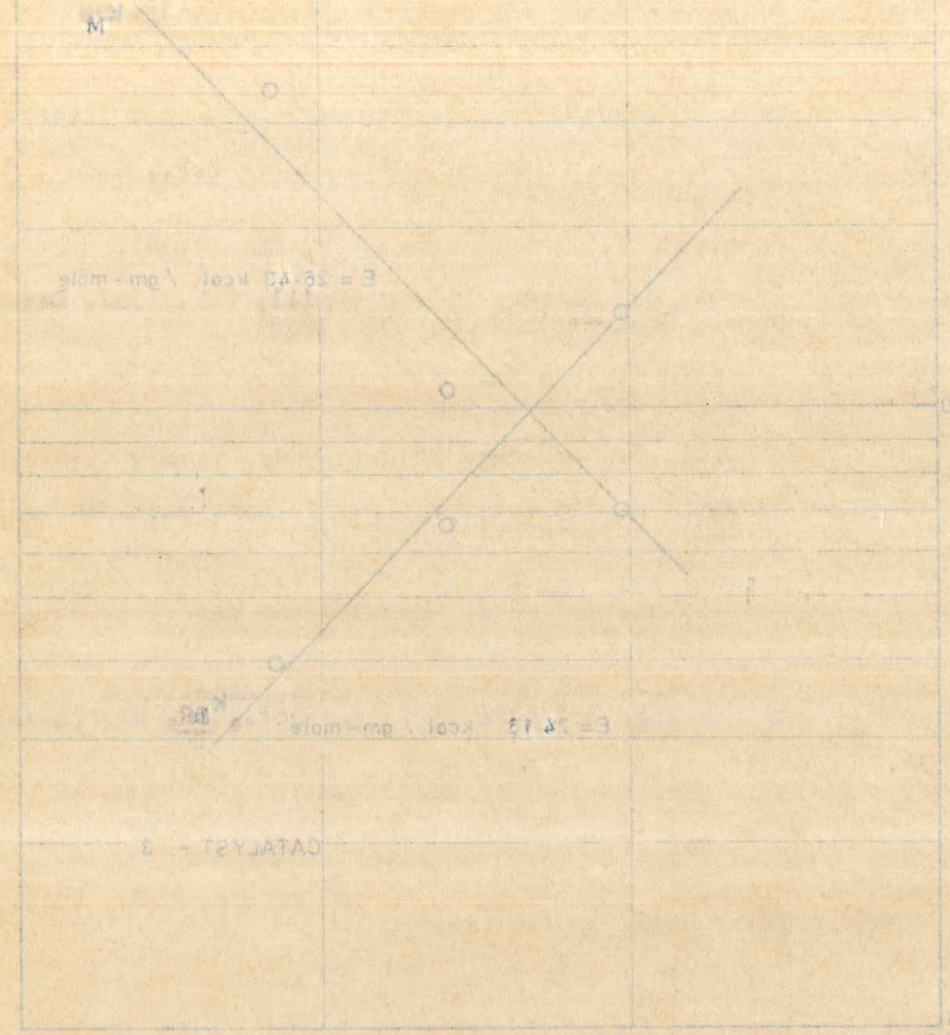

References

1. Balandin, A.A., Advances in Catalysis, 10, 96 (1958).

2. Balandin, A.A. and Ponomarev, A.A., J. Gen. Chem. (S.S.S.R.), (Eng. Transl.), 26, 1301 (1956).

3. Bretton, R.H., Wan, S.U. and Dodge, B.F., Ind. Eng. Chem., 44, 594 (1952).

4. Corrigan, T.E., Chem. Eng., 62, 201 (1955).

5. Happel, J., Blanck, H. and Hamill, T.D., Ind. Eng. Chem., Fundamentals, 5, 291 (1966).

6. Hayashi, R., Hudgins, R.R. and Graydon, W.F., Can. J. Chem. Eng., 41, 220 (1963).

7. Horiuti, J., Advances in Catalysis, 9, 339 (1957).

8. Horiuti, J. and Takezawa, N., J. Res. Inst. Cat., Hokkaido University, 8, 170 (1960).

9. Hougen, O.A. and Watson, K.M., "Chemical Process Principles, Vol. III, Kinetics and Catalysis," John Wiley & Sons, Inc., New York (1947).

10. Ioffe, I.I. and Lyubarskii, L.G., Kinetika i Kataliz, 3, 261 (1962); Chem. Abst., 58, 55g (1963).

11. Kittrell, J.R., Hunter, W.G. and Watson, C.C., A. I. Ch. E. J., 11, 1051 (1965).

12. Ibid., A. I. Ch. E. J., 12, 5 (1966).

13. Kittrell, J.R., Mezaki, R. and Watson, C.C., Brit. Chem. Eng., 11, 15 (1966).

14. Ibid., Ind. Eng. Chem., 57, 18 (1965).

15. Lapidus, L. and Peterson, T.I., A. I. Ch. E. J., 11, 891 (1965).

16. Mars, P. and van Krevelen, D.W., Chem. Eng. Sci., 3, 41 (1954); Special Supplement.

17. Yang, K.H. and Hougen, O.A., Chem. Eng. Prog., 46, 146 (1950).

CHAPTER-5

CONTROLLING REGIMES IN BENZENE OXIDATION

Chapter 5

CONTROLLING REGIMES IN BENZENE OXIDATIONS

5.1 GENERAL THEORETICAL DEVELOPMENT

The effect of temperature on the rate constants can form a rational basis for distinguishing between the regimes of control in a chemical reaction. At relatively low temperatures chemical reaction is normally the controlling mechanism, since the reaction rate is quite low (being an exponential function of temperature). This is characterized by an activation energy of over 10 kcal./gm-mole (frequently > 20 kcal./gm-mole). In the usual Arrhenius plot a steep line therefore results for the chemical control regime, as shown by line (1) of Figure 5.1

As the temperature is raised the exponential dependence of rate on temperature leads to a situation where chemical reaction becomes extremely fast and the rate of transfer of the reactants to the reaction zone becomes the controlling step. In this case the effect of temperature would be reflected by its effect on the physical properties (mainly diffusion) which characterize mass transfer. Thus a line with a considerably lower slope, corresponding to an activation energy of about 2 kcal./gm-mole (usually < 1 kcal./gm-mole), is obtained

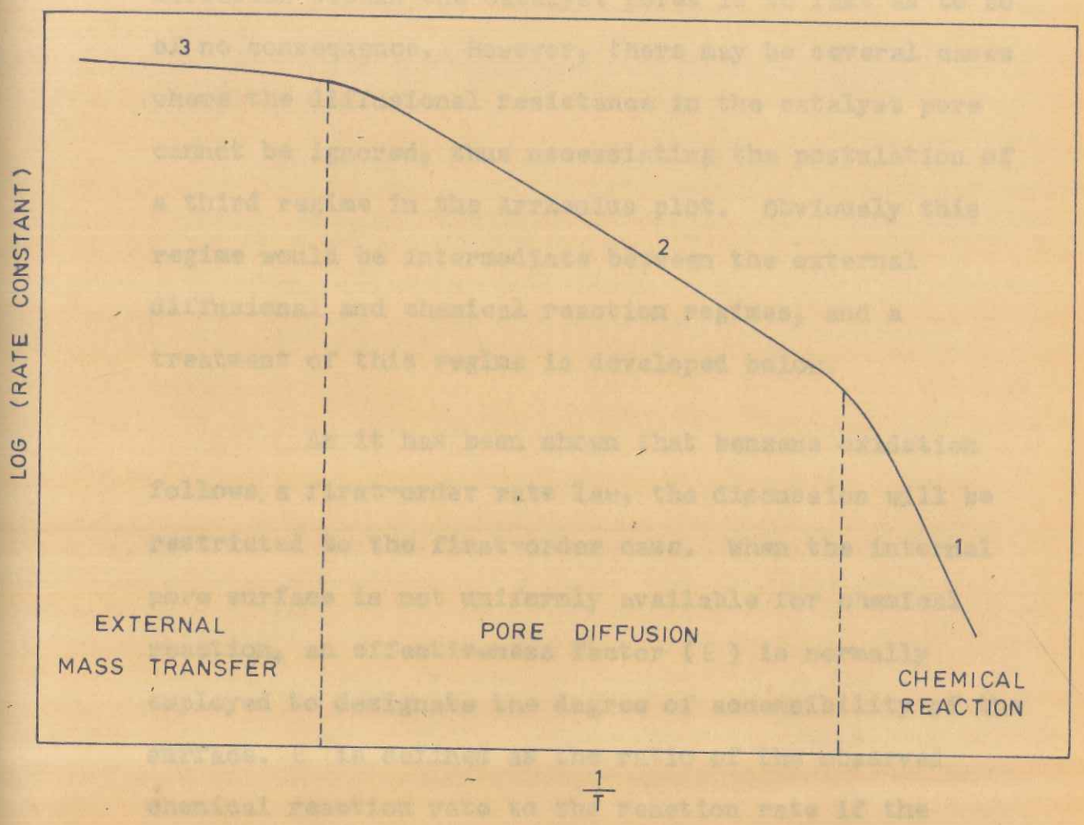

FIG. 5.1. REGIMES OF CONTROL IN A GAS-SOLID REACTION

in the Arrhenius plot as shown by line (3) of Figure 5.1.

The discussion presented above assumes that diffusion within the catalyst pores is so fast as to be of no consequence. However, there may be several cases where the diffusional resistance in the catalyst pore cannot be ignored, thus necessiating the postulation of a third regime in the Arrhenius plot. Obviously this regime would be intermediate between the external diffusional and chemical reaction regimes, and a treatment of this regime is developed below.

As it has been shown that benzene oxidation follows a first-order rate law, the discussion will be restricted to the first-order case. When the internal pore surface is not uniformly available for chemical reaction, an effectiveness factor (ϵ) is normally employed to designate the degree of accessibility of the surface. ϵ is defined as the ratio of the observed chemical reaction rate to the reaction rate if the concentration of the reactant within the pores is uniformly equal to the concentration at the surface. Thus the reaction rate (expressed in concentration units) can be represented as

$$r_c = \epsilon k_c C \qquad .. \qquad (5.1)$$

It has been shown that ϵ is a function of the Thiele

modulus, which for a first-order reaction is defined by,

$$\emptyset = L \sqrt{k_c/D_e} \qquad .. \qquad (5.2)$$

where

L = characteristic length defined by

v_p/a_p

The general nature of the $\epsilon - \emptyset$ plot for a first-order reaction is shown in Figure 5.3. For values of $\emptyset$ greater than 2, one may write,

$$\epsilon = \frac{1}{L \sqrt{k_c/D_e}} \qquad .. \qquad (5.3)$$

or

$$\epsilon = 1/L \sqrt{D_e/k_c} \qquad .. \qquad (5.4)$$

Substituting Equation (5.4) in Equation (5.1),

$$r_c = 1/L \sqrt{D_e k_c} \cdot C \qquad .. \qquad (5.5)$$

The effective diffusion coefficient D_e and the reaction velocity constant k_c can be expressed in the form of the usual Arrhenius equation:

$$k_c = A_r \, e^{-E_r/RT} \qquad .. \qquad (5.6)$$

$$D_e = A_D\, e^{-E_D/RT} \qquad .. \qquad (5.7)$$

where E_r and E_D are the activation energies for reaction and diffusion respectively.

Substituting Equations (5.6) and (5.7) in (5.5),

$$r_c = 1/L \left[A_D\, A_r\, e^{-E_r/RT} \cdot e^{-E_D/RT} \right]^{\frac{1}{2}} C \qquad .. \qquad (5.8)$$

or

$$r_c = K' e^{-\frac{(E_r + E_D)}{2RT}} \qquad .. \qquad (5.9)$$

where

$$K' = 1/L\, (A_D\, A_r)^{\frac{1}{2}}$$

Comparing Equation (5.9) with the standard form,

$$r_c = A\, e^{-E/RT} \qquad .. \qquad (5.10)$$

we obtain

$$E = \frac{E_D + E_r}{2} \qquad .. \qquad (5.11)$$

or

$$E = E_r/2 \text{ (if } E_D \text{ is low compared to } E_r)$$

Thus the value of the activation energy, E, in the pore diffusion region tends to be half the value for the chemical control regime.

Line (2) of Figure 5.1 represents the regime where internal pore diffusion is operative. It is thus possible to have all the three regimes of control with a suitable variation of temperature or catalyst properties (like pore size and characteristic length).

It has been pointed out by Petersen (6) that external mass transfer can never by itself be the controlling step in a chemical reaction, and that whenever experimental results indicate external mass transfer control, there is also a simultaneous diffusional resistance, the magnitude of which is invariably greater than the mass transfer resistance. This concept will be developed further in the next section for the oxidation of benzene.

5.2 IDENTIFICATION OF THE CONTROLLING REGIMES IN BENZENE OXIDATION

Arrhenius plots of the different rate constants for the two catalysts employed in this study are shown

in Figures 3.1 and 3.2. It will be seen that for all the constants the activation energy in the higher temperature range is considerably lower than for the lower temperature range. The temperature ranges and the corresponding activation energies are:

310 - 350°C.	--	20 kcal./gm-mole.
350 - 400°C.	--	2 kcal./gm-mole.

Obviously in the lower temperature range (310-350°C.) chemical reaction controls, where as in the higher temperature range (350-400°C.) external diffusion (mass transfer) would appear to be the limiting resistance. The transition from one region to another is generally not as abrupt as has been found in this case. It is likely that, if the transition region is studied more closely, a gradual shift in the mechanism would be observed. This was not done in the present study since the shift in the mechanism was unmistakable.

The magnitude of the activation energy in the high temperature range appears to be somewhat higher than for external diffusion control (for which it should generally be less than 1 kcal./gm-mole), but too low for pore diffusion alone to be the controlling step (for which the magnitude of the activation energy should be E (chemical)/2, or about 10 kcal./gm-mole). Therefore

it appears desirable to examine this regime further. As a first step in this direction, the effect of pore diffusion was experimentally determined and also evaluated from the criterion proposed by Weisz and Prater (9).

Experiments were carried out at 350°C. with catalyst - 3 of the following size ranges:

-5 +12, -12 +22, -22 +36, -36 +60 (B.S.S. mesh)

It was found that the data obtained for each of these size ranges followed first-order kinetics. In order to elucidate the role of pore diffusion it is necessary to express the observed rate constants as a function of the particle size. For this purpose the rate constant (k_1+k_3) for the total oxidation of benzene was used in all the calculations since the behaviour of the individual constants, k_1, k_2 and k_3, is similar to that of the rate constant for total benzene disappearance (k_1+k_3). Henceforth the rate constant for total benzene disappearance, (k_1+k_3), will be designated as k.

Since the absence of pore diffusion cannot be assumed *a priori* the rate constants determined would be ϵ k (and not merely k) in accordance with Equation (5.1). A plot of ϵ k vs. particle size should give a line which levels off as the particle size is decreased, the

asymptotic value corresponding to the intrinsic rate constant, k. The effectiveness factor, , for any size can then be determined from the relation,

$$\epsilon = \epsilon\, k/k \qquad .. \qquad (5.12)$$

A plot of k (experimentally determined value of the rate constant for different particle sizes) as a function of particle size is shown in Figure 5.2. The values of ϵ for the different particle sizes were determined in accordance with Equation (5.12), and are listed in Table - 5.1. It can be seen that ϵ is practically unity for all the catalyst sizes, leading to the conclusion that pore diffusion is not significant. This is further examined below.

The Thiele modulus, $\emptyset$, for the present catalyst (catalyst - 3) was evaluated as follows: The effective diffusivity, D_e, was first calculated from the equation presented below (8) (since unpelletted silica gel particles were used, it was assumed that Knudsen flow was operative):

$$D_e = 19{,}400 \frac{\theta^2}{\tau S \rho_p} \sqrt{T/M} \qquad .. \qquad (5.13)$$

Assuming a tortuosity factor (τ) of 1.2 and using the

Table - 5.1

Experimental effectiveness factors for different values of the Thiele modulus

Particle size B.S.S. mesh	$kx10^3$	ϵ	$\emptyset$
- 5 +12	1.811	0.873	0.1612
-12 +22	2.033	0.977	0.0713
-22 +36	2.043	0.984	0.0379
-36 +60	2.081	1.000	0.0228

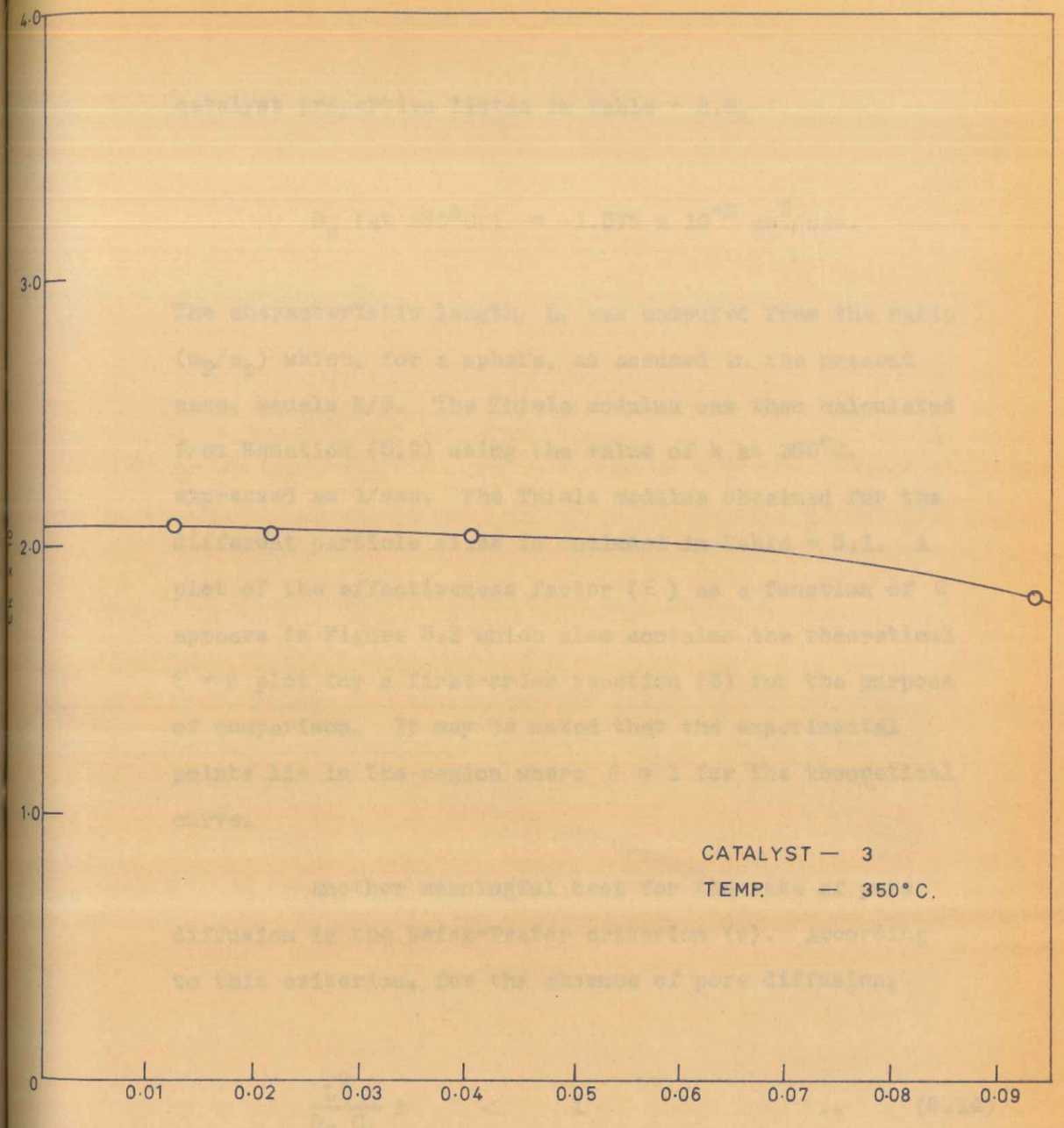

FIG. 5·2. EFFECT OF PARTICLE SIZE ON OBSERVED RATE CONSTANT

catalyst properties listed in Table - 3.6,

$$D_e \text{ (at } 350^\circ\text{C.)} = 1.575 \times 10^{-3} \text{ cm.}^2\text{/sec.}$$

The characteristic length, L, was computed from the ratio (v_p/a_p) which, for a sphere, as assumed in the present case, equals R/3. The Thiele modulus was then calculated from Equation (5.2) using the value of k at 350°C. expressed as 1/sec. The Thiele modulus obtained for the different particle sizes is included in Table - 5.1. A plot of the effectiveness factor (ϵ) as a function of $\emptyset$ appears in Figure 5.3 which also contains the theoretical $\epsilon - \emptyset$ plot for a first-order reaction (8) for the purpose of comparison. It may be noted that the experimental points lie in the region where $\epsilon = 1$ for the theoretical curve.

Another meaningful test for the rate of pore diffusion is the Weisz-Prater criterion (9). According to this criterion, for the absence of pore diffusion,

$$\frac{L^2}{D_e C_i} r \quad < \quad 1 \qquad .. \qquad (5.14)$$

Making use of the following representative values,

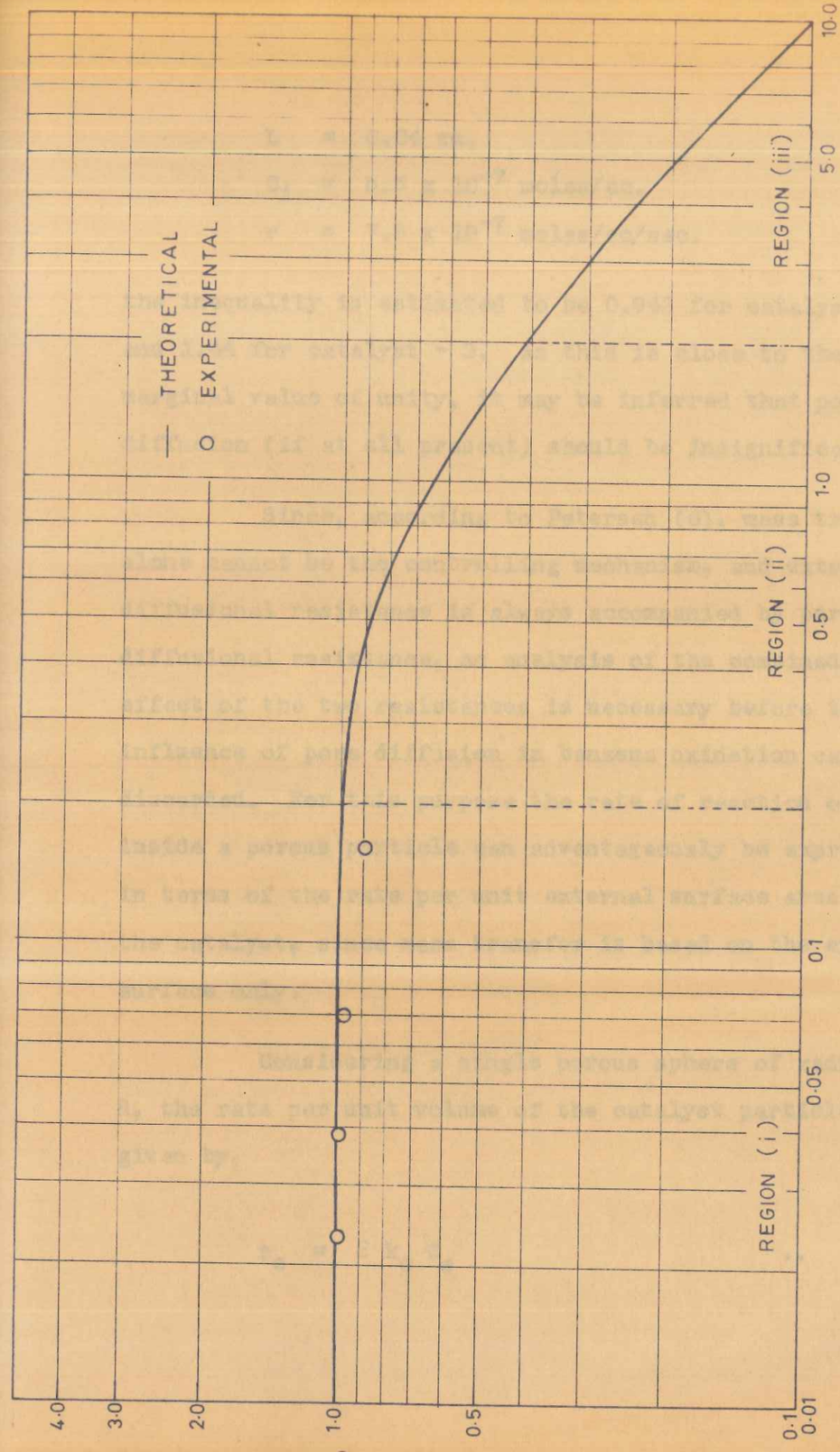

FIG. 5·3. THEORETICAL EFFECTIVENESS FACTOR (ε) CURVE FOR A FIRST-ORDER REACTION, SHOWING ALSO THE EXPERIMENTAL VALUES OF ε

$L = 0.04$ cm.

$C_i = 5.5 \times 10^{-7}$ moles/cc.

$r = 7.8 \times 10^{-7}$ moles/cc/sec.

the inequality is estimated to be 0.943 for catalyst - 2 and 1.44 for catalyst - 3. As this is close to the marginal value of unity, it may be inferred that pore diffusion (if at all present) should be insignificant.

Since, according to Petersen (6), mass transfer alone cannot be the controlling mechanism, and external diffusional resistance is always accompanied by pore diffusional resistance, an analysis of the combined effect of the two resistances is necessary before the influence of pore diffusion in benzene oxidation can be discarded. For this purpose the rate of reaction occurring inside a porous particle can advantageously be expressed in terms of the rate per unit external surface area of the catalyst, since mass transfer is based on the external surface only.

Considering a single porous sphere of radius, R, the rate per unit volume of the catalyst particle is given by,

$$r_c = \epsilon k_c C_s \qquad .. \qquad (5.15)$$

where,

C_s = surface concentration of the reactant

r_c = reaction rate based on concentration units, $\frac{\text{gm-mole}}{\text{hr. gm. cat.}}$

k_c = velocity constant, $\frac{\text{cc.}}{\text{hr. gm. cat.}}$

If the rate is expressed as gm-mole/hr.cc. of catalyst (r'_c),

$$r'_c = r_c \rho_p \quad .. \quad (5.16)$$

giving

$$r'_c = \epsilon k_c \rho_p C_s \quad .. \quad (5.17)$$

If the reaction velocity constant is now expressed in terms of unit surface area of the catalyst,

$$k_c = k_s S \quad .. \quad (5.18)$$

where k_s has the units (cm./hr.) and S is the surface area (cm^2.) per unit weight (gm.) of the catalyst. Substituting Equation (5.18) in Equation (5.17),

$$r'_c = \epsilon k_s S \rho_p C_s \quad .. \quad (5.19)$$

For a single particle of spherical shape, the

rate is given by,

$$r'_p = 4/3\,\pi R^3 (k_s S \rho_p C_s) \epsilon \quad .. \quad (5.20)$$

Since the surface area is $4\pi R^2$, the rate (r'_{pe}) for a spherical particle per unit external surface area will be given by,

$$r'_{pe} = R/3 (k_s S \rho_p C_s) \epsilon \quad .. \quad (5.21)$$

This may be expressed as,

$$r'_{pe} = k'_s C_s \quad .. \quad (5.22)$$

where

$$k'_s = \frac{R k_s S \rho_p}{3} \epsilon \quad .. \quad (5.23)$$

The constant, k'_s, is obviously a rate constant based on external surface area (as against k_s based on the total surface area) and has the units of length/time (cm./hr. in this case).

The basic differential equation for a non-porous spherical catalyst pellet immersed in a large medium of stagnant reactant is (6):

$$D \frac{d}{dR'} \left[R'^2 \frac{dC}{dR'} \right] = 0 \quad .. \quad (5.24)$$

where R' represents the radial coordinate. The boundary condition for this equation is given by,

$$r'_{pe} = D\left(\frac{dC}{dR'}\right)_{R'=R} \qquad .. \qquad (5.25)$$

This condition denotes that the heterogeneous rate based on external surface area should be equal to the rate of diffusion at the surface of the particle. Equation (5.25) can be made dimensionless by the following transformations:

$$\bar{C} = \frac{C - C_b}{C_b} \qquad .. \qquad (5.26)$$

and

$$\bar{R} = R'/R \qquad .. \qquad (5.27)$$

the resulting equation being

$$r'_{pe} = \left(\frac{D\ C_b}{R}\right)\left(\frac{d\bar{C}}{d\bar{R}}\right)_{\bar{R}=1} \qquad .. \qquad (5.28)$$

Equation (5.22) can also be expressed in dimensionless form,

$$r'_{pe} = k'_s\ C_b\ (1 + \bar{C}_s) \qquad .. \qquad (5.29)$$

by using the transformation,

$$\bar{C}_s = \frac{C_s - C_b}{C_b} \quad .. \quad (5.30)$$

Combining Equations (5.28) and (5.29),

$$\left(\frac{d\bar{C}}{d\bar{R}}\right)_{\bar{R}=1} = \left(\frac{k'_s R}{D}\right)(1 + \bar{C}_s) \quad .. \quad (5.31)$$

or

$$\left(\frac{d\bar{C}}{d\bar{R}}\right)_{\bar{R}=1} = \Theta\,(1 + \bar{C}_s) \quad .. \quad (5.32)$$

where

$$\Theta = \left(\frac{k'_s R}{D}\right) \quad .. \quad (5.33)$$

From Equations (5.33) and (5.23),

$$\Theta = \frac{R^2 k_s S \rho_p}{3D} \epsilon \quad .. \quad (5.34)$$

This may be written as,

$$\Theta = \frac{R^2 (k_s S \rho_p)}{3D_e} \left(\frac{D_e}{D}\right) \epsilon \quad .. \quad (5.35)$$

or

$$\theta = 3\phi^2\left(\frac{D_e}{D}\right)\epsilon \qquad .. \qquad (5.36)$$

where,

$$\phi = R/3\sqrt{\frac{k_s S \rho_p}{D_e}} \qquad .. \qquad (5.37)$$

Equation (5.36) represents the relationship between the dimensionless group, θ (calculated on the basis of unit external surface area), the Thiele modulus, ϕ (which is a measure of internal pore diffusion) and a tortuosity term represented by (D_e/D). It now remains to eliminate ϵ from this equation, so that a relationship can be obtained exclusively between θ and ϕ for a given ratio of (D_e/D).

One can identify three regions in the $\epsilon - \phi$ plot:

(i) $\phi < 0.2$, where $\epsilon = 1$.

(ii) $0.2 < \phi < 2$, transition region.

(iii) $\phi \geqslant 2$, where $\epsilon = 1/\phi$.

Region (iii) has been discussed by Petersen (6) in detail. The present reaction, however, falls in region (i). In the following paragraphs, the development of Petersen for

region (iii) is briefly summarized, and the treatment is then extended to region (i).

Region (iii)

As mentioned above, for this region $\epsilon = 1/\phi$, and Equation (5.36) reduces to,

$$\theta = 3\phi\left(\frac{D_e}{D}\right) \qquad .. \qquad (5.38)$$

Let us now consider Figure 5.4 in which concentration gradients are shown both for external diffusion and internal pore diffusion. The existence of a concentration gradient inside the pore is accounted for by the introduction of the effectiveness factor, ϵ . Similarly the existence of an external mass transfer gradient can be accounted for by a mass transfer factor, δ . If this is done, the reaction rates can be expressed in terms of the bulk concentration (which is the concentration measured experimentally). Thus we may define a mass transfer factor, δ, as

$$C_s = \delta C_b \qquad .. \qquad (5.39)$$

δ can be expressed in terms of the dimensionless concentration, $\bar{C}_s$, by combining Equations (5.30) and (5.39). Thus,

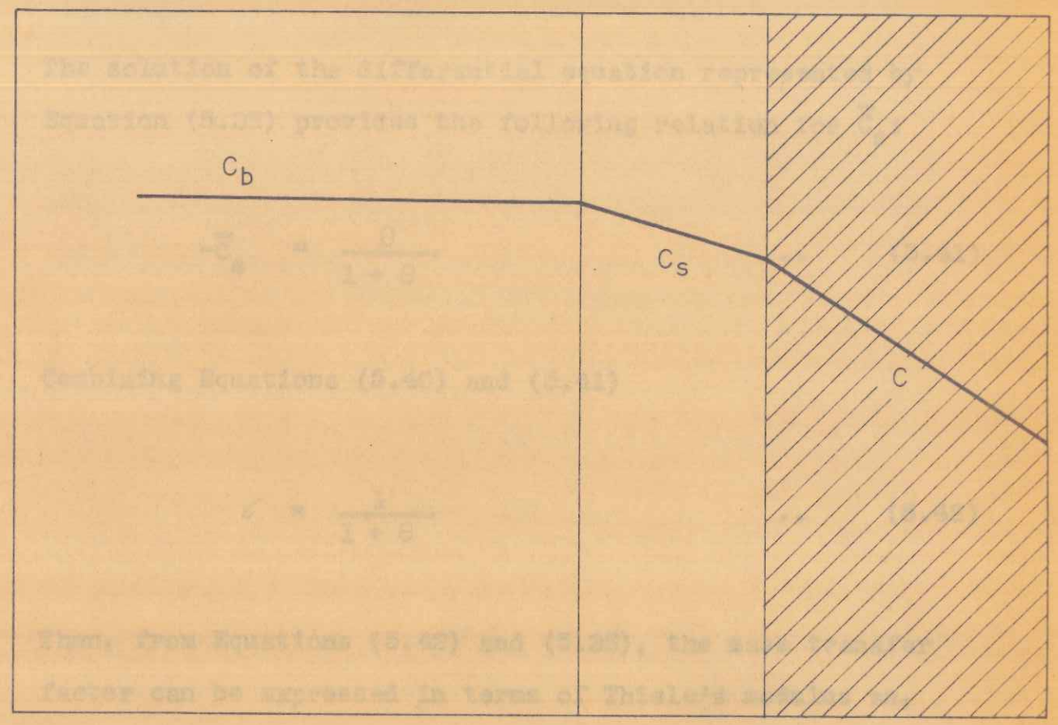

FIG. 5.4. CONCENTRATION PROFILES IN A SYSTEM WHERE EXTERNAL MASS TRANSFER AND PORE DIFFUSION ARE SIMULTANEOUSLY OPERATIVE

$$\sigma = 1 + \bar{C}_s \qquad .. \qquad (5.40)$$

The solution of the differential equation represented by Equation (5.32) provides the following relation for $\bar{C}_s$:

$$-\bar{C}_s = \frac{\theta}{1+\theta} \qquad .. \qquad (5.41)$$

Combining Equations (5.40) and (5.41)

$$\sigma = \frac{1}{1+\theta} \qquad .. \qquad (5.42)$$

Then, from Equations (5.42) and (5.38), the mass transfer factor can be expressed in terms of Thiele's modulus as,

$$\sigma = \frac{1}{1 + 3\emptyset\,(D_e/D)} \qquad .. \qquad (5.43)$$

Equation (5.43) fulfills the objective of this development, viz., to relate the mass transfer factor (σ) with the Thiele modulus ($\emptyset$).

It must be emphasised that Equation (5.43) holds good for region (iii) only, and is not operative for benzene oxidation, where ϵ is almost unity. Extrapolation of Equation (5.43) to $\epsilon = 1$ is not warranted since one

would then cross over to region (i).

Region (i)

As stated earlier, the present study on the oxidation of benzene falls in region (i) of the $\epsilon - \emptyset$ curve, where ϵ is unity. For this region, Equation (5.36) can be written as,

$$\theta = 3\emptyset^2 \frac{D_e}{D} \qquad .. \quad (5.44)$$

Combining this with Equation (5.42),

$$\zeta = \frac{1}{1 + 3\emptyset^2 (D_e/D)} \qquad .. \quad (5.45)$$

In this region $\emptyset$ is always less than about 0.2, and since (D_e/D) is of the order of 0.1 or less, from Equation (5.45) it may be seen that ζ is also substantially unity. In the case of benzene oxidation,

$$\frac{D_e}{D} = 5.102 \times 10^{-3}$$

and therefore ζ is far closer to unity than in cases where (D_e/D) is of the order of 0.1.

From the development presented above it would appear that in region (i), where the effect of pore diffusion is absent, the effect of mass transfer is also absent. This fact, combined with the conclusion in respect of region (iii), suggests that external mass transfer cannot be operative in the region where ϵ is unity and that, when it becomes operative (in the region $\epsilon < 1$), the resistance due to pore diffusion is of a higher order. In the case of benzene oxidation, since $\epsilon = 1$, it follows that external mass transfer is also negligible. It may be recalled that this was anticipated in Chapter 3, where external mass transfer was estimated to be negligible from the charts of Hougen et al (10).

In the lower temperature range one can conclude from the magnitude of the activation energy that chemical reaction is the controlling step. In spite of the low activation energy observed in the higher temperature range, it may be concluded (in view of the absence of diffusional effects) that in this region also probably chemical reaction controls, the fall in activation energy being due to a change in the structure or chemical character of the catalyst used. A similar fall in the activation energy at higher temperatures has been reported by Pinchbeck (7) and Ioffe et al (5) in the oxidation of naphthalene; by Dixon (1) in his review on the oxidation of maleic anhydride carried out by Holsen (4); and by

Hedden (3) in the oxidation of coal by air.

Hammar (2) reported mass transfer to be the controlling step in the oxidation of benzene, though a high value of the activation energy (28 ± 4 kcal./gm-mole) was obtained. In view of this inherent discrepancy, it would be logical to speculate that chemical reaction is the limiting step.

On the basis of the findings reported in this chapter, it may be concluded that:

(1) Chemical reaction appears to be the controlling resistance over the entire temperature range.

(2) While in the temperature range, 310-350°C., this conclusion is substantiated by the magnitude of the activation energy (which is about 20 kcal./gm-mole), in the higher temperature range (350-400°C.) an activation energy of 2 kcal./gm-mole seems to suggest mass transfer control.

(3) A detailed analysis of external diffusion and pore diffusion indicates that neither of these is operative and that the low activation energy in the higher temperature range is attributable to a favourable change in the structure or orientation of the catalyst.

References

1. Dixon, J.K. and Longfield, J.E., "Catalysis," (P.H. Emmett, ed.); Vol. VII, Chap. 3, Reinhold Publishing Corporation, New York (1960).

2. Hammar, C.G.B., Svensk Kem. Tid., 64, 165 (1952); Chem. Abst., 46, 3945d (1952).

3. Hedden, K., Chem. Eng. Sci., 14, 317 (1961).

4. Holsen, J.N., Ph.D. Thesis, "An investigation of the catalytic vapour phase oxidation of benzene," Washington Univ., St. Louis, Missouri (1954).

5. Ioffe, I.I. and Sherman, Yu. G., J. Phys. Chem., (U.S.S.R.), 28, 2095 (1954); Chem. Abst., 50, 10691 (1956).

6. Petersen, E.E., "Chemical Reaction Analysis," Prentice-Hall, Inc., New Jersey (1965).

7. Pinchbeck, P.H., Chem. Eng. Sci., 6, 105 (1957).

8. Satterfield, C.N. and Sherwood, T.K., "The Role of Diffusion in Catalysis," Addison-Wesley Publishing Co. (1963).

9. Weisz, P.B. and Prater, C.D., Advances in Catalysis, 6, 144 (1954).

10. Yoshida, F., Ramaswamy, D. and Hougen, O.A., Am. Inst. Chem. Eng., Convention, Washington, D.C., December 1960.

NOMENCLATURE

NOMENCLATURE

a	-	constant.
a_m	-	external surface area of pellet per unit mass, $cm.^2/gm.$
a_v	-	external surface area per unit volume of catalyst bed, $cm.^2/cm.^3$
A	-	Arrhenius constant.
C	-	concentration, gm-mole/cc.
$\overline{C}$	-	dimensionless concentration, $\frac{C - C_b}{C_b}$.
C_b	-	bulk concentration, gm-mole/cc.
C_s	-	surface concentration, gm-mole/cc.
d_p	-	particle diameter, cm.
D	-	bulk diffusion coefficient, $cm.^2/sec.$
D_e	-	effective diffusion coefficient, $cm.^2/sec.$
E	-	activation energy, kcal./gm-mole.
F	-	feed rate, gm-mole/hr.
G	-	mass velocity, $gm./hr.cm.^2$
G_m	-	molal mass velocity, $gm\text{-}mole/hr.cm.^2$
k_1, k_2, k_3	-	reaction velocity constants for the steps 1, 2 and 3 shown in the reaction scheme, gm-mole/(hr.) (gm. cat.) (atm.).
k_a, k_B	-	specific rate of adsorption of oxygen and benzene respectively, gm-mole/(hr.) (gm. cat.) (atm.).
k_c	-	reaction velocity constant, cc./(hr.) (gm. cat.).

k_r	-	specific rate of total reaction of benzene, gm-mole/(hr.) (gm. cat.) (atm.).
k_{ro}	-	specific rate of total reaction of benzene at the initial condition, gm-mole/(hr.) (gm. cat.) (atm.).
k_s	-	reaction velocity constant per unit surface area, cm./hr.
k_s'	-	reaction velocity constant based on external surface area, cm./hr.
k_{1s}, k_{2s}, k_{3s}	-	rate constants in the Hougen-Watson models.
K'	-	constant.
$K_B, K_C, K_M,$ K_O, K_W	-	adsorption constants for benzene, carbon dioxide, maleic anhydride, oxygen and water, respectively.
l	-	active site.
L	-	characteristic length, cm.
m	-	order of reaction.
M	-	molecular weight.
n	-	moles of oxygen used per mole of the hydrocarbon reacted; also number of active sites.
p	-	partial pressure, atm.
r_1, r_2, r_3	-	reaction rates for steps 1, 2 and 3 shown in the reaction scheme, gm-mole/(hr.) (gm. cat.).
r_c	-	reaction rate, gm-mole/(hr.) (gm. cat.).
r_c'	-	reaction rate, gm-mole/(hr.) (cc. cat.).

r_o - total reaction rate at the initial condition, gm-mole/(hr.) (gm. cat.).

R - gas constant, cal./°K./gm-mole; also radius of the pellet, cm.

R' - radial coordinate.

R" - rate number, $\frac{r}{a_m G_m}$.

Re - Reynolds number, $\frac{G}{a_v \mu}$.

S - surface area per unit weight of catalyst, $cm.^2/gm.$

S_B - fraction of catalyst surface covered with benzene.

Sc - Schmidt number, $\frac{\mu \rho}{D}$.

T - temperature, °K.

W - weight of the catalyst, gm.

x - mole of benzene converted to products per mole of feed.

x_C - mole of benzene converted to carbon dioxide per mole of feed.

x_M - mole of benzene converted to maleic anhydride per mole of feed.

GREEK LETTERS

α, β - constants.

γ - stoichiometric number of the rate controlling step.

Δ - reciprocal of the adsorption term.

ϵ - effectiveness factor.

θ - dimensionless group, $\frac{k_s' R}{D}$

θ' - pore volume, cc./cc.

ρ - density, gm./cc.

σ - mass transfer factor.

Σ - summation.

τ - tortuosity factor.

ϕ - Thiele modulus, $L \sqrt{k/D_e}$.

μ - Viscosity. gm./cm. hr.

APPENDICES

APPENDIX - A

Tables of experimental data

Table - A.1

Experimental data for catalyst - 1
at 400°C.

benzene:air	W/F	$p_B x10^2$	$p_O x10^1$	$p_M x10^3$	$p_C x10^2$	$p_W x10^2$
1	2	3	4	5	6	7
	0	1.785	1.927	-	-	-
	60	1.518	1.762	1.187	1.1389	0.6889
	93	1.400	1.688	1.651	1.6635	0.9979
	132	1.312	1.652	1.713	1.9402	1.1425
1:50	162	1.258	1.594	2.052	2.3534	1.3833
	190	1.220	1.568	2.106	2.5582	1.4911
	228	1.185	1.542	2.124	2.7666	1.5970
	280	1.170	1.529	1.963	2.9067	1.6509
	0	1.154	1.938	-	-	-
	62	0.987	1.827	0.865	0.6504	0.4117
	90	0.932	1.788	1.038	0.9141	0.5608
	132	0.871	1.723	1.304	1.1741	0.7174
1:80	160	0.830	1.719	1.471	1.3475	0.8208
	192	0.798	1.695	1.557	1.5085	0.9099
	204	0.792	1.691	1.592	1.5362	0.9273
	250	0.790	1.688	1.673	1.5108	0.9803
	310	0.754	1.655	1.638	1.8084	1.0679

Table - A.1 (contd.)

1	2	3	4	5	6	7
	0	0.835	1.945	-	-	-
	61	0.718	1.874	0.538	0.4692	0.2967
	107	0.651	1.831	0.803	0.7906	0.4755
	154	0.624	1.815	0.985	0.8674	0.5322
1:110	183	0.587	1.791	1.043	1.0643	0.6364
	212	0.576	1.785	1.102	1.1085	0.6644
	230	0.573	1.783	1.135	1.1177	0.6723
	321	0.550	1.767	1.177	1.2361	0.7356
	0	0.663	1.949	-	-	-
	61	0.574	1.901	0.404	0.3691	0.2249
	98	0.537	1.872	0.584	0.5221	0.3197
	124	0.515	1.858	0.649	0.6268	0.3783
1:140	155	0.493	1.845	0.754	0.7161	0.4334
	180	0.481	1.837	0.822	0.7646	0.4645
	203	0.472	1.832	0.848	0.8017	0.4856
	242	0.458	1.823	0.903	0.8635	0.5219
	337	0.447	1.815	0.929	0.9245	0.5551

Table - A.2

Experimental data for catalyst - 2
at 310°C.

benzene:air	W/F	$p_B x10^2$	$p_O x10^1$	$p_M x10^3$	$p_C x10^2$	$p_W x10^2$
1:50	0	1.8317	1.9233	-	-	-
	70	1.7454	1.8556	0.5128	0.3124	0.2075
	107	1.7091	1.8520	0.6887	0.4597	0.2987
	149	1.6896	1.8424	0.8590	0.5092	0.3405
	185	1.6736	1.8334	0.9579	0.5653	0.3784
	230	1.6659	1.8260	0.9012	0.6341	0.4072
1:80	0	1.1533	1.9375	-	-	-
	75	1.1107	1.9130	0.2456	0.1570	0.1031
	118	1.0791	1.8954	0.4509	0.2645	0.1773
	164	1.0670	1.8869	0.4705	0.3294	0.2117
	197	1.0528	1.8789	0.5570	0.3798	0.2456
	240	1.0492	1.8764	0.5628	0.3990	0.2558
1:110	0	0.8416	1.9440	-	-	-
	69	0.8155	1.9290	0.1506	0.0963	0.0632
	107	0.8103	1.9250	0.1936	0.1171	0.0801
	154	0.7945	1.9170	0.2886	0.1668	0.1122
	190	0.7868	1.9130	0.3341	0.1951	0.1309
	238	0.7696	1.9040	0.3972	0.2560	0.1671

Table - A.3

Experimental data for catalyst - 2
at 330°C.

benzene:air	W/F	$p_B x10^2$	$p_O x10^1$	$p_M x10^3$	$p_C x10^2$	$p_W x10^2$
1:50	0	1.8317	1.9234	-	-	-
	69	1.7067	1.8525	0.7601	0.4454	0.2987
	104	1.6593	1.8250	1.0294	0.6224	0.4141
	149	1.5954	1.7871	1.2437	0.9202	0.5844
	194	1.5791	1.7628	1.4213	1.0568	0.6705
	228	1.5383	1.7473	1.5789	1.1554	0.7356
1:80	0	1.1533	1.9375	-	-	-
	72	1.0770	1.8941	0.4590	0.2737	0.1828
	113	1.0415	1.8738	0.6689	0.4029	0.2683
	155	1.0088	1.8522	0.7600	0.5607	0.3575
	209	0.9957	1.8447	0.8442	0.6075	0.3882
	250	0.9606	1.8229	0.9941	0.7579	0.4780
1:110	0	0.8416	1.9441	-	-	-
	68	0.8005	1.9207	0.2491	0.1467	0.0983
	111	0.7567	1.9003	0.4376	0.2799	0.1837
	149	0.7408	1.8845	0.5327	0.3913	0.2489
	195	0.7235	1.8763	0.6227	0.4425	0.2835
	235	0.7133	1.8682	0.6766	0.4989	0.3171

Table - A.4

Experimental data for catalyst - 2
at 350°C.

benzene:air	W/F	$p_B x10^2$	$p_O x10^1$	$p_M x10^3$	$p_C x10^2$	$p_W x10^2$
1	2	3	4	5	6	7
1:50	0	1.8318	1.9233	-	-	-
	61	1.5969	1.7879	1.3555	0.8668	0.5689
	99	1.4899	1.7230	1.8666	1.3042	0.8388
	131	1.4213	1.6814	2.1982	1.5837	1.0117
	173	1.3485	1.6421	2.7055	1.8171	1.1791
	199	1.3188	1.6245	2.8612	1.9329	1.2526
	230	1.2965	1.6148	3.0957	1.9732	1.2962
	313	1.2267	1.5741	3.4822	2.2373	1.4669
1:80	0	1.1533	1.9375	-	-	-
	65	1.0090	1.8551	0.8199	0.5376	0.3508
	107	0.9345	1.8072	1.1267	0.8619	0.5436
	150	0.8878	1.7799	1.3839	1.0393	0.6581
	178	0.8649	1.7667	1.5143	1.1242	0.7135
	219	0.8311	1.7470	1.7022	1.2508	0.7959
	244	0.8144	1.7358	1.7484	1.3367	0.8417
	319	0.7892	1.7204	1.8706	1.4363	0.9052

Table - A.4 (contd.)

1	2	3	4	5	6	7
1:110	0	0.8416	1.9441	-	-	-
	68	0.7381	1.8839	0.5823	0.3881	0.2523
	104	0.6942	1.8573	0.7894	0.5714	0.3632
	149	0.6525	1.8318	0.9846	0.7408	0.4688
	187	0.6263	1.8150	1.0789	0.8601	0.5379
	222	0.6177	1.8110	1.1588	0.8796	0.5557
	267	0.5973	1.7984	1.2473	0.9665	0.6079
	302	0.5845	1.7900	1.2902	1.0266	0.6423
1:140	0	0.6626	1.9479	-	-	-
	64	0.5882	1.9045	0.4108	0.2817	0.1819
	102	0.5595	1.8864	0.5545	0.4069	0.2232
	138	0.5298	1.8700	0.7209	0.5079	0.3260
	178	0.5103	1.8589	0.8415	0.5769	0.3726
	215	0.4954	1.8504	0.9296	0.6308	0.4083
	252	0.4823	1.8431	1.0137	0.6758	0.4393
	334	0.4652	1.8333	1.1145	0.7381	0.4805

Table - A.5

Experimental data for catalyst - 2
at 375°C.

benzene:air	W/F	$p_B x10^2$	$p_O x10^1$	$p_M x10^3$	$p_C x10^2$	$p_W x10^2$
1	2	3	4	5	6	7
1:50	0	1.8318	1.9233	-	-	-
	62	1.5749	1.7751	1.5332	0.9496	0.6226
	96	1.4760	1.7145	1.9508	1.3521	0.8831
	144	1.3665	1.6538	2.6469	1.7313	1.1311
	182	1.2861	1.6042	3.0041	2.0747	1.3366
	219	1.2493	1.5849	3.2807	2.1823	1.4195
	245	1.2267	1.5715	3.4584	2.2450	1.4692
	301	1.1868	1.5501	3.6819	2.3954	1.5667
1:80	0	1.1533	1.9375	-	-	-
	65	0.9939	1.8448	0.8961	0.5978	0.3885
	103	0.9318	1.8061	1.1567	0.8659	0.5486
	140	0.8857	1.7873	1.4508	1.0251	0.6576
	187	0.8342	1.7489	1.6918	1.2379	0.7881
	222	0.8144	1.7391	1.8591	1.2894	0.8306
	250	0.7979	1.7286	1.9214	1.3634	0.8738
	322	0.7634	1.7064	2.0425	1.5219	0.9652

Table - A.5 (contd.)

1	2	3	4	5	6	7
	0	0.8416	1.9441	-	-	-
	62	0.7288	1.8785	0.6312	0.4242	0.2752
	107	0.6799	1.8483	0.8491	0.6303	0.4001
	139	0.6461	1.8288	1.0435	0.7556	0.4822
1:110	181	0.6172	1.8105	1.1538	0.8346	0.5577
	212	0.5956	1.7972	1.2531	0.9747	0.6126
	258	0.5824	1.7898	1.3381	1.0200	0.6438
	322	0.5674	1.7801	1.3869	1.0904	0.6839
	0	0.6626	1.9479	-	-	-
	61	0.5765	1.8978	0.4817	0.3233	0.2098
	100	0.5399	1.8753	0.6440	0.4778	0.3033
	140	0.5167	1.8616	0.7692	0.5673	0.3606
1:140	177	0.4881	1.8433	0.8759	0.6964	0.4358
	208	0.4790	1.8371	0.8958	0.7429	0.4610
	250	0.4661	1.8298	0.9720	0.7895	0.4919
	319	0.4508	1.8201	1.0336	0.8566	0.5314

Table - A.6

Experimental data for catalyst -2
at 400°C.

benzene:air	W/F	$p_B x10^2$	$p_O x10^1$	$p_M x10^3$	$p_C x10^2$	$p_W x10^2$
1	2	3	4	5	6	7
1:50	0	1.7965	1.9223	-	-	-
	46	1.6026	1.8144	1.257	0.6600	0.4557
	53	1.5629	1.7875	1.347	0.8623	0.5659
	107	1.4172	1.6997	2.065	1.4508	0.9311
	135	1.3432	1.6538	2.389	1.7640	1.1208
	189	1.2390	1.5979	3.126	2.0944	1.3598
	226	1.1997	1.5746	3.322	2.2492	1.4580
	240	1.1749	1.5584	3.413	2.3642	1.5234
	305	1.1494	1.5488	3.736	2.3897	1.5676
	346	1.1246	1.5282	3.664	2.5655	1.6492
1:80	0	1.1533	1.9375	-	-	-
	53	1.0113	1.8578	0.899	0.4931	0.3359
	119	0.9157	1.7962	1.234	0.9330	0.5893
	147	0.8856	1.7815	1.496	1.0085	0.6533
	177	0.8419	1.7533	1.643	1.2109	0.7698
	238	0.7998	1.7275	1.836	1.3864	0.8768
	268	0.7802	1.7164	1.978	1.4474	0.9215
	322	0.7531	1.7003	2.099	1.5615	0.9907

Table - A.6 (contd.)

1	2	3	4	5	6	7
	0	0.8341	1.9435	-	-	-
	70	0.7140	1.8686	0.592	0.4837	0.3512
	117	0.6668	1.8426	0.817	0.6748	0.4199
	175	0.6260	1.8205	1.105	0.8066	0.5138
1:110	190	0.6172	1.8105	1.201	0.8713	0.5557
	240	0.5872	1.7968	1.285	0.9677	0.6121
	266	0.5720	1.7871	1.369	1.0246	0.6492
	322	0.5488	1.7730	1.451	1.1311	0.7106
	0	0.6625	1.9478	-	-	-
	60	0.5800	1.8991	0.474	0.3187	0.2034
	98	0.5471	1.8791	0.629	0.4539	0.2866
	140	0.5099	1.8518	0.616	0.6686	0.3959
1:140	222	0.4750	1.8364	0.976	0.7344	0.4648
	234	0.4660	1.8299	0.983	0.7851	0.4909
	272	0.4529	1.8221	1.053	0.8360	0.5234
	346	0.4385	1.8140	1.140	0.8873	0.5577

Table - A.7

Experimental data for catalyst - 3
at 310°C.

benzene:air	W/F	$p_B x10^2$	$p_O x10^1$	$p_M x10^3$	$p_C x10^2$	$p_W x10^2$
1:50	0	1.8317	1.9232	-	-	-
	58	1.7454	1.8741	0.5165	0.3110	0.2071
	100	1.7212	1.8609	0.6832	0.3894	0.2630
	130	1.7040	1.8505	0.7656	0.4597	0.3064
	169	1.6888	1.8396	0.8279	0.5371	0.3513
	235	1.6628	1.8387	1.0367	0.5986	0.4029
1:80	0	1.1533	1.9375	-	-	-
	64	1.1092	1.9122	0.2584	0.1610	0.1063
	107	1.0812	1.8965	0.4336	0.2590	0.1728
	132	1.0679	1.8888	0.5097	0.3081	0.2050
	194	1.0497	1.8779	0.6032	0.3801	0.2504
	236	1.0413	1.8733	0.6585	0.4084	0.2701
1:110	0	0.8416	1.9441	-	-	-
	70	0.8136	1.9279	0.1607	0.1033	0.0677
	110	0.8022	1.9210	0.2154	0.1501	0.0966
	140	0.7947	1.9170	0.2709	0.1728	0.1135
	190	0.7847	1.9111	0.3206	0.2125	0.1383
	248	0.7779	1.9075	0.3425	0.2447	0.1566

Table - A.8

Experimental data for catalyst - 3
at 330°C

benzene:air	W/F	$p_B x10^2$	$p_O x10^1$	$p_M x10^3$	$p_C x10^2$	$p_W x10^2$
1:50	0	1.8317	1.9233	-	-	-
	63	1.7038	1.8522	0.8151	0.4410	0.2947
	104	1.6161	1.7978	1.2089	0.8099	0.5258
	130	1.5987	1.7867	1.2748	0.8880	0.5715
	168	1.5789	1.7766	1.4323	0.9436	0.6151
	220	1.5322	1.7491	1.6796	1.1250	0.7305
1:80	0	1.1533	1.9375	-	-	-
	70	1.0783	1.8957	0.4786	0.2583	0.1790
	107	1.0411	1.8748	0.7162	0.3869	0.2650
	132	1.0235	1.8650	0.8165	0.4518	0.3018
	187	0.9777	1.8353	0.9826	0.6601	0.4283
	237	0.9645	1.8271	1.0391	0.7171	0.4624
1:110	0	0.8416	1.9441	-	-	-
	68	0.7891	1.9132	0.2912	0.1981	0.1281
	112	0.7589	1.8948	0.4637	0.3204	0.2066
	138	0.7347	1.8812	0.5840	0.4076	0.2622
	193	0.7262	1.8763	0.6236	0.4428	0.2837
	244	0.7072	1.8654	0.7423	0.5095	0.3289

Table - A.9

Experimental data for catalyst - 3
at 350°C.

benzene:air	W/F	$p_B x10^2$	$p_O x10^1$	$p_M x10^3$	$p_C x10^2$	$p_W x10^2$
1	2	3	4	5	6	7
1:50	0	1.800	1.925	-	-	-
	75	1.516	1.775	1.583	0.9126	0.6934
	90	1.490	1.760	1.655	1.0384	0.7671
	120	1.404	1.721	2.300	1.2216	0.9557
	139	1.370	1.700	2.415	1.3725	1.0473
	162	1.345	1.684	2.540	1.4605	1.1102
	200	1.284	1.652	2.845	1.6635	1.2575
	244	1.258	1.638	2.950	1.7713	1.3276
	310	1.262	1.640	2.862	1.7839	1.3204
1:80	0	1.171	1.942	-	-	-
	81	0.982	1.845	1.053	0.6025	0.3888
	103	0.952	1.824	1.147	0.7309	0.5371
	128	0.928	1.812	1.310	0.7928	0.5926
	177	0.880	1.784	1.532	0.9726	0.6642
	203	0.858	1.780	1.720	1.0053	0.7601
	255	0.831	1.763	1.918	1.0742	0.8244
	318	0.830	1.760	1.882	1.0988	0.8314

Table - A.9 (contd.)

1	2	3	4	5	6	7
	0	0.815	1.885	-	-	-
	75	0.686	1.820	0.686	0.4258	0.3186
	102	0.657	1.800	0.880	0.5026	0.3871
	150	0.633	1.789	0.985	0.6003	0.4519
1:110	211	0.610	1.773	1.062	0.7083	0.5179
	270	0.602	1.770	1.110	0.7322	0.5370
	294	0.595	1.768	1.180	0.7331	0.5496
	338	0.594	1.766	1.140	0.7607	0.5563
	0	0.663	1.950	-	-	-
	79	0.565	1.910	0.517	0.3259	0.2339
	96	0.543	1.885	0.610	0.4108	0.2968
	147	0.527	1.877	0.755	0.4333	0.3299
1:140	168	0.521	1.875	0.802	0.4459	0.3432
	215	0.510	1.870	0.901	0.4638	0.3671
	280	0.495	1.860	0.940	0.5354	0.4088
	346	0.491	1.855	0.982	0.5791	0.4101

Table - A.10

Experimental data for catalyst - 3
at 375°C

benzene:air	W/F	$p_B x10^2$	$p_O x10^1$	$p_M x10^3$	$p_C x10^2$	$p_W x10^2$
1	2	3	4	5	6	7
1:50	0	1.735	1.930	-	-	-
	65	1.456	1.768	1.560	1.0328	0.6689
	75	1.413	1.720	1.750	1.1902	0.7755
	129	1.291	1.646	2.365	1.6867	1.0878
	211	1.206	1.600	2.880	1.9860	1.2717
	282	1.180	1.583	3.050	2.0725	1.3469
	352	1.188	1.580	2.740	2.1556	1.3547
1:80	0	1.183	1.940	-	-	-
	76	0.980	1.825	1.122	0.7319	0.4863
	92	0.980	1.821	1.183	0.7589	0.4875
	124	0.915	1.787	1.650	0.9472	0.6399
	202	0.852	1.745	1.835	1.2392	0.8093
	246	0.835	1.738	1.988	1.2841	0.8439
	322	0.824	1.728	1.940	1.3669	0.8808

Table - A.10 (contd.)

1	2	3	4	5	6	7
	0	0.842	1.940	-	-	-
	77	0.710	1.867	0.736	0.4957	0.3217
	116	0.677	1.850	0.943	0.5925	0.3933
1:110	135	0.642	1.828	1.035	0.7675	0.4931
	202	0.630	1.820	1.105	0.8221	0.5261
	270	0.614	1.810	1.238	0.8579	0.5496
	360	0.602	1.807	1.284	0.9157	0.5912
	0	0.667	1.950	-	-	-
	73	0.573	1.890	0.500	0.2969	0.2160
	92	0.554	1.882	0.560	0.4369	0.2756
1:140	141	0.530	1.870	0.765	0.5172	0.3354
	183	0.516	1.862	0.910	0.5378	0.3648
	283	0.497	1.850	0.991	0.6198	0.4124
	312	0.492	1.848	1.082	0.6419	0.4253

Table - A.11

Experimental data for catalyst - 3
at 400°C.

benzene:air	W/F	$p_B x10^2$	$p_O x10^1$	$p_M x10^3$	$p_C x10^2$	$p_W x10^2$
1	2	3	4	5	6	7
1:50	0	1.760	1.920	-	-	-
	74	1.418	1.720	1.740	1.3731	0.8729
	123	1.317	1.665	2.720	1.6834	1.0922
	143	1.298	1.670	2.510	1.5899	1.1238
	224	1.200	1.608	3.440	2.0201	1.3564
	280	1.165	1.576	3.380	2.2404	1.4593
	308	1.162	1.574	3.270	2.2932	1.4761
1:80	0	1.140	1.940	-	-	-
	95	0.910	1.180	1.220	0.8966	0.5739
	128	0.894	1.179	1.460	0.8904	0.5924
	185	0.843	1.177	1.778	1.0527	0.7092
	224	0.820	1.176	1.925	1.1370	0.7667
	280	0.790	1.174	1.998	1.2942	0.8506
	305	0.791	1.173	1.955	1.3062	0.8505

Table - A.11 (contd.)

1	2	3	4	5	6	7
1:110	0	0.843	1.950	-	-	-
	76	0.715	1.890	0.674	0.4671	0.3171
	97	0.700	1.886	0.761	0.5470	0.3429
	105	0.693	1.882	0.753	0.5898	0.3627
	136	0.673	1.870	0.995	0.6145	0.4090
	211	0.640	1.850	1.091	0.7763	0.5006
	272	0.613	1.838	1.240	0.8677	0.5619
	293	0.608	1.830	1.342	0.8567	0.5679
1:140	0	0.650	1.970	-	-	-
	74	0.581	1.895	0.500	0.3148	0.2104
	140	0.517	1.880	0.858	0.4438	0.3108
	215	0.487	1.860	0.941	0.5891	0.3935
	286	0.478	1.852	1.005	0.6209	0.4148
	338	0.467	1.846	1.033	0.8811	0.4438

Table - A.12

Experimental data for catalyst - 4
at 400°C.

benzene:air	W/F	$p_B x10^2$	$p_O x10^1$	$p_M x10^3$	$p_C x10^2$	$p_W x10^2$
1	2	3	4	5	6	7
1:50	0	1.8318	1.8593	-	-	-
	68	1.3743	1.6579	2.586	1.7098	1.1135
	116	1.2035	1.5553	3.440	2.3937	1.5409
	127	1.1702	1.5392	3.736	2.4751	1.6113
	152	1.1247	1.5163	4.165	2.6004	1.7107
	180	1.0549	1.4693	4.284	2.9473	1.9021
	231	0.9974	1.4411	4.784	3.0924	2.0246
	294	0.9479	1.4026	4.726	3.4126	2.1734
	318	0.9305	1.3846	4.579	3.5756	2.2456
1:80	0	1.1533	1.9367	-	-	-
	60	0.8824	1.7819	1.537	1.0084	0.6579
	88	0.8115	1.7401	1.915	1.2827	0.8329
	93	0.7839	1.7207	1.962	1.4292	0.9108
	122	0.7422	1.6996	2.298	1.5454	1.0025
	161	0.6755	1.6602	2.652	1.8037	1.1671
	205	0.6343	1.6381	2.942	1.9357	1.2586
	250	0.6025	1.6198	3.136	2.0487	1.3381
	318	0.5795	1.6037	3.172	2.1721	1.4033

Table - A.12 (contd.)

1	2	3	4	5	6	7
1:110	0	0.8416	1.9550	-	-	-
	62	0.6479	1.8430	1.109	0.7182	0.4700
	73	0.6226	1.8276	1.221	0.8254	0.5315
	124	0.5491	1.7851	1.651	1.0942	0.7133
	144	0.5302	1.7765	1.834	1.1344	0.7507
	183	0.4888	1.7507	2.009	1.3128	0.8574
	216	0.4659	1.7369	2.122	1.4051	0.9148
	221	0.4662	1.7391	2.189	1.3770	0.9074
	294	0.4358	1.7222	2.383	1.4815	0.9791
1:140	0	0.6579	1.9480	-	-	-
	70	0.5080	1.8621	0.882	0.5466	0.3615
	109	0.4710	1.8434	1.186	0.6469	0.4421
	139	0.4276	1.8184	1.434	0.8076	0.5473
	222	0.3623	1.7802	1.784	1.0598	0.7083
	267	0.3423	1.7680	1.888	1.1383	0.7579
	304	0.3302	1.7608	1.950	1.1862	0.7882
	326	0.3283	1.7603	1.981	1.1853	0.7907

Table - A.13

Experimental data for catalyst - 5
at 400°C.

benzene:air	W/F	$p_B x10^2$	$p_O x10^1$	$p_M x10^3$	$p_C x10^2$	$p_W x10^2$
1	2	3	4	5	6	7
1:50	0	1.8318	1.9234	-	-	-
	64	1.3645	1.6459	2.432	1.8307	1.1586
	102	1.1818	1.5375	3.383	2.5462	1.6114
	136	1.1027	1.4882	3.720	2.8861	1.8151
	177	1.0098	1.4145	4.284	3.4276	2.0373
	222	0.9364	1.3889	4.445	3.5566	2.2416
	250	0.9228	1.3913	4.396	3.5171	2.2872
	302	0.8761	1.4156	4.150	3.3206	2.2686
1:80	0	1.1677	1.9372	-	-	-
	64	0.8756	1.7630	1.494	1.1401	0.7176
	103	0.7737	1.7010	1.985	1.5525	0.9723
	140	0.7205	1.6698	2.267	1.7544	1.1011
	183	0.6588	1.6346	2.636	1.9797	1.2474
	254	0.5911	1.5916	2.896	2.2729	1.4224
	262	0.5900	1.5919	2.932	2.2648	1.4220
	282	0.5808	1.5853	2.944	2.3144	1.4480
	318	0.5641	1.5714	2.898	2.4318	1.5021

Table - A.13 (contd.)

1	2	3	4	5	6	7
	0	0.8416	1.9441	-	-	-
	64	0.6377	1.8235	1.077	0.7921	0.5038
	103	0.5635	1.7763	1.361	1.1237	0.6980
1:110	140	0.5100	1.7462	1.645	1.3163	0.8300
	194	0.4606	1.7141	1.920	1.5364	0.9509
	240	0.4399	1.7005	2.037	1.6301	1.0013
	250	0.4358	1.6936	2.106	1.6852	1.0068
	310	0.4176	1.6846	2.176	1.7411	1.0544
	0	0.6579	1.9480	-	-	-
	64	0.5067	1.8590	0.782	0.5878	0.3688
	98	0.4511	1.8259	1.098	0.8011	0.5104
	135	0.4136	1.8043	1.316	0.9394	0.6014
1:140	175	0.3790	1.7837	1.495	1.0751	0.6871
	257	0.3283	1.7521	1.710	1.2934	0.8177
	272	0.3262	1.7534	1.801	1.2691	0.8147
	305	0.3169	1.7471	1.827	1.3151	0.8403

Table - A.14

Experimental conversions to maleic anhydride (x_M) and carbon dioxide (x_C) for catalyst - 1 at 400°C.

benzene:air	W/F	x_M	x_C
1:50	0	-	-
	60	0.0665	0.0835
	93	0.0925	0.1235
	132	0.0960	0.1680
	162	0.1150	0.1800
	190	0.1180	0.1980
	228	0.1190	0.2170
	280	0.1102	0.2498
1:80	0	-	-
	62	0.0750	0.0690
	90	0.0900	0.1020
	132	0.1130	0.1320
	160	0.1275	0.1529
	192	0.1350	0.1730
	204	0.1380	0.1760
	250	0.1450	0.1700
	310	0.1420	0.1740
1:110	0	-	-
	61	0.0645	0.0756
	107	0.0962	0.1239
	154	0.1180	0.1340
	183	0.1250	0.1710
	212	0.1320	0.1775
	230	0.1360	0.1780
	321	0.1410	0.2000
1:140	0	-	-
	61	0.0610	0.0725
	98	0.0831	0.1021
	124	0.0980	0.1250
	155	0.1138	0.1422
	180	0.1240	0.1510
	203	0.1280	0.1590
	242	0.1362	0.1718
	337	0.1402	0.1858

Table - A.15

Experimental conversions to maleic anhydride (x_M) and carbon dioxide (x_C) for catalyst - 2 at 310°C.

benzene:air	W/F	x_M	x_C
1:50	0	-	-
	70	0.0280	0.0191
	107	0.0376	0.0293
	149	0.0469	0.0307
	185	0.0523	0.0340
	230	0.0492	0.0413
1:80	0	-	-
	75	0.0213	0.0156
	118	0.0391	0.0252
	164	0.0408	0.0340
	197	0.0483	0.0388
	240	0.0488	0.0414
1:110	0	-	-
	69	0.0179	0.0131
	107	0.0255	0.0167
	154	0.0343	0.0216
	190	0.0397	0.0254
	238	0.0447	0.0358

Table - A.16

Experimental conversions to maleic anhydride (x_M) and carbon dioxide (x_C) for catalyst - 2 at 330°C.

benzene:air	W/F	x_M	x_C
1:50	0	-	-
	69	0.0415	0.0267
	104	0.0562	0.0379
	149	0.0679	0.0611
	194	0.0776	0.0703
	228	0.0862	0.0764
1:80	0	-	-
	72	0.0398	0.0263
	113	0.0580	0.0389
	155	0.0659	0.0594
	209	0.0732	0.0634
	250	0.0862	0.0808
1:110	0	-	-
	68	0.0352	0.0248
	111	0.0520	0.0381
	149	0.0633	0.0564
	195	0.0740	0.0663
	235	0.0804	0.0720

Table - A.17

Experimental conversions to maleic anhydride (x_M) and carbon dioxide (x_C) for catalyst - 2 at 350°C.

benzene:air	W/F	x_M	x_C
1:50	0	-	-
	61	0.0740	0.0542
	99	0.1019	0.0847
	131	0.1200	0.1041
	173	0.1477	0.1161
	199	0.1562	0.1238
	230	0.1690	0.1232
	313	0.1901	0.1402
1:80	0	-	-
	65	0.0711	0.0540
	107	0.0977	0.0920
	150	0.1200	0.1102
	178	0.1313	0.1187
	219	0.1478	0.1315
	244	0.1516	0.1422
	319	0.1622	0.1535
1:110	0	-	-
	68	0.0692	0.0538
	104	0.0938	0.0813
	149	0.1170	0.1077
	187	0.1282	0.1276
	222	0.1377	0.1283
	267	0.1482	0.1420
	322	0.1533	0.1522
1:140	0	-	-
	64	0.0620	0.0552
	102	0.0837	0.0818
	138	0.1088	0.0915
	178	0.1270	0.1028
	215	0.1403	0.1119
	252	0.1530	0.1190
	334	0.1682	0.1296

Table - A.18

Experimental conversions to maleic anhydride (x_M) and carbon dioxide (x_C) for catalyst - 2 at 375°C.

benzene:air	W/F	x_M	x_C
	0	-	-
	62	0.0807	0.0595
	96	0.1065	0.0877
	144	0.1445	0.1095
1:50	182	0.1640	0.1339
	219	0.1791	0.1389
	245	0.1888	0.1415
	301	0.2010	0.1511
	0	-	-
	65	0.0777	0.0605
	103	0.1003	0.0917
	140	0.1258	0.1062
1:80	187	0.1467	0.1300
	222	0.1612	0.1326
	250	0.1666	0.1415
	322	0.1771	0.1609
	0	-	-
	62	0.0750	0.0590
	107	0.1009	0.0912
	139	0.1240	0.1083
1:110	181	0.1371	0.1295
	212	0.1489	0.1434
	258	0.1590	0.1490
	322	0.1648	0.1610
	0	-	-
	61	0.0727	0.0571
	100	0.0972	0.0878
	140	0.1161	0.1040
1:140	177	0.1322	0.1311
	208	0.1352	0.1418
	250	0.1467	0.1497
	319	0.1560	0.1636

Table - A.19

Experimental conversions to maleic anhydride (x_M) and carbon dioxide (x_C) for catalyst - 2 at 400°C.

benzene:air	W/F	x_M	x_C
	0	-	-
	46	0.0700	0.0379
	53	0.0750	0.0550
	107	0.1150	0.0961
	135	0.1330	0.1193
1:50	189	0.1740	0.1363
	226	0.1852	0.1470
	240	0.1900	0.1560
	305	0.2080	0.1522
	346	0.2040	0.1700
	0	-	-
	53	0.780	0.0459
	119	0.1070	0.0990
	147	0.1298	0.1023
1:80	177	0.1425	0.1275
	238	0.1592	0.1473
	268	0.1715	0.1520
	322	0.1820	0.1650
	0	-	-
	70	0.0710	0.0730
	117	0.0980	0.1025
	175	0.1325	0.1170
1:110	190	0.1440	0.1261
	240.	0.1541	0.1420
	266	0.1642	0.1500
	322	0.1740	0.1683
	0	-	-
	60	0.0715	0.0630
	98	0.0950	0.0892
	140	0.0930	0.1372
1:140	222	0.1474	0.1356
	234	0.1485	0.1480
	272	0.1590	0.1573
	346	0.1722	0.1658

Table - A.20

Experimental conversions to maleic anhydride (x_M) and carbon dioxide (x_C) for catalyst - 3 at 310°C.

benzene:air	W/F	x_M	x_C
1:50	0	-	-
	58	0.0282	0.0189
	100	0.0373	0.0230
	130	0.0418	0.0279
	169	0.0452	0.0338
	235	0.0566	0.0356
1:80	0	-	-
	64	0.0224	0.0158
	107	0.0376	0.0249
	132	0.0442	0.0298
	194	0.0523	0.0375
	236	0.0571	0.0440
1:110	0	-	-
	70	0.0191	0.0141
	110	0.0256	0.0212
	140	0.0322	0.0235
	190	0.0381	0.0294
	248	0.0407	0.0349

Table - A.21

Experimental conversions to maleic anhydride (x_M) and carbon dioxide (x_C) for catalyst - 3 at 330°C.

benzene:air	W/F	x_M	x_C
1:50	0	-	-
	63	0.0445	0.0253
	104	0.0660	0.0517
	130	0.0696	0.0576
	168	0.0782	0.0598
	220	0.0917	0.0718
1:80	0	-	-
	70	0.0415	0.0235
	107	0.0621	0.0352
	132	0.0708	0.0417
	187	0.0852	0.0670
	237	0.0901	0.0736
1:110	0	-	-
	68	0.0346	0.0277
	112	0.0551	0.0451
	138	0.0694	0.0576
	193	0.0741	0.0630
	244	0.0882	0.0715

Table - A.22

Experimental conversions to maleic anhydride (x_M) and carbon dioxide (x_C) for catalyst - 3 at 350°C.

benzene:air	W/F	x_M	x_C
1:50	0	-	-
	75	0.0881	0.0700
	90	0.0920	0.0813
	120	0.1283	0.0922
	139	0.1343	0.1056
	162	0.1419	0.1128
	200	0.1585	0.1280
	244	0.1710	0.1311
	310	0.1597	0.1397
1:80	0	-	-
	81	0.0900	0.0711
	103	0.0983	0.0882
	128	0.1125	0.0945
	177	0.1313	0.1172
	203	0.1476	0.1191
	255	0.1645	0.1267
	318	0.1612	0.1308
1:110	0	-	-
	75	0.0841	0.0707
	102	0.1082	0.0823
	150	0.1208	0.0993
	211	0.1303	0.1192
	270	0.1366	0.1231
	294	0.1451	0.1222
	338	0.1408	0.1286
1:140	0	-	-
	79	0.0780	0.0690
	96	0.0925	0.0881
	147	0.1143	0.0907
	168	0.1267	0.0956
	215	0.1369	0.0945
	280	0.1421	0.1115
	346	0.1481	0.1210

Table - A.23

Experimental conversions to maleic anhydride (x_M) and carbon dioxide (x_C) for catalyst - 3 at 375°C.

benzene:air	W/F	x_M	x_C
1:50	0	-	-
	65	0.0903	0.0695
	75	0.1015	0.0811
	129	0.1365	0.1177
	211	0.1664	0.1363
	232	0.1767	0.1410
	352	0.1582	0.1558
1:80	0	-	-
	76	0.0953	0.0753
	92	0.1001	0.0698
	124	0.1395	0.0877
	202	0.1550	0.1238
	246	0.1683	0.1251
	322	0.1642	0.1382
1:110	0	-	-
	77	0.0875	0.0692
	116	0.1122	0.0804
	135	0.1235	0.1119
	202	0.1314	0.1190
	270	0.1473	0.1235
	360	0.1527	0.1305
1:140	0	-	-
	73	0.0752	0.0655
	92	0.0857	0.0808
	141	0.1145	0.0916
	183	0.1366	0.0897
	283	0.1485	0.1003
	312	0.1510	0.1105

Table - A.24

Experimental conversions to maleic anhydride (x_M) and carbon dioxide (x_C) for catalyst - 3 at 400°C.

benzene:air	W/F	x_M	x_C
1:50	0	-	-
	74	0.108	0.096
	123	0.142	0.099
	143	0.154	0.112
	224	0.188	0.133
	280	0.191	0.148
	308	0.185	0.155
1:80	0	-	-
	95	0.107	0.095
	128	0.128	0.093
	185	0.156	0.102
	224	0.169	0.110
	280	0.175	0.137
	306	0.172	0.134
1:110	0	-	-
	76	0.079	0.066
	97	0.089	0.078
	105	0.088	0.087
	136	0.117	0.088
	211	0.128	0.116
	272	0.146	0.123
	293	0.158	0.117
1:140	0	-	-
	74	0.077	0.055
	140	0.132	0.070
	215	0.145	0.103
	286	0.154	0.108
	338	0.159	0.120

Table - A.25

Experimental conversions to maleic anhydride (x_M) and carbon dioxide (x_C) for catalyst - 3A at 350°C.

benzene:air	W/F	x_M	x_C
1:50	0	-	-
	62.5	0.0792	0.0763
	102	0.1211	0.0862
	130	0.1368	0.1175
	175	0.1676	0.1363
	217	0.1800	0.1502
1:80	0	-	-
	69	0.0871	0.0803
	106	0.1115	0.0946
	130	0.1263	0.1675
	188	0.1552	0.1328
	230	0.1715	0.1382
1:140	0	-	-
	63	0.0771	0.0654
	97	0.0983	0.0884
	126	0.1158	0.0985
	175	0.1382	0.1106
	221	0.1400	0.1231

Table - A.26

Experimental conversions to maleic anhydride (x_M) and carbon dioxide (x_C) for catalyst - 3B at 350°C.

benzene:air	W/F	x_M	x_C
1:50	0	-	-
	64	0.0690	0.0669
	98	0.1029	0.0968
	122	0.1381	0.1217
	181	0.1682	0.1521
	222	0.1718	0.1726
1:80	0	-	-
	62	0.0720	0.0650
	65	0.0755	0.0623
	95	0.0982	0.0906
	120	0.1273	0.1124
	190	0.1661	0.1388
	212	0.1730	0.1475
1:140	0	-	-
	68	0.0671	0.0512
	99	0.0901	0.0895
	126	0.1133	0.1128
	190	0.1398	0.1309
	220	0.1449	0.1340
	225	0.1471	0.1331

Table - A.27

Experimental conversions to maleic anhydride (x_M) and carbon dioxide (x_C) for catalyst - 3C at 350°C.

benzene:air	W/F	x_M	x_C
1:50	0	-	-
	60	0.0728	0.0797
	93	0.1197	0.1025
	125	0.1488	0.1242
	180	0.1822	0.1475
	221	0.1927	0.1678
1:80	0	-	-
	54	0.0701	0.0536
	94	0.1092	0.0986
	133	0.1408	0.1153
	169	0.1583	0.1304
	250	0.1896	0.1581
1:140	0	-	-
	51	0.0592	0.0497
	93	0.1070	0.0913
	125	0.1255	0.1015
	178	0.1497	0.1214
	222	0.1611	0.1262

Table - A.28

Experimental conversions to maleic anhydride (x_M) and carbon dioxide (x_C) for catalyst - 4 at 400°C.

benzene:air	W/F	x_M	x_C
1:50	0	-	-
	68	0.1412	0.1085
	116	0.1878	0.1552
	127	0.2040	0.1572
	152	0.2241	0.1619
	180	0.2339	0.1902
	231	0.2612	0.1943
	294	0.2580	0.2245
	318	0.2500	0.2426
1:80	0	-	-
	60	0.1333	0.1013
	88	0.1661	0.1300
	93	0.1702	0.1498
	122	0.1993	0.1569
	161	0.2300	0.1840
	205	0.2551	0.1947
	250	0.2720	0.2054
	318	0.2751	0.2222
1:110	0	-	-
	62	0.1318	0.0983
	73	0.1451	0.1151
	124	0.1962	0.1513
	144	0.2180	0.1520
	183	0.2388	0.1804
	216	0.2522	0.1942
	221	0.2601	0.1860
	294	0.2332	0.1990
1:140	0	-	-
	70	0.1380	0.0998
	109	0.1803	0.1038
	139	0.2181	0.1319
	222	0.2712	0.1781
	267	0.2870	0.1927
	304	0.2964	0.2017
	326	0.3011	0.1989

Table - A.29

Experimental conversions to maleic anhydride (x_M) and carbon dioxide (x_C) for catalyst - 5 at 400°C.

benzene:air	W/F	x_M	x_C
1:50	0	-	-
	64	0.1328	0.1223
	102	0.1847	0.1701
	136	0.2031	0.1949
	177	0.2339	0.2148
	222	0.2427	0.2461
	250	0.2400	0.2562
	302	0.2266	0.2951
1:80	0	-	-
	64	0.1280	0.1221
	103	0.1700	0.1677
	140	0.1942	0.1888
	183	0.2258	0.2100
	254	0.2511	0.2436
	262	0.2480	0.2458
	282	0.2522	0.2504
	318	0.2482	0.2687
1:110	0	-	-
	64	0.1200	0.1142
	103	0.1618	0.1686
	140	0.1955	0.1984
	194	0.2282	0.2245
	240	0.2421	0.2352
	250	0.2503	0.2319
	310	0.2586	0.2452
1:140	0	-	-
	64	0.1188	0.1110
	98	0.1670	0.1473
	135	0.2001	0.1713
	175	0.2273	0.1966
	257	0.2600	0.2410
	272	0.2739	0.2302
	305	0.2777	0.2406

Table - A.30

Comparison of the rates (r) calculated by the modified Hinshelwood model for total benzene disappearance and the rates (r_1) calculated by the Hougen-Watson model for maleic anhydride formation with the corresponding experimental rates

Temperature - 330°C. Catalyst - 2

benzene:air	W/F	$rx10^4$ Exptl.	$rx10^4$ Calc.	Error, %	r_1x10^4 Exptl.	r_1x10^4 Calc.	Error, %
1:50	0	11.60	11.62	- 0.2	8.70	11.37	-30.7
	69	7.70	8.07	- 4.8	5.77	6.00	- 3.9
	104	7.21	6.61	+ 8.3	5.41	5.07	+ 6.3
	149	5.33	5.79	- 8.6	4.00	4.43	-10.8
	194	3.84	3.62	+ 5.7	2.88	4.05	-
	228	3.00	2.79	+ 7.0	2.25	3.70	-
1:80	0	10.60	10.54	+ 0.5	7.96	7.16	+10.0
	72	7.20	7.32	- 1.6	5.40	4.58	+15.2
	113	6.41	6.18	+ 3.4	4.80	3.87	+19.4
	155	4.58	4.77	- 3.7	3.45	3.53	- 2.3
	209	3.63	4.20	-16.6	2.70	3.35	-24.0
	250	2.28	2.56	-10.9	1.71	2.99	-
1:110	0	9.82	9.63	+ 1.7	7.35	5.22	+29.0
	68	6.80	7.43	- 9.2	5.10	3.91	+23.4
	111	6.05	6.16	- 1.8	2.50	3.18	+29.3
	149	5.22	4.86	+ 6.1	3.92	2.90	+25.5
	195	3.56	3.91	- 9.8	2.68	2.68	nil
	235	2.63	2.62	nil	1.96	2.54	-
	Average error:			5.8			15.7

Table - A.31

Comparison of the rates (r) calculated by the modified Hinshelwood model for total benzene disappearance and the rates (r_1) calculated by the Hougen-Watson model for maleic anhydride formation with the corresponding experimental rates

Temperature - 310°C. Catalyst - 3

benzene:air	W/F	$r \times 10^4$ Exptl.	$r \times 10^4$ Calc.	Error, %	$r_1 \times 10^4$ Exptl.	$r_1 \times 10^4$ Calc.	Error, %
	0	7.60	7.62	- 0.3	5.46	7.20	+27.2
	58	4.31	4.02	+ 6.5	3.24	2.50	+21.8
	100	2.88	2.87	+ 0.3	2.25	2.04	+ 5.1
1:50	130	2.15	2.02	+ 6.0	1.64	1.85	-15.6
	169	1.75	1.22	+29.5	1.25	1.74	-34.8
	235	1.33	-	-	1.05	1.44	-
	0	6.75	6.75	nil	5.03	4.54	+ 9.7
	64	3.80	4.41	-16.0	2.89	2.33	+17.6
	107	2.60	2.59	+ 0.3	1.90	1.71	+11.8
1:80	132	2.17	1.81	+16.6	1.62	1.54	+ 4.9
	194	1.80	1.47	+18.4	1.26	1.35	- 7.1
	236	1.46	-	-	1.19	1.26	- 5.8
	0	6.00	6.10	- 1.6	4.47	3.31	+25.9
	70	3.60	4.34	-20.5	2.52	2.07	+18.1
	110	2.65	3.50	-32.0	1.80	1.82	- 1.1
1:110	140	2.00	2.43	-21.5	1.43	1.62	- 8.7
	190	1.67	2.00	-19.7	1.24	1.48	-19.3
	248	1.20	1.34	-11.7	0.89	1.41	-
	Average error:			12.5			14.7

APPENDIX - B

Figures

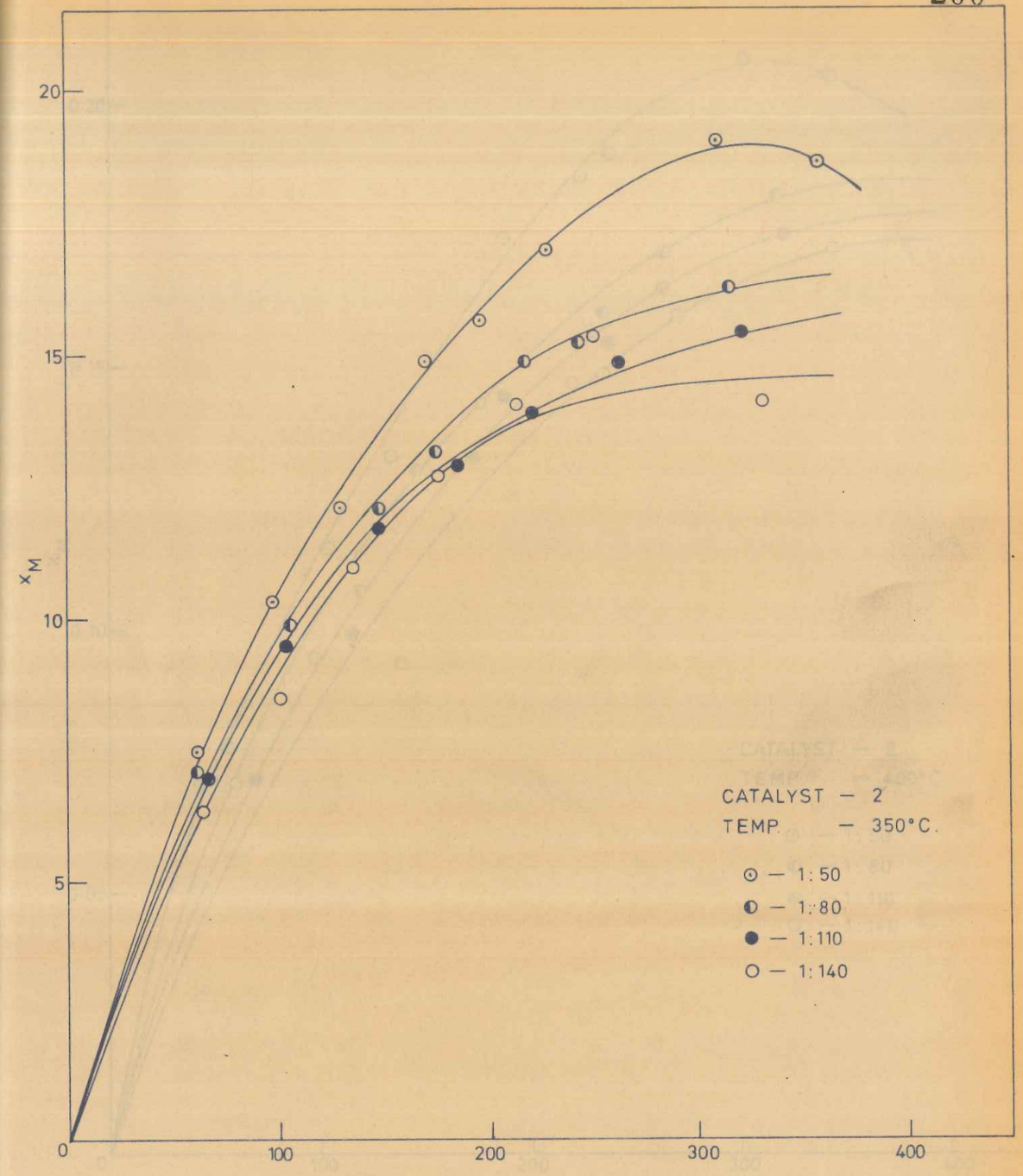

FIG. B·1. CONVERSION TO MALEIC ANHYDRIDE (x_M) AS A FUNCTION OF W/F FOR CATALYST 2 AT TEMPERATURE 350° C

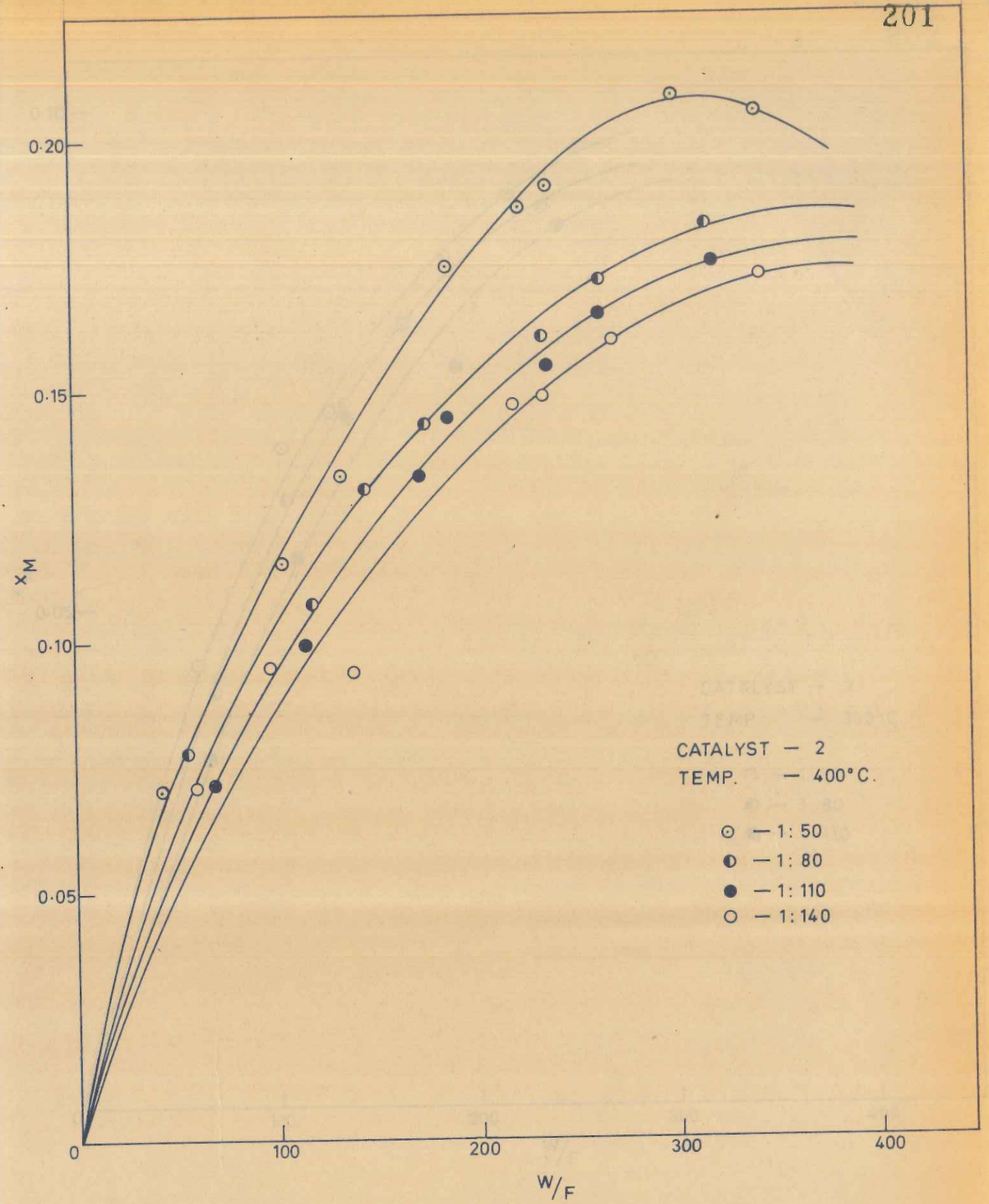

FIG. B·2. CONVERSION TO MALEIC ANHYDRIDE (x_M) AS A FUNCTION OF $W/_F$ FOR CATALYST 2 AT TEMPERATURE 400°C.

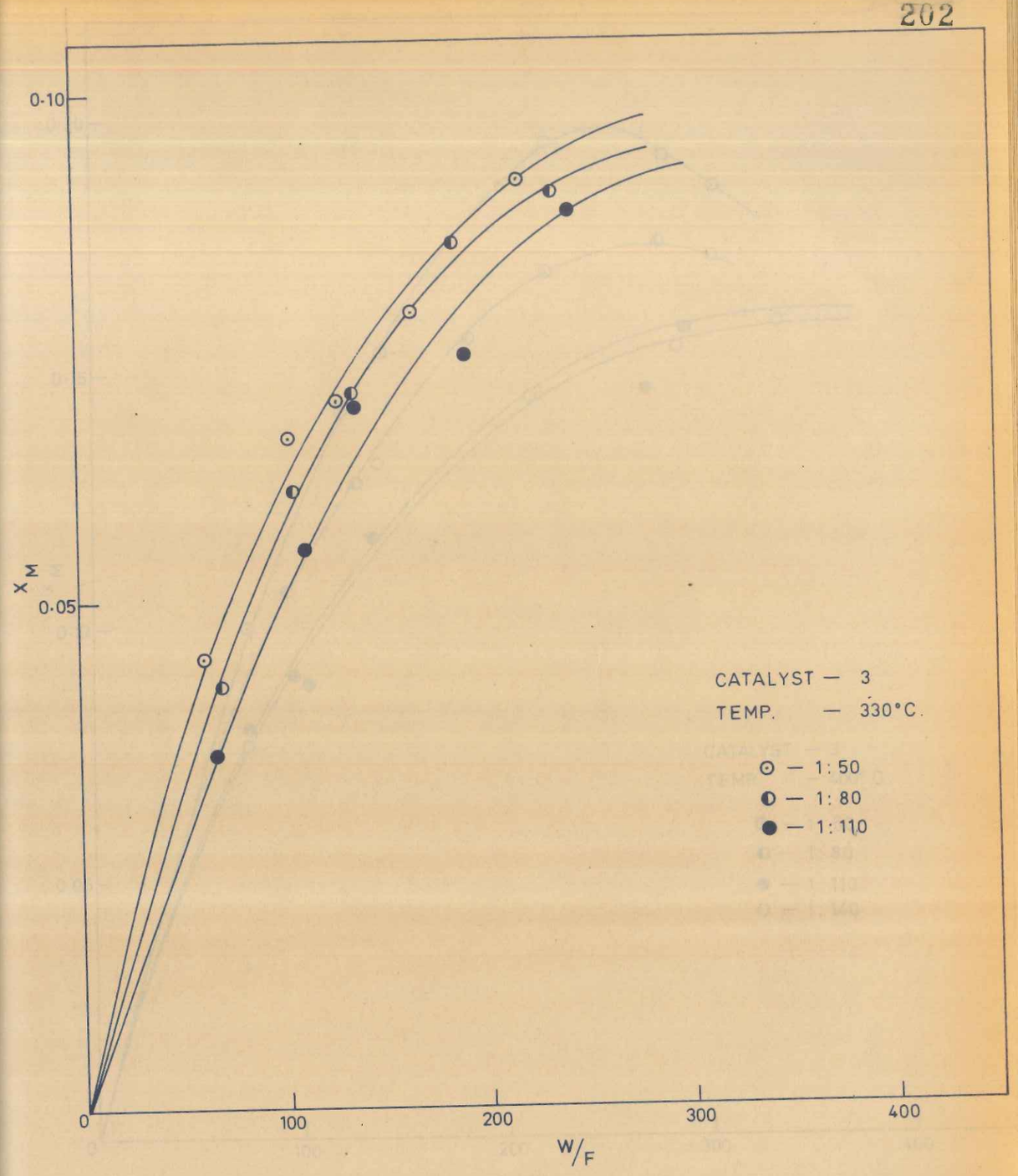

FIG. B·3. CONVERSION TO MALEIC ANHYDRIDE (x_M) AS A FUNCTION OF W/F FOR CATALYST 3 AT TEMPERATURE 330°C.

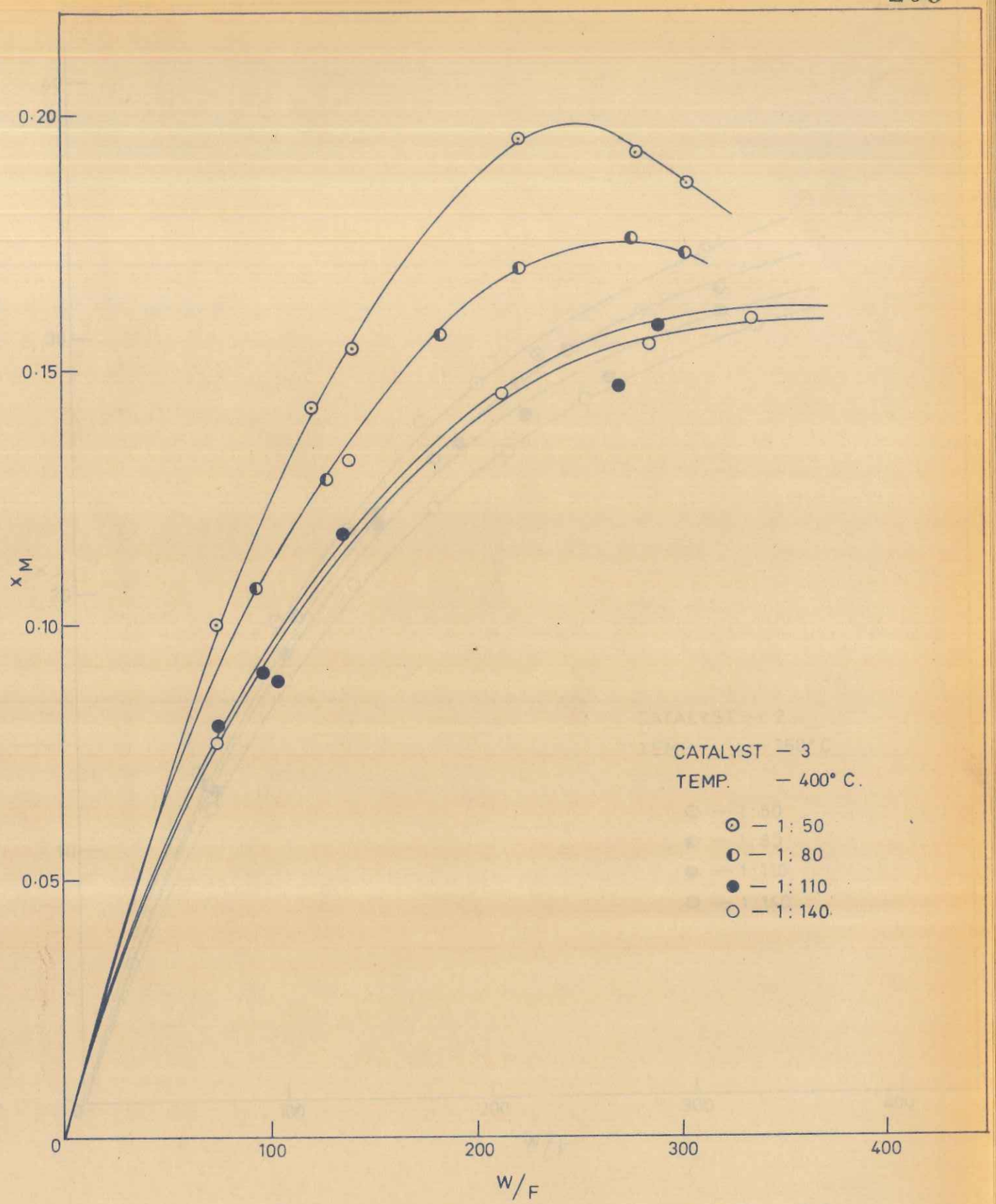

FIG. B·4 CONVERSION TO MALEIC ANHYDRIDE (x_M) AS A FUNCTION OF $W/_F$ FOR CATALYST 3, AT TEMPERATURE 400° C.

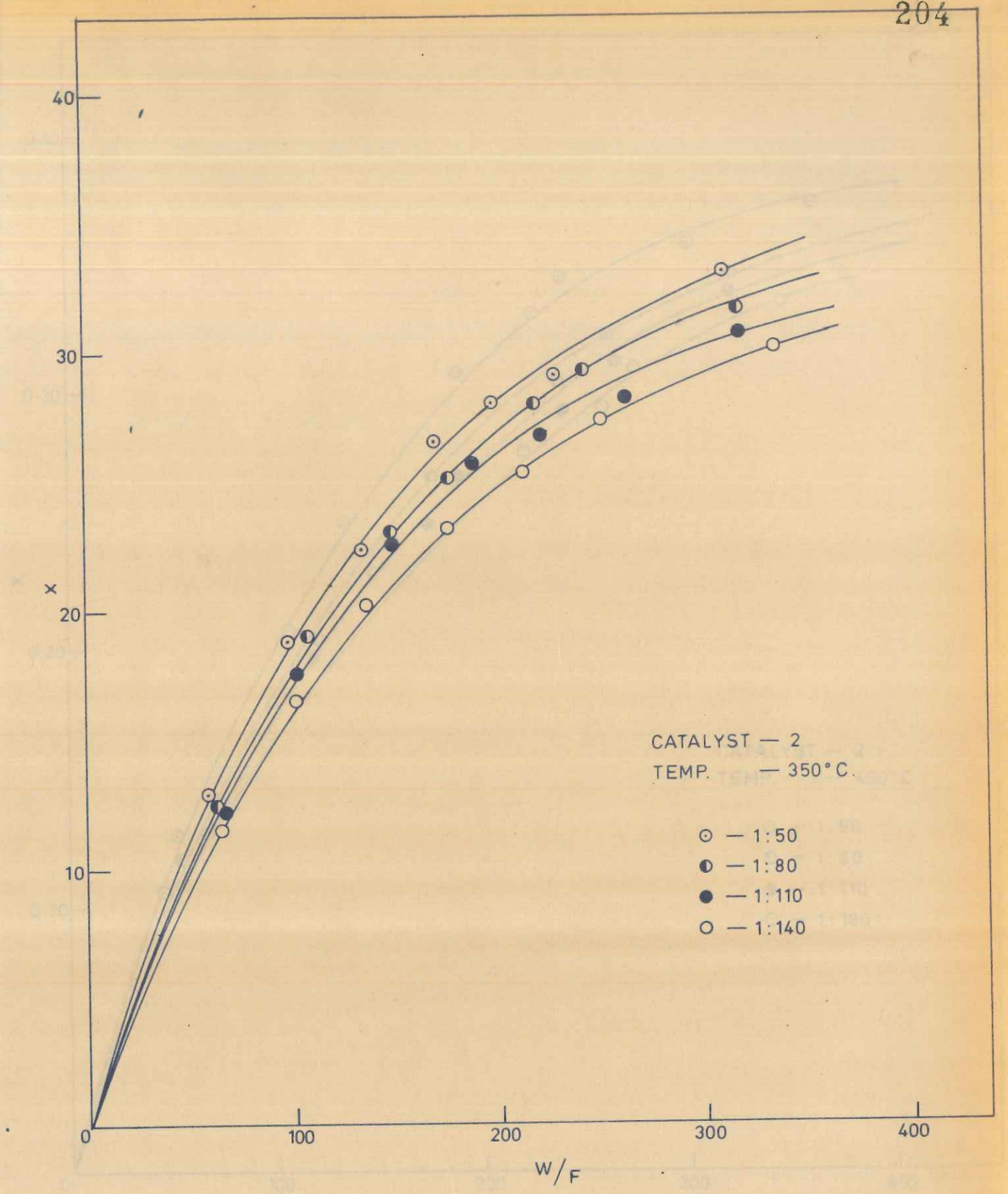

FIG. B·5 BENZENE CONVERSION, x (experimental), AS A FUNCTION OF W/F FOR CATALYST 2, AT TEMPERATURE 350°C.

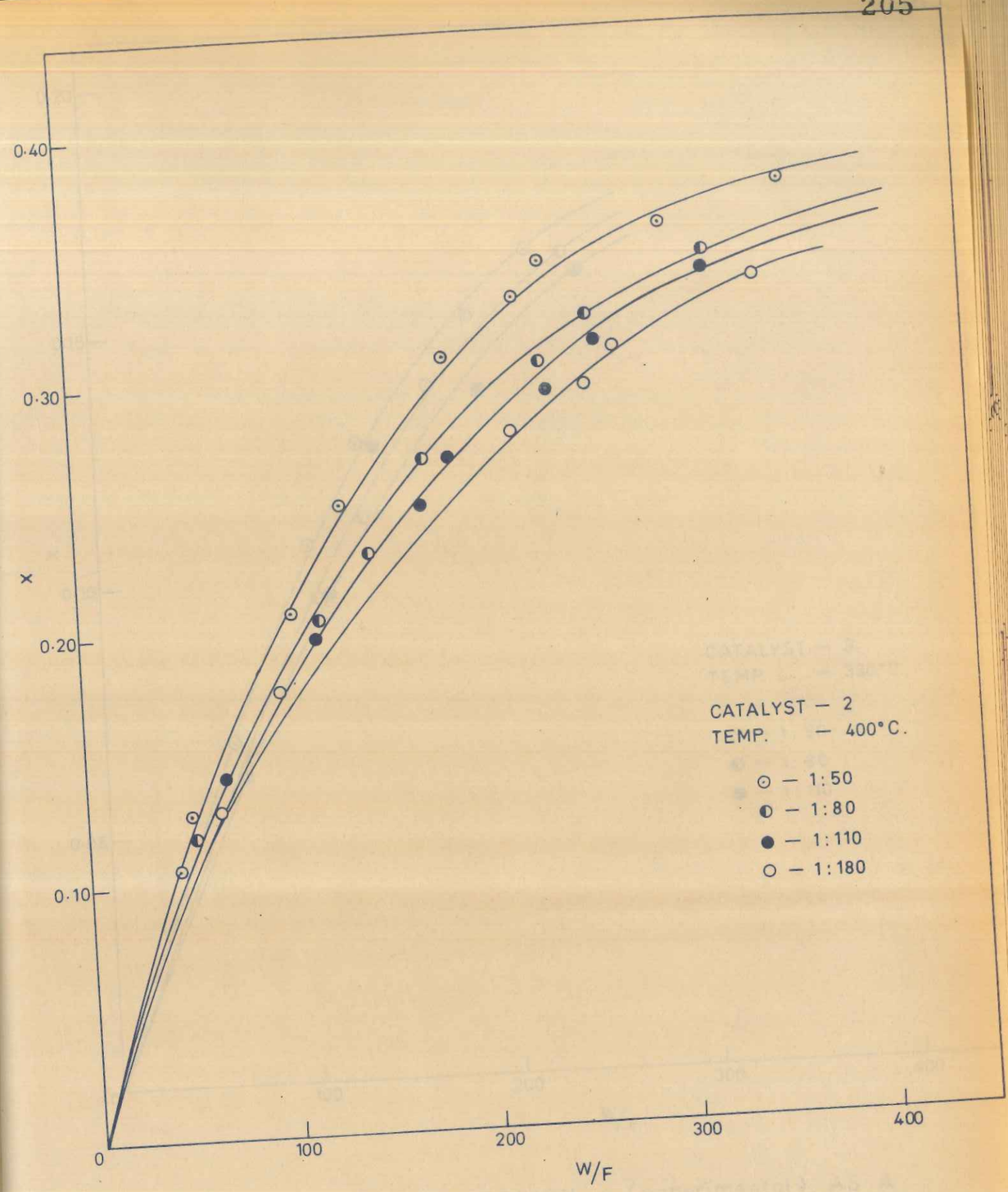

FIG. B·6. BENZENE CONVERSION, x (experimental), AS A FUNCTION OF W/F FOR CATALYST 2, AT TEMPERATURE 400°C.

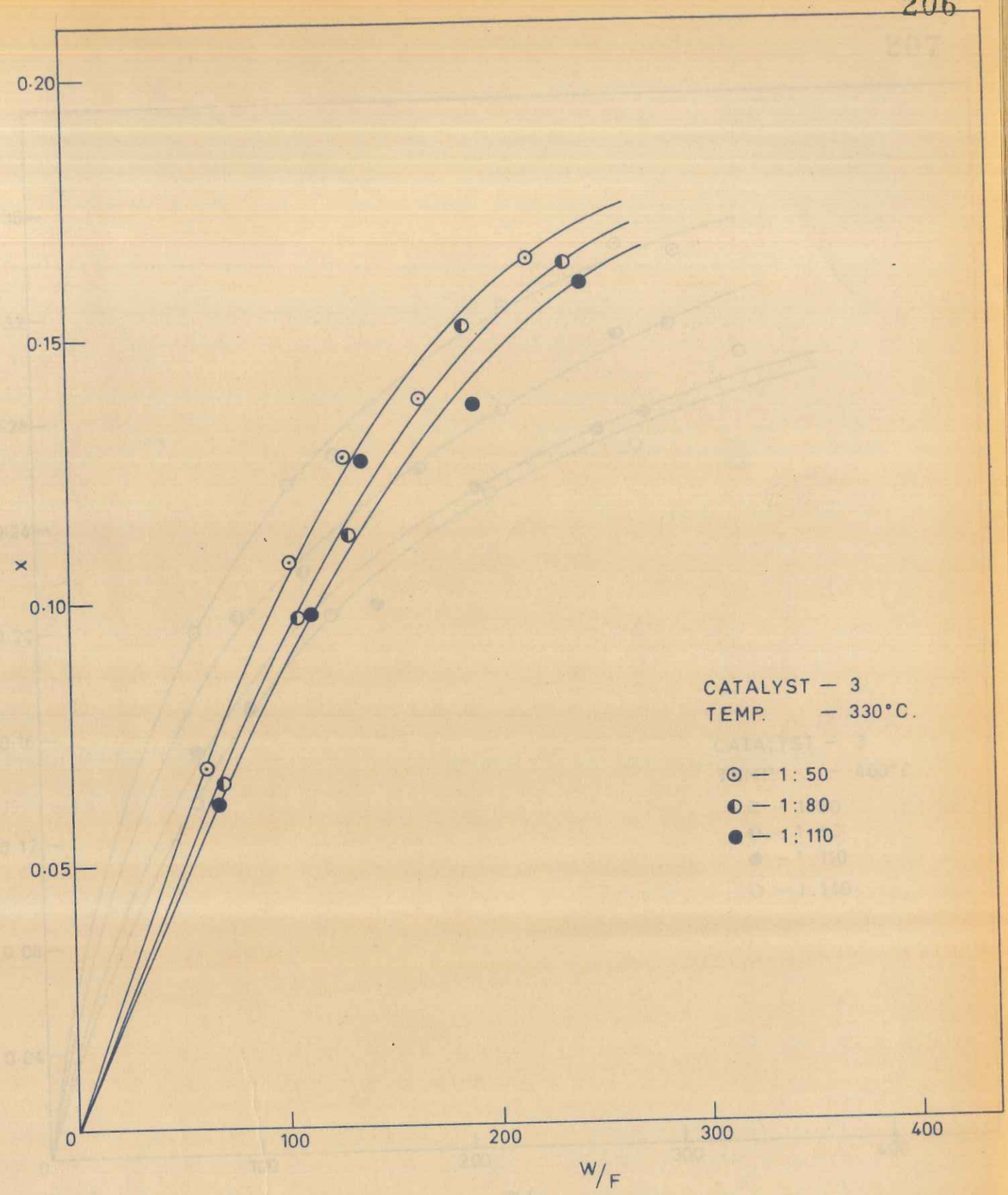

FIG. B·7. BENZENE CONVERSION, x (experimental), AS A FUNCTION OF W/F FOR CATALYST 3, AT TEMPERATURE 330°C.

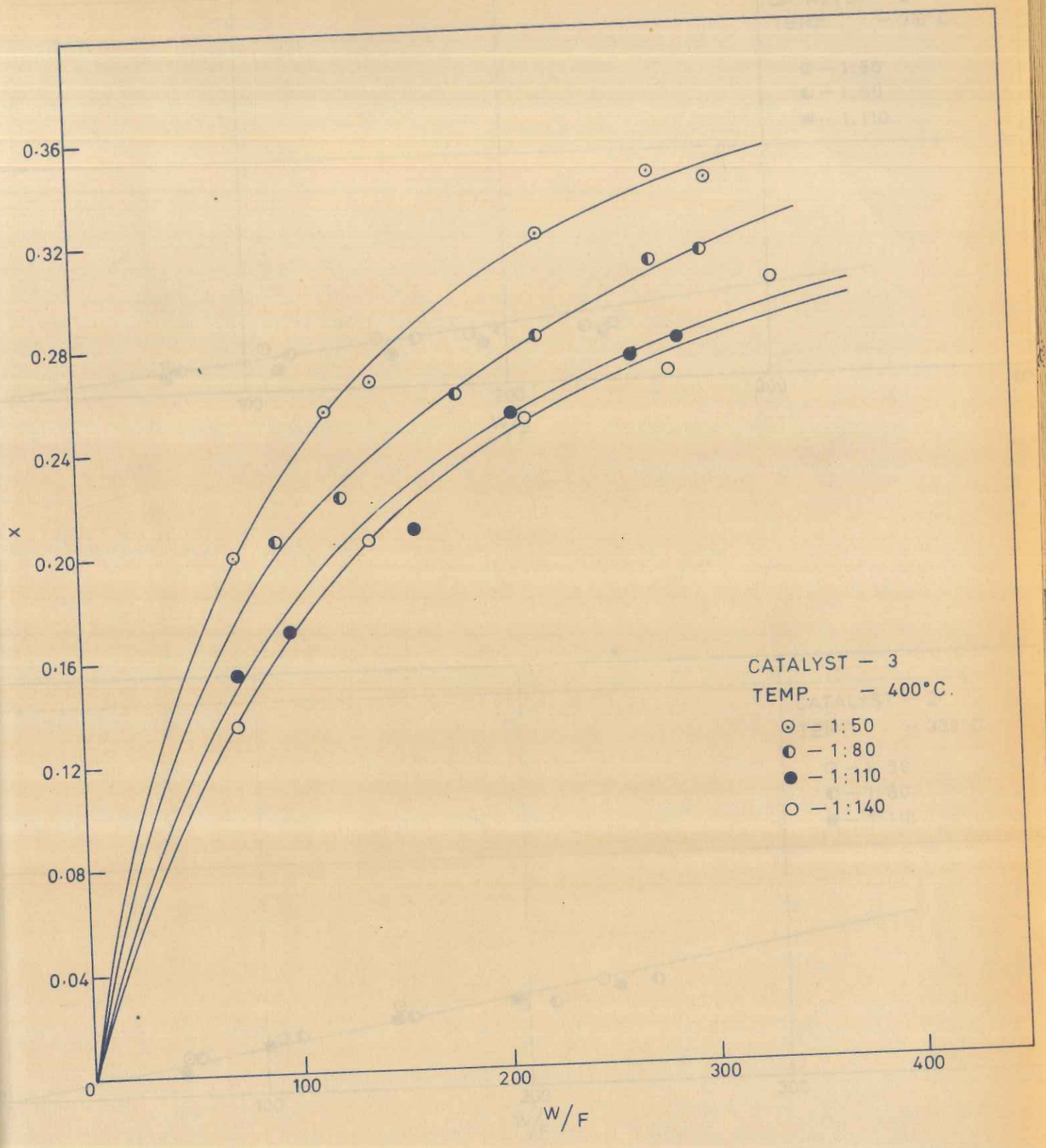

FIG. B·8. BENZENE CONVERSION, x (experimental), AS A FUNCTION OF W/F FOR CATALYST 3, AT TEMPERATURE 400°C.

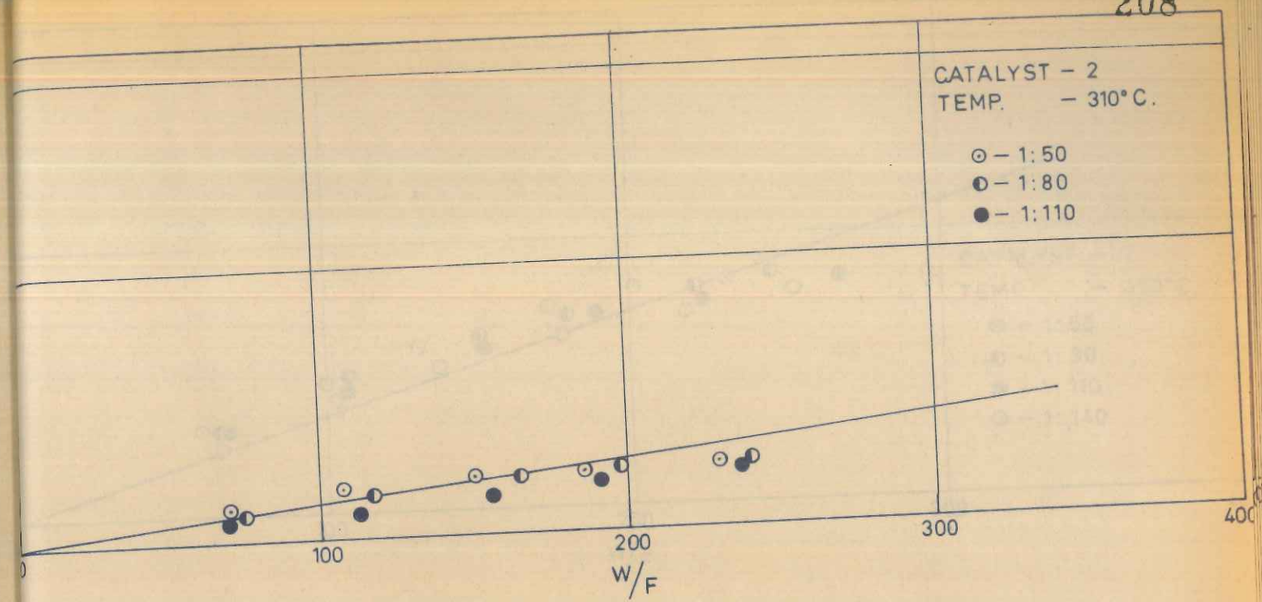

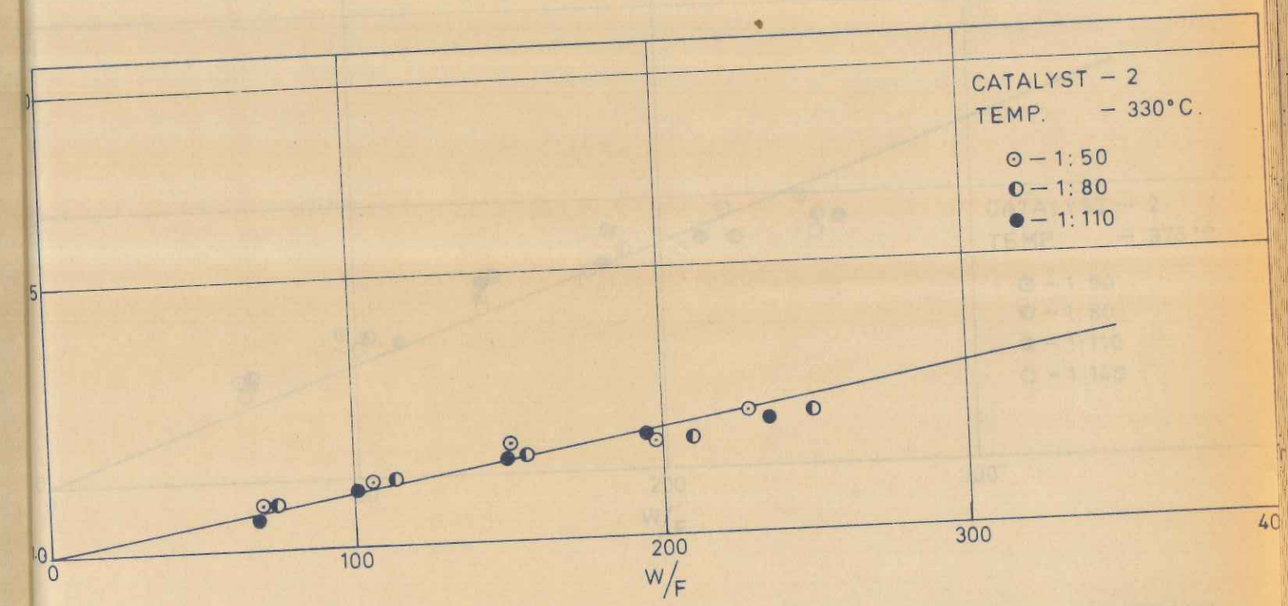

FIG. B·9. PLOTS OF EQUATION (3·4) FOR DETERMINING THE CONSTANT (k_1+k_3) FOR CATALYST-2, AT TEMPERATURES 310 & 330°C.

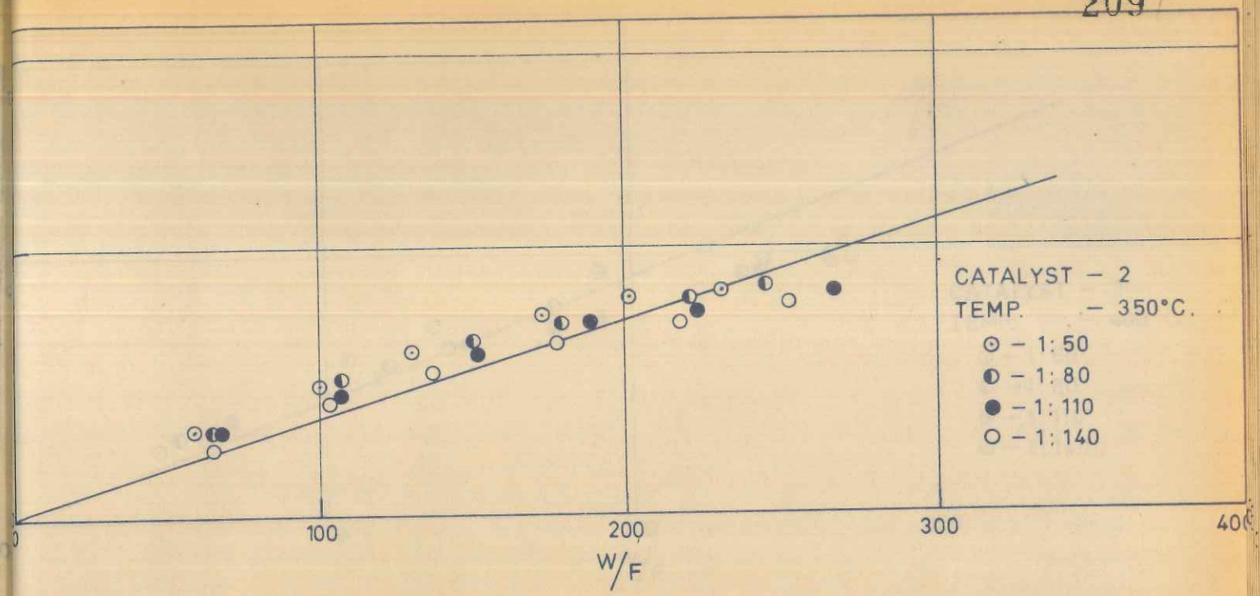

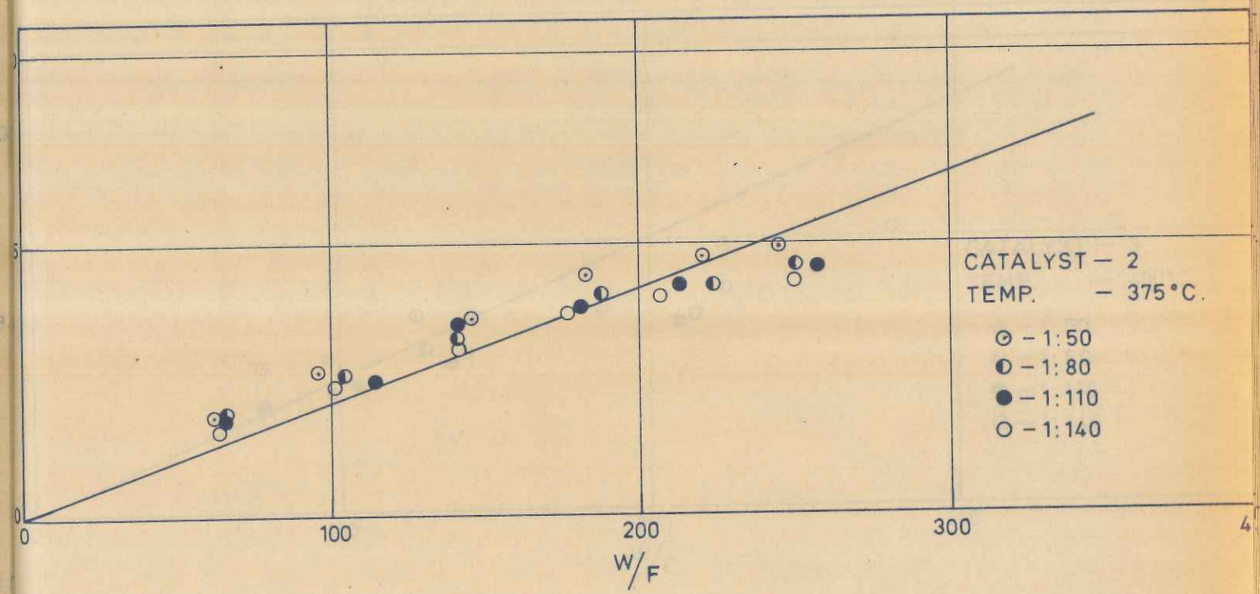

FIG. B·10 PLOTS OF EQUATION (3·4) FOR DETERMINING THE CONSTANT (k_1+k_3) FOR CATALYST – 2 AT TEMPERATURES 350 & 375°C.

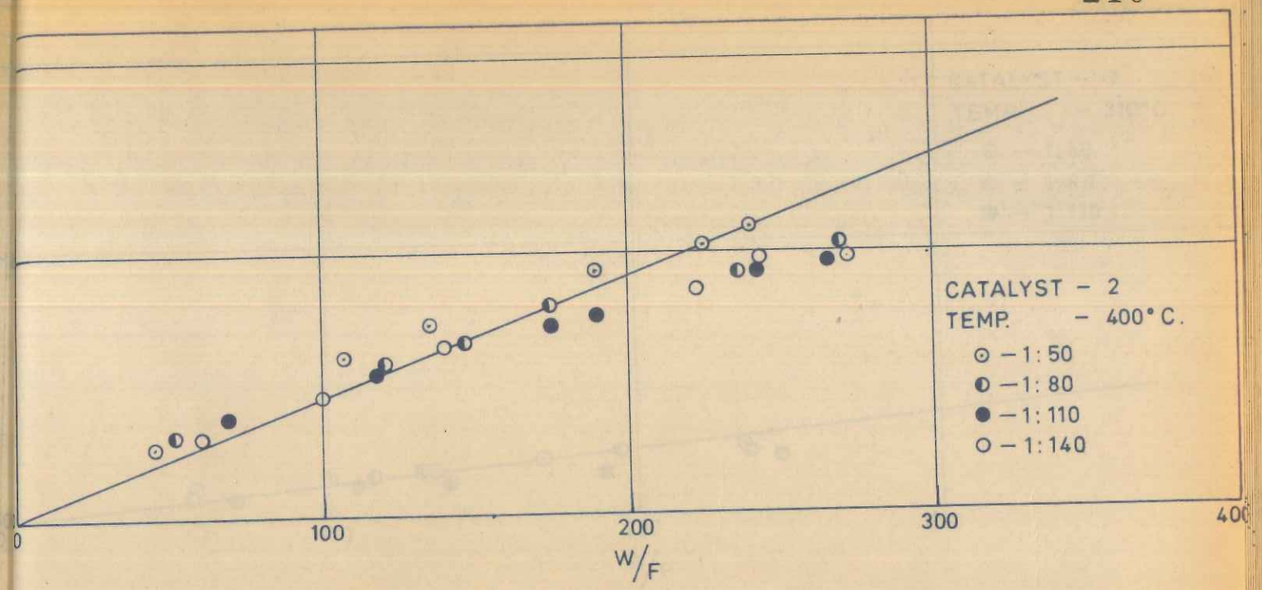

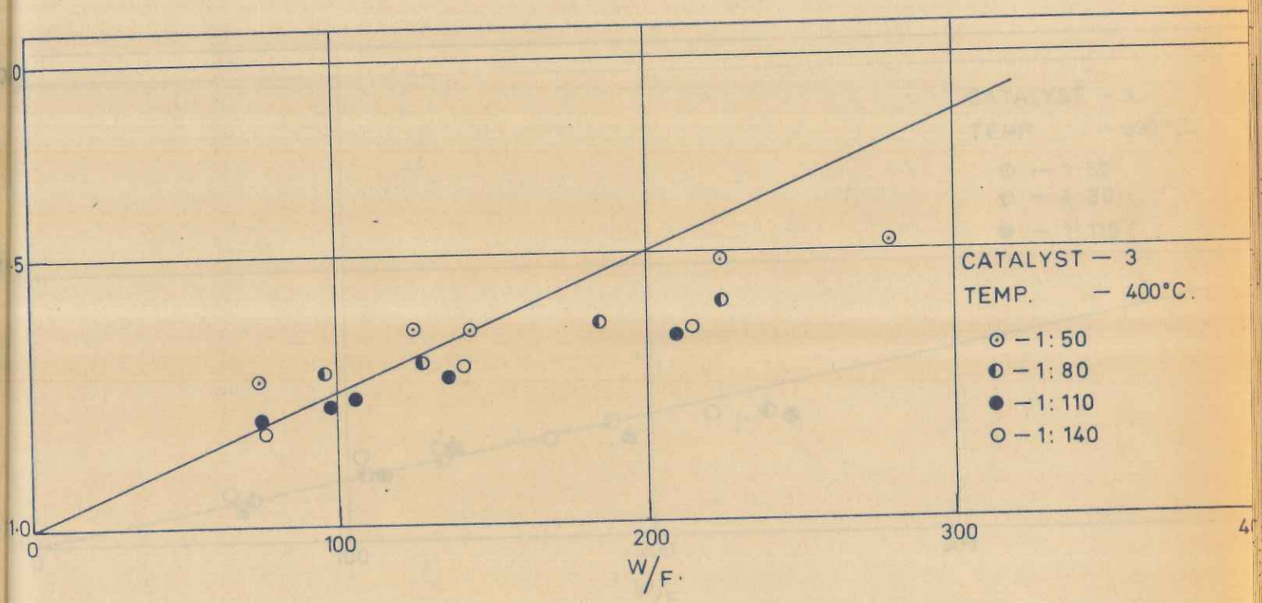

FIG. B·11. PLOTS OF EQUATION (3·4) FOR DETERMINING THE CONSTANT $(k_1 + k_3)$ FOR CATALYSTS 2 & 3 AT TEMPERATURE 400°C.

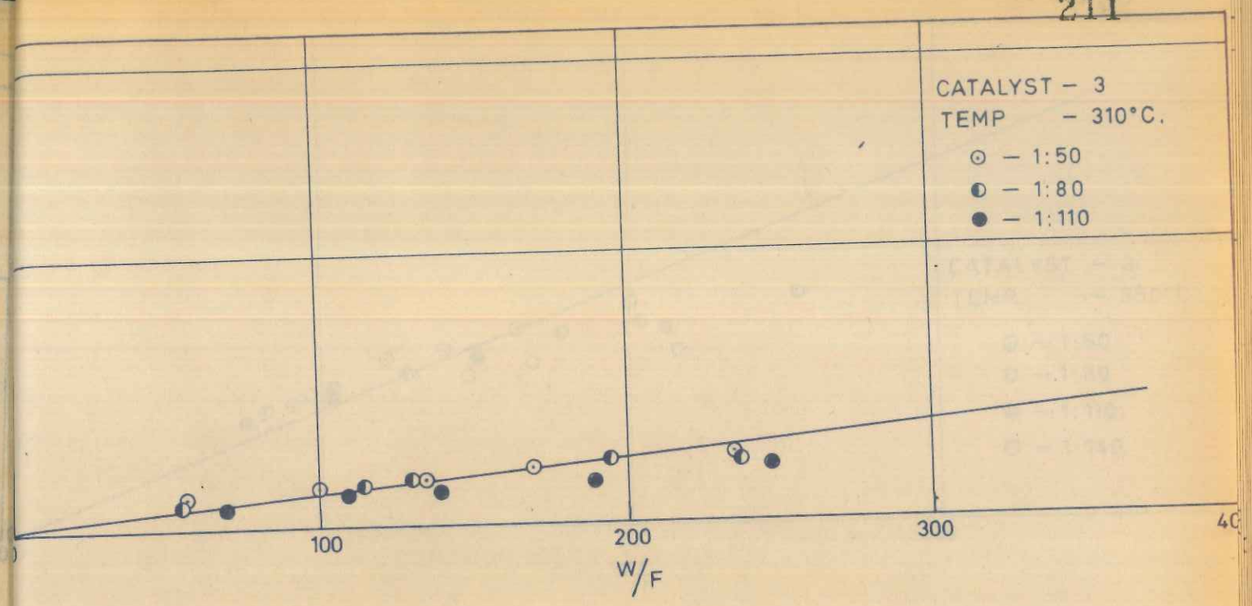

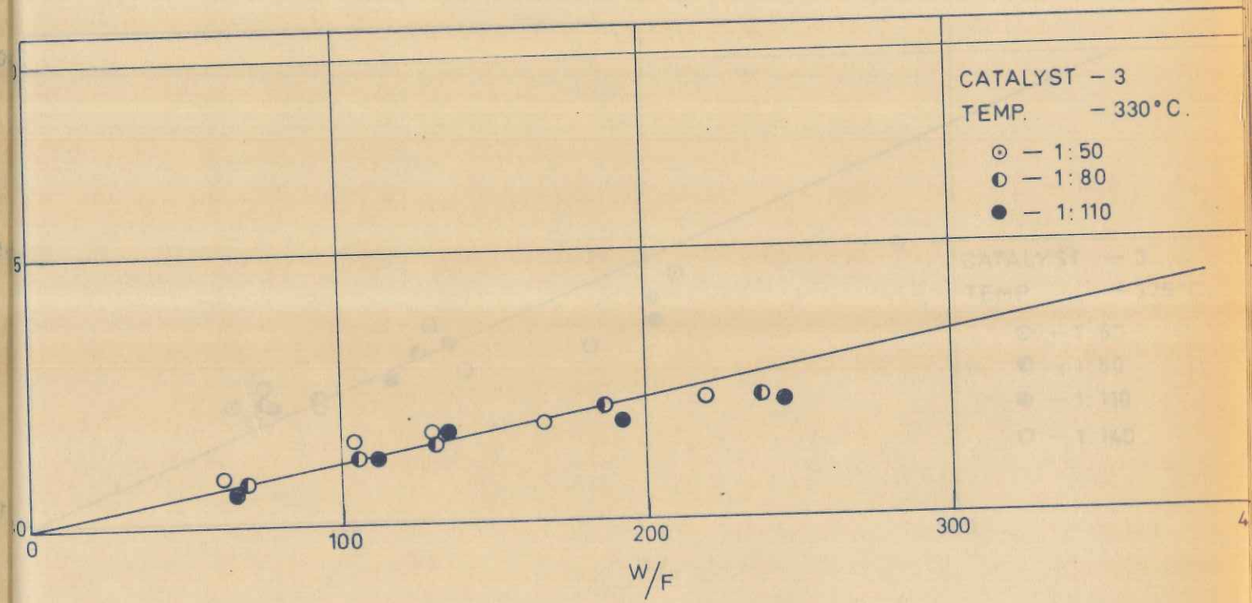

FIG. B·12. PLOTS OF EQUATION (3·4) FOR DETERMINING THE CONSTANT $(k_1 + k_3)$ FOR CATALYST-3, AT TEMPERATURES 310 & 330°C.

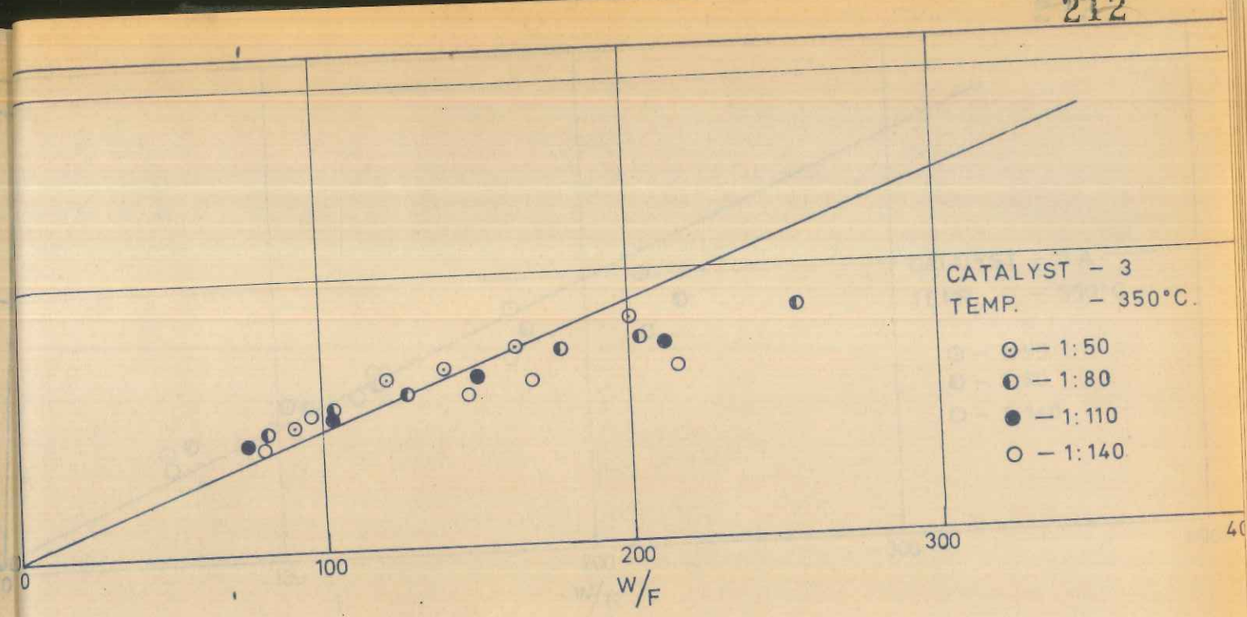

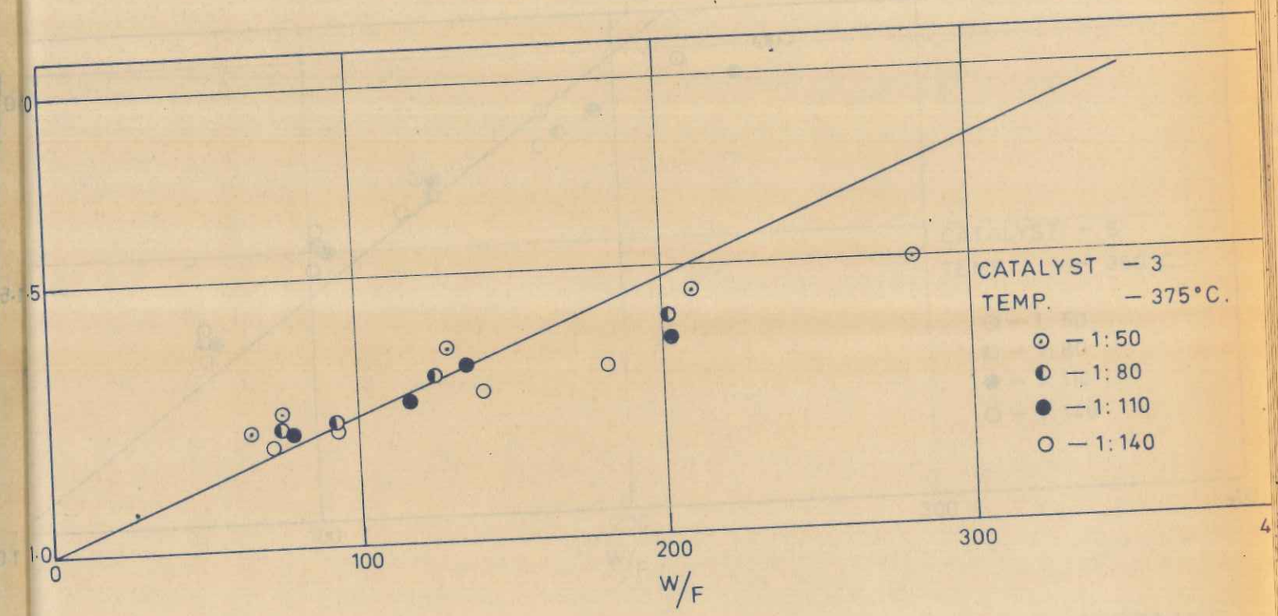

FIG. B·13. PLOTS OF EQUATION (3·4) FOR DETERMINING THE CONSTANT $(k_1 + k_3)$ FOR CATALYST-3 AT TEMPERATURES 350 & 375° C.

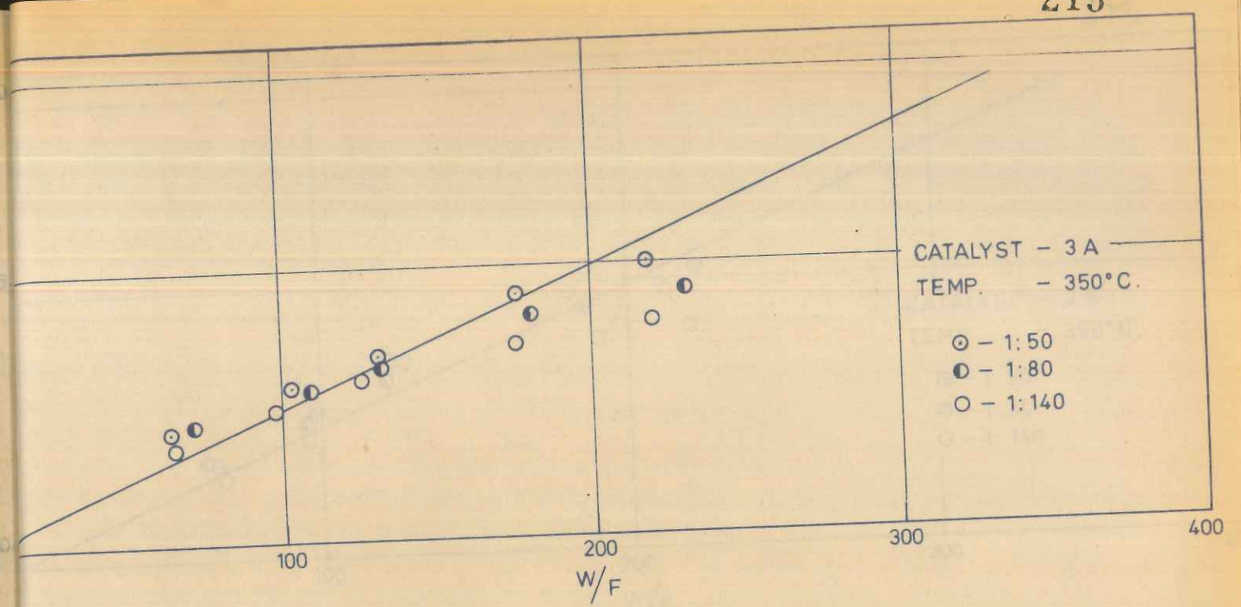

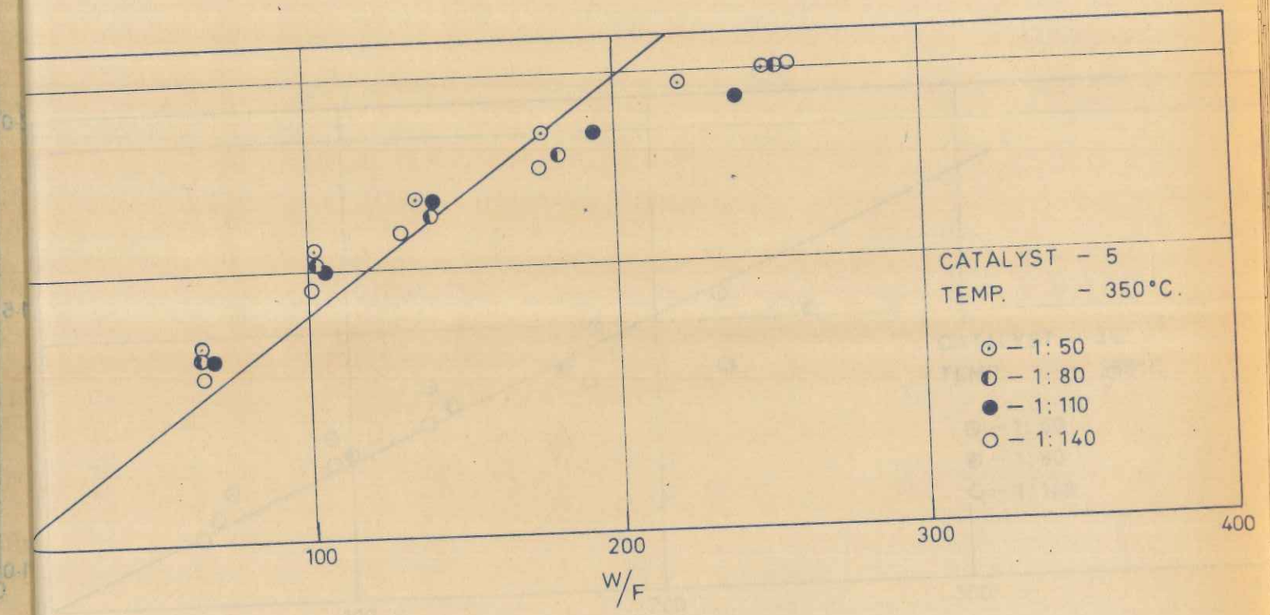

B·14. PLOTS OF EQUATION (3-4) FOR DETERMINING THE CONSTANT $(k_1 + k_3)$ FOR CATALYSTS-3A & 5 AT TEMPERATURE 350° C.

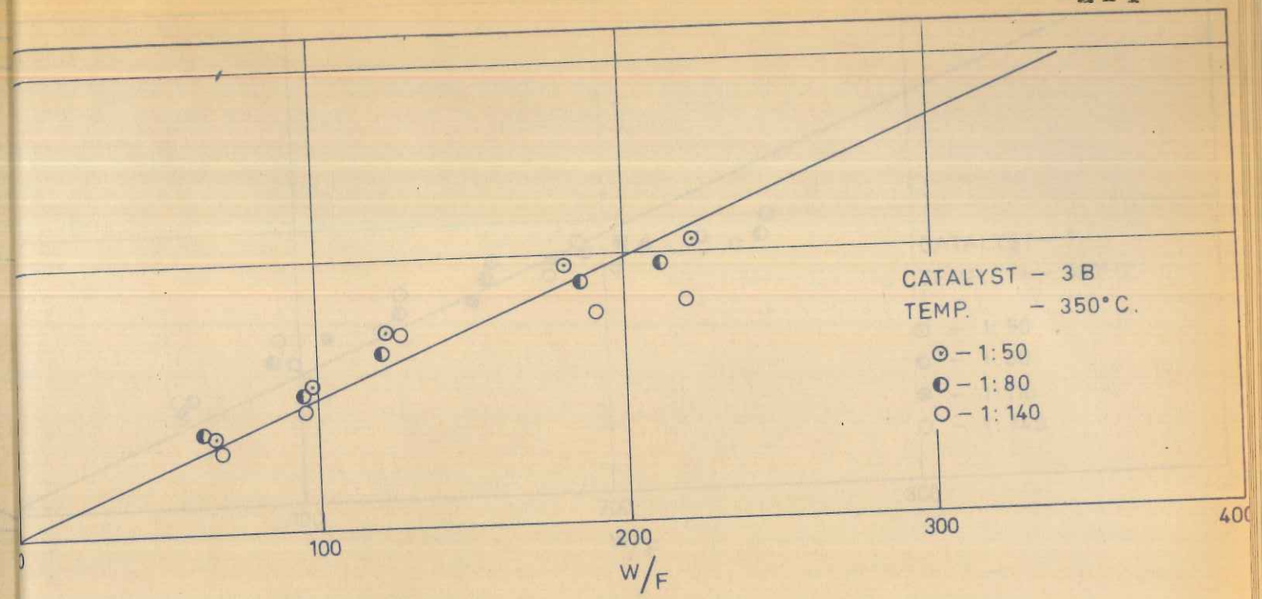

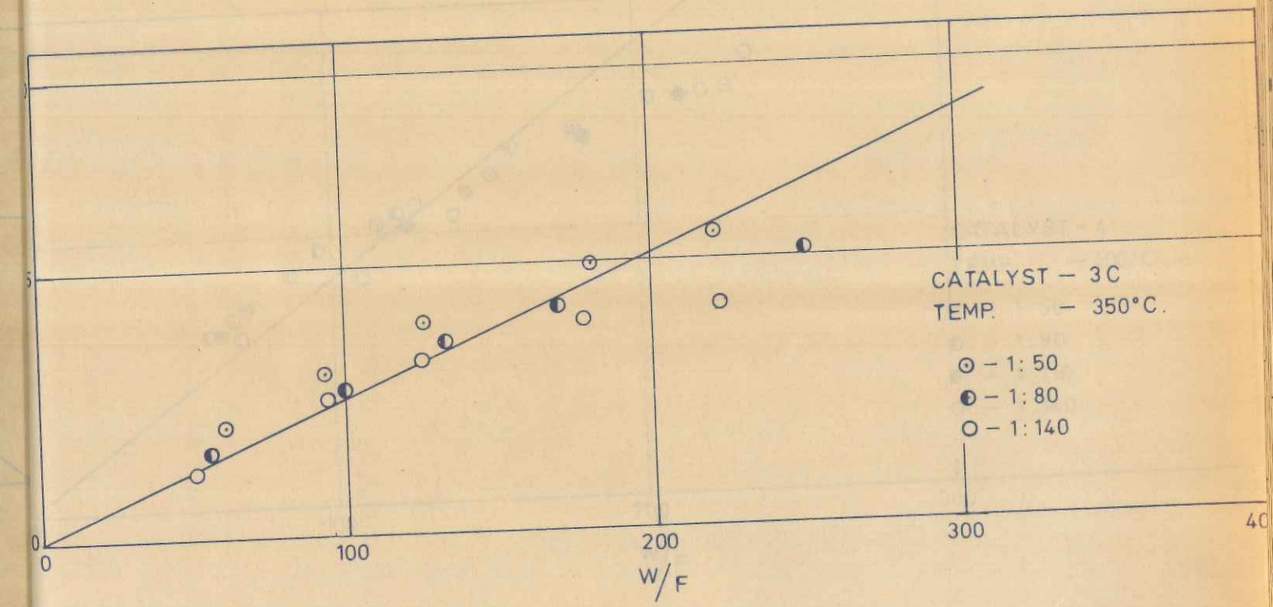

FIG. B·15. PLOTS OF EQUATION (3·4) FOR DETERMINING THE CONSTANT $(k_1 + k_3)$ FOR CATALYSTS – 3B & 3C AT TEMPERATURE 350°C.

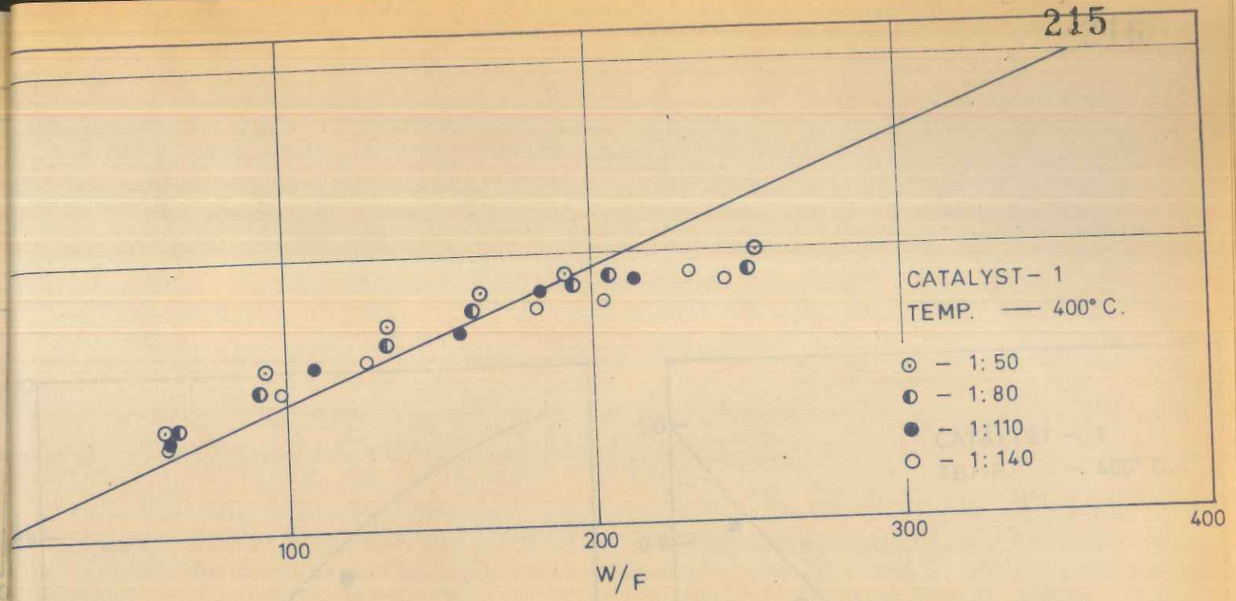

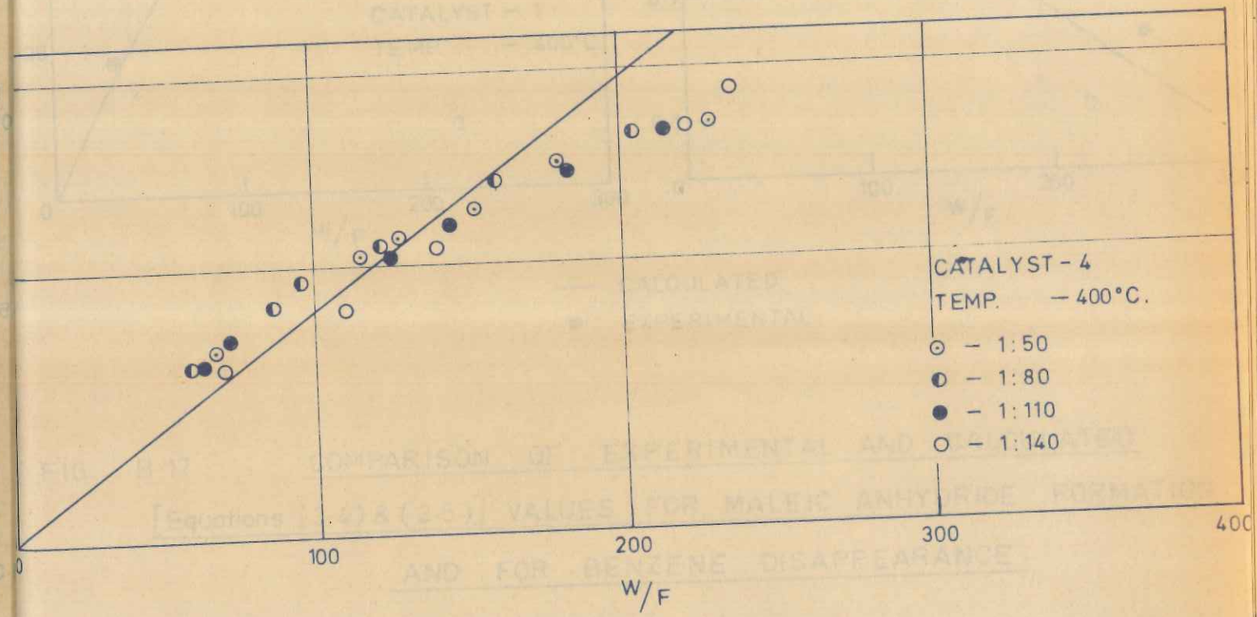

FIG. B·16. PLOTS OF EQUATION (3·4) FOR DETERMINING THE CONSTANT $(k_1 + k_3)$ FOR CATALYSTS – 1 & 4 AT TEMPERATURE 400° C.

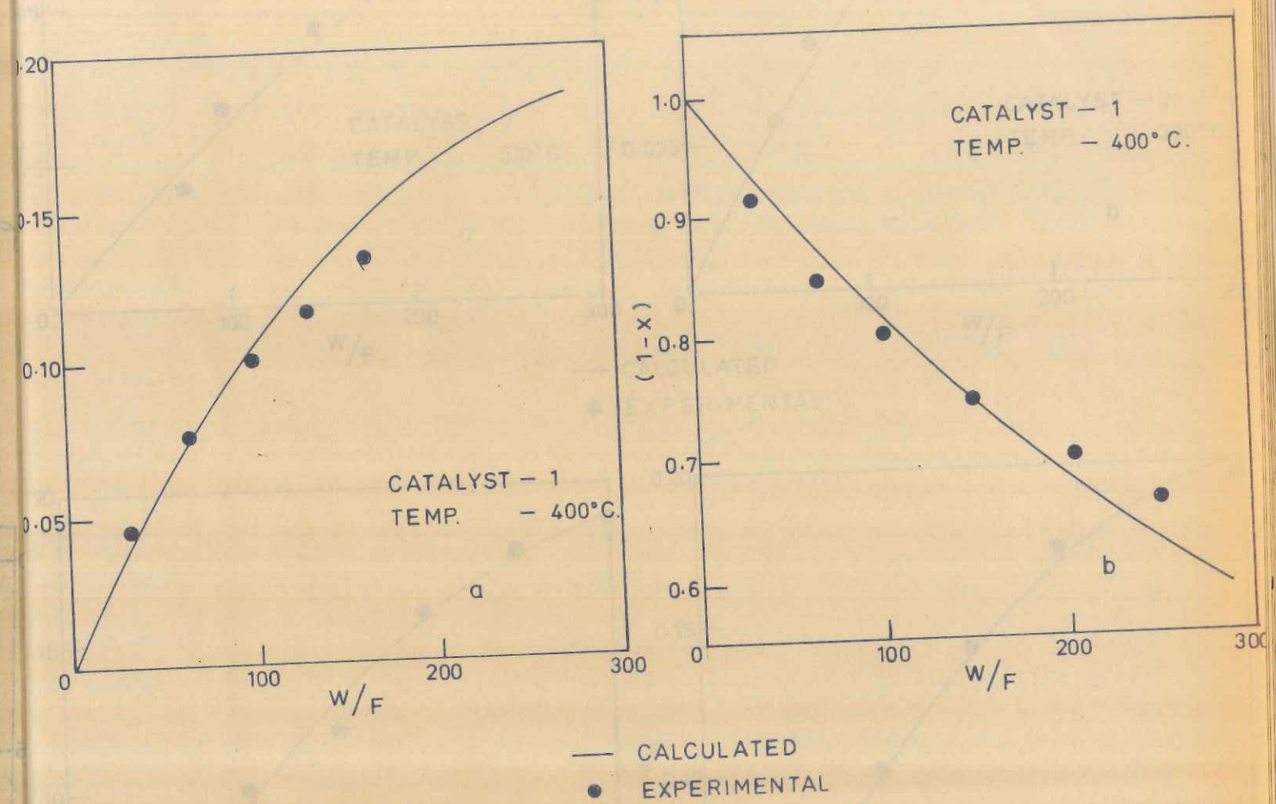

FIG. B·17. COMPARISON OF EXPERIMENTAL AND CALCULATED [Equations (3·4) & (3·5)] VALUES FOR MALEIC ANHYDRIDE FORMATION AND FOR BENZENE DISAPPEARANCE

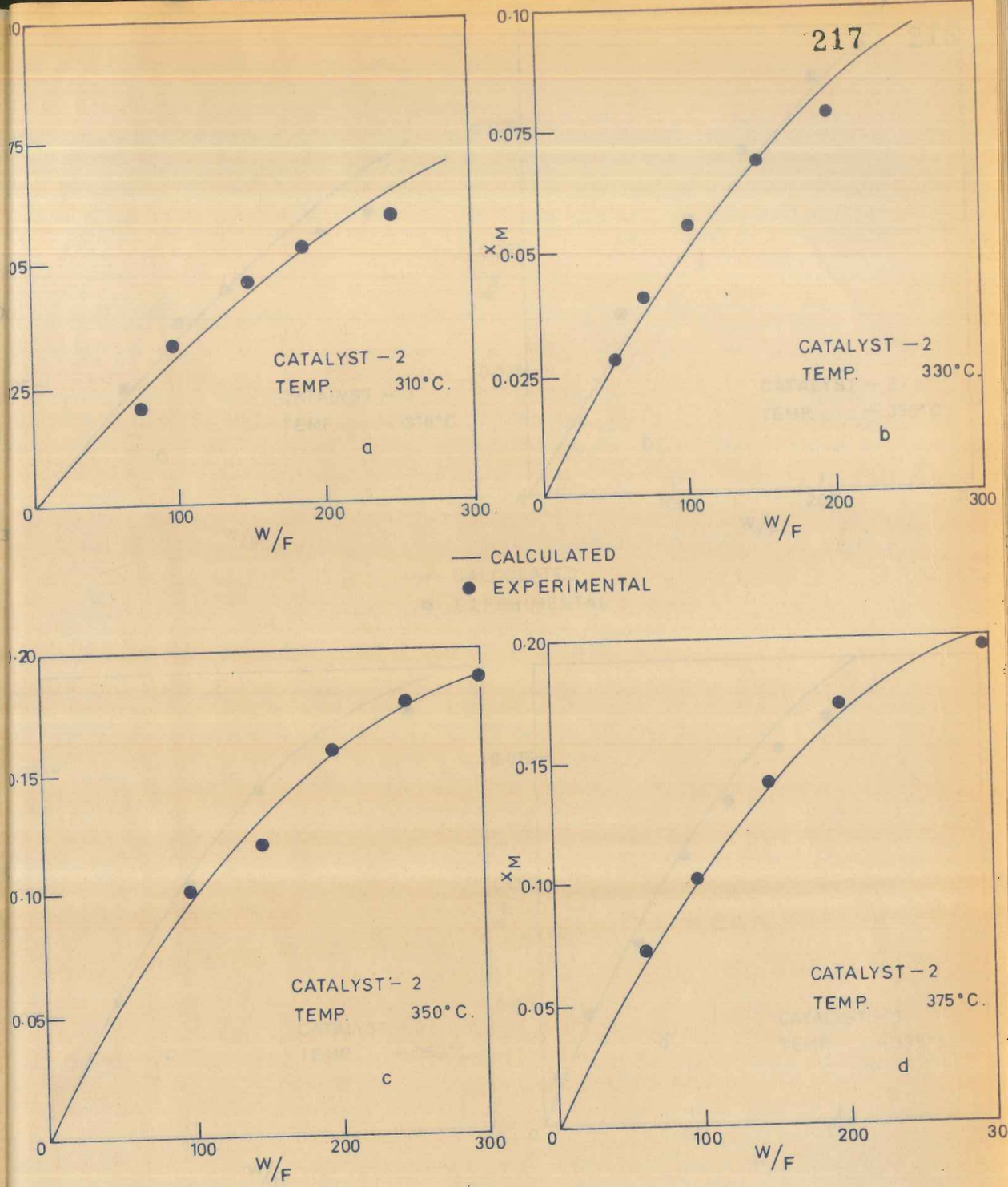

FIG. B·18. COMPARISON OF EXPERIMENTAL AND CALCULATD [Equation (3·5)] VALUES FOR MALEIC ANHYDRIDE FORMATION

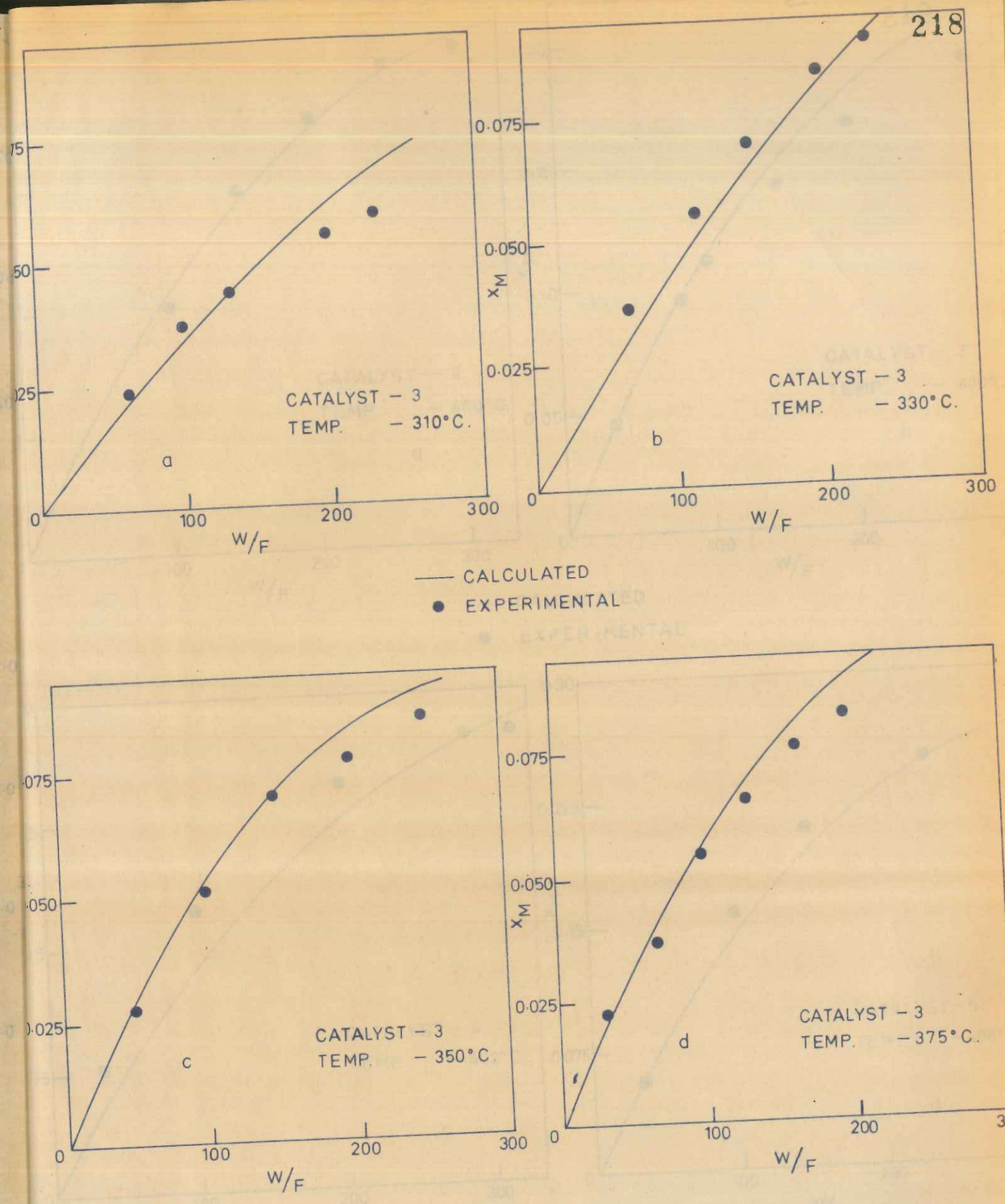

FIG. B·19. COMPARISON OF EXPERIMENTAL AND CALCULATED [Equation (3·5)] VALUES FOR MALEIC ANHYDRIDE FORMATION

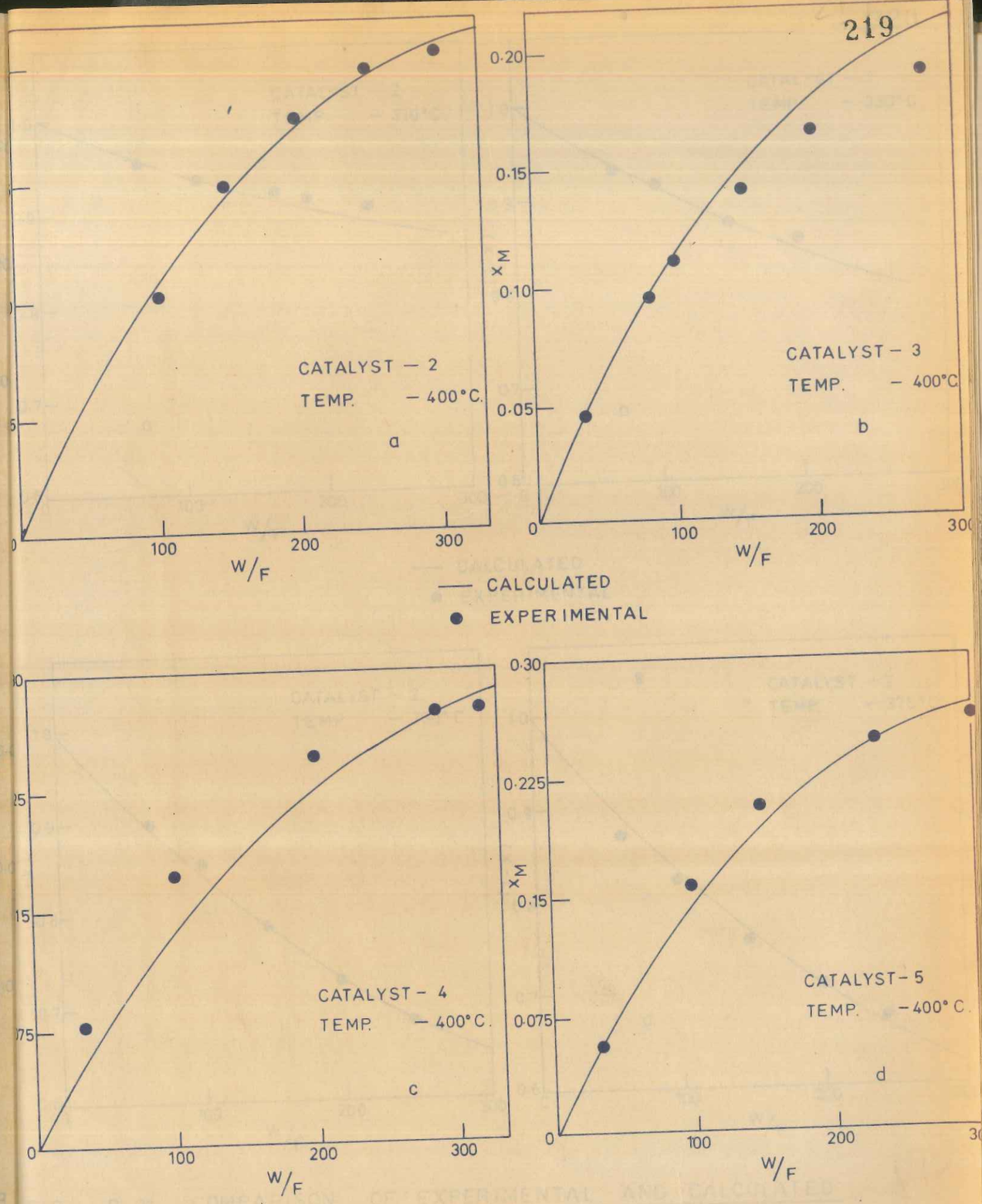

FIG. B·20. COMPARISON OF EXPERIMENTAL AND CALCULATED [Equation (3·5)] VALUES FOR MALEIC ANHYDRIDE FORMATION

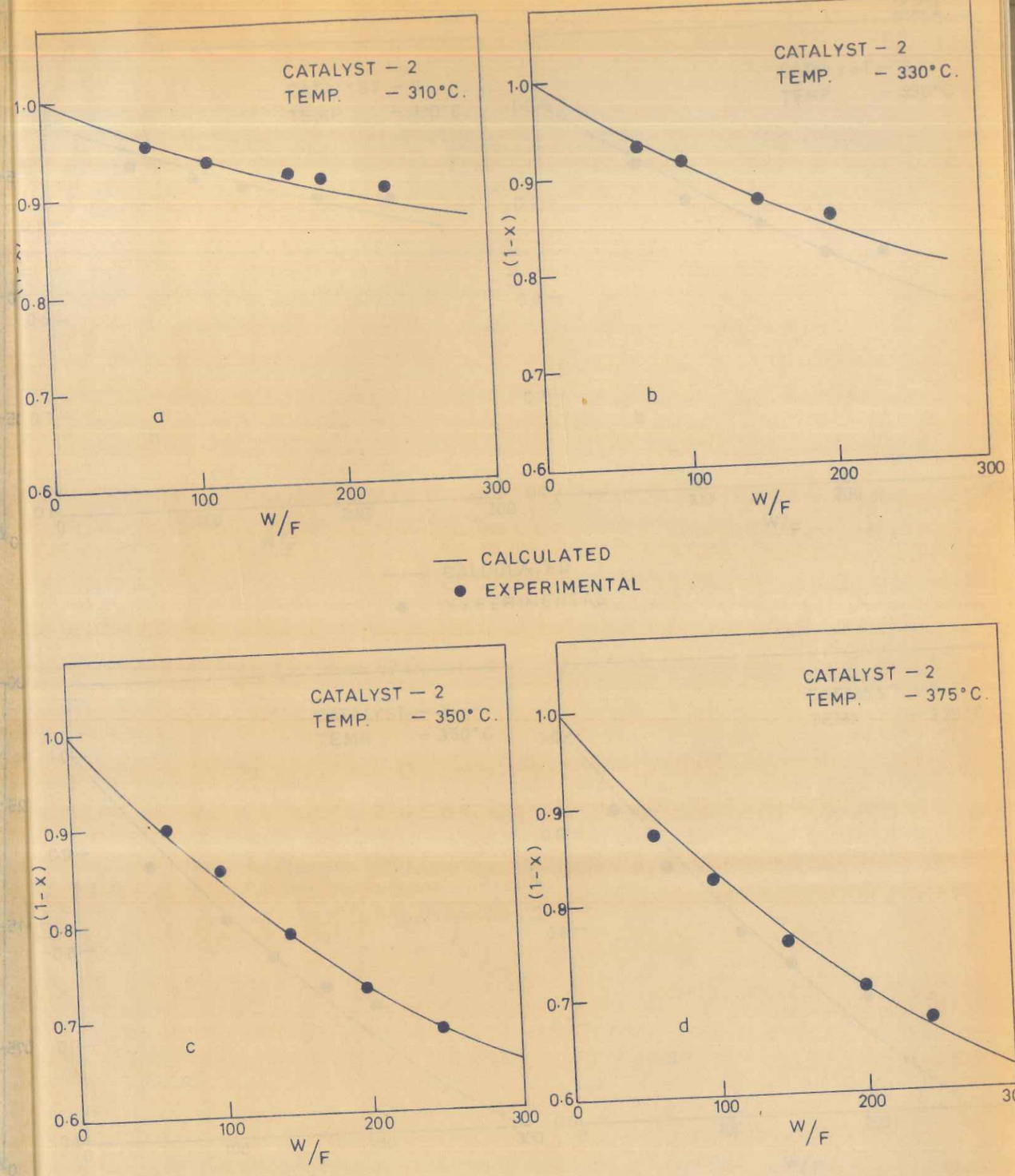

FIG. B·21. COMPARISON OF EXPERIMENTAL AND CALCULATED [Equation (3·4)] VALUES FOR BENZENE DISAPPEARANCE

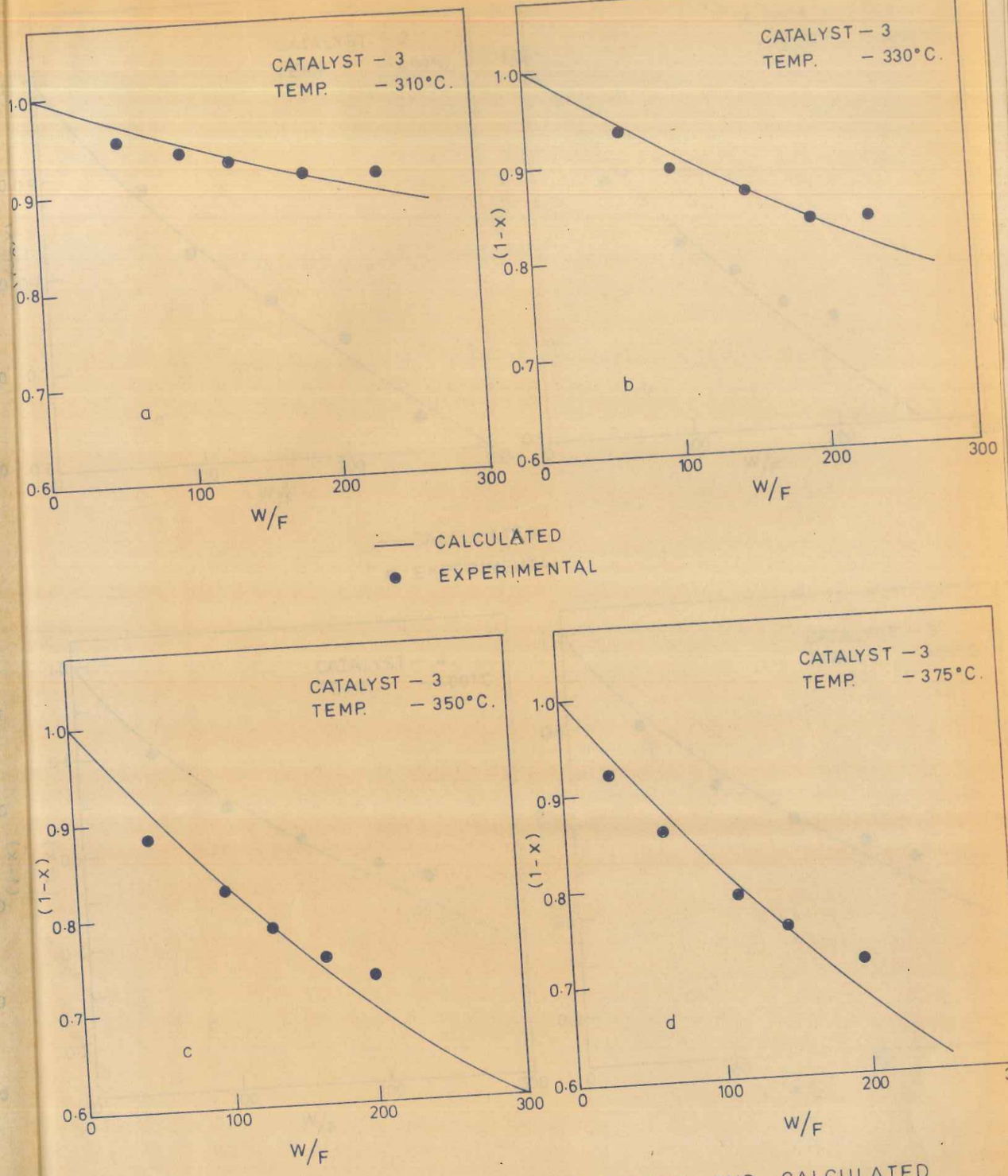

FIG. B·22. COMPARISON OF EXPERIMENTAL AND CALCULATED [Equation (3·4)] VALUES FOR BENZENE DISAPPEARANCE

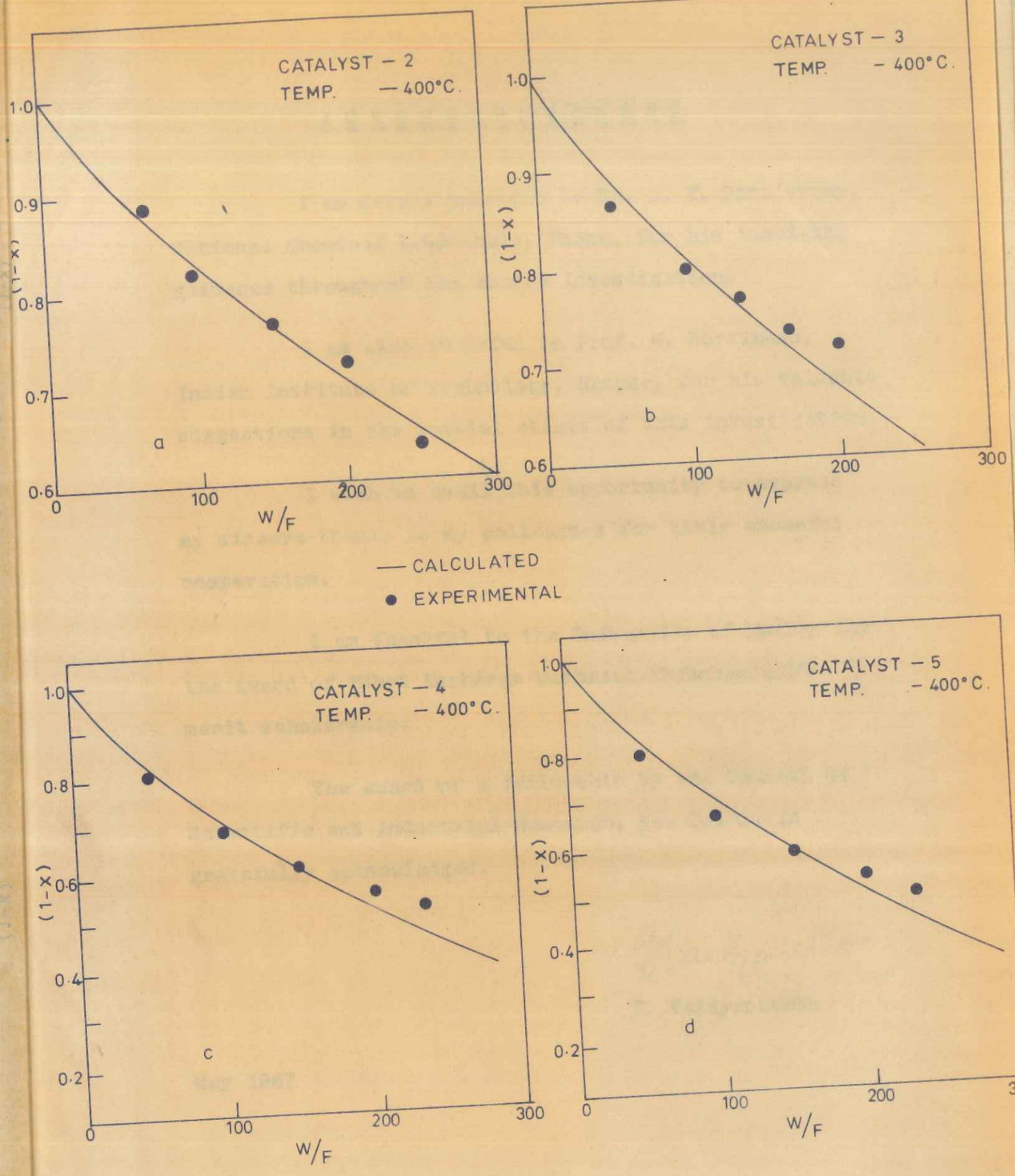

FIG. B·23. COMPARISON OF EXPERIMENTAL AND CALCULATED [Equation (3.4)] VALUES FOR BENZENE DISAPPEARENCE

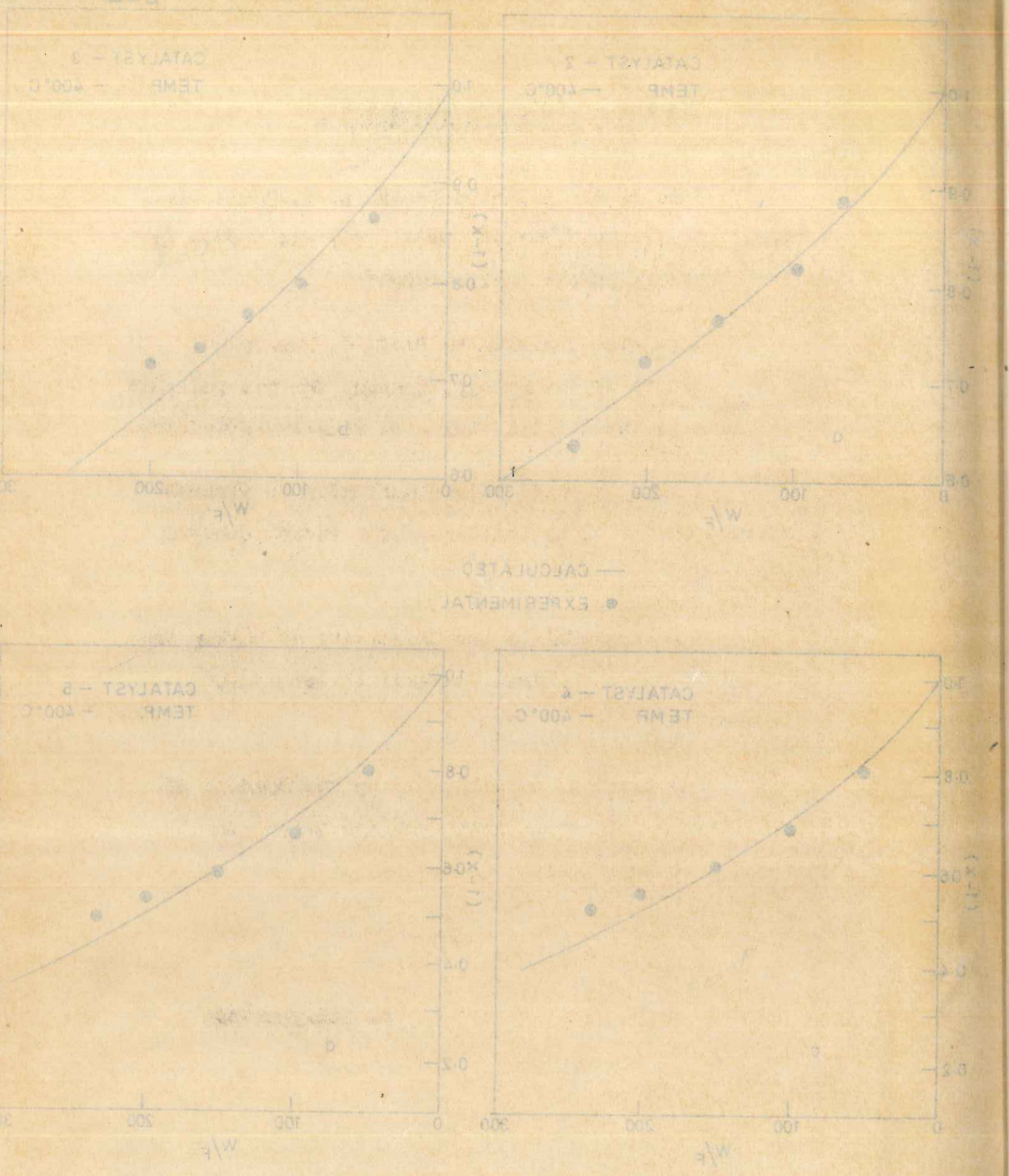

A C K N O W L E D G E M E N T

I am deeply indebted to Dr. L. K. Doraiswamy, National Chemical Laboratory, Poona, for his inspiring guidance throughout the entire investigation.

I am also thankful to Prof. G. Narsimhan, Indian Institute of Technology, Kanpur, for his valuable suggestions in the initial stages of this investigation.

I wish to avail of this opportunity to express my sincere thanks to my colleagues for their cheerful cooperation.

I am thankful to the University of Bombay for the award of "Shri Kushiram Wadhumal Khubchandani" merit scholarship.

The award of a fellowship by the Council of Scientific and Industrial Research, New Delhi, is gratefully acknowledged.

K. Vaidyanathan

May 1967

TH-435

TH-435